microRNA as Predictive Biomarkers of Canine Mammary Tumors

by

Eric James Fish

A dissertation submitted to the Graduate Faculty of
Auburn University
in partial fulfillment of the
requirements for the Degree of
Doctor of Philosophy

Auburn, Alabama
August 3, 2019

Keywords: microRNA, canine mammary tumor, estrogen receptor, biomarkers, epigenetics

Approved by

R. Curtis Bird, Chair and Graduate Advisor, Professor of Pathobiology
Russell C. Cattley, Tyler & Frances Young Professor of Pathobiology
Pete W. Christopherson, Associate Professor of Pathobiology
Annette N. Smith, Robert & Charlotte Lowder Distinguished Professor in Oncology

Abstract

Canine mammary tumors (CMT) are one of the most common forms of cancer in intact female dogs. CMTs share clinical, epidemiologic, and genetic features with women with breast cancer (BC). BC and CMT cells have altered profiles of microRNA (miRNA), small 18-22 nucleotide non-coding RNA molecules that down-regulate gene translation. Human BC cells secrete exosomes that contain microRNA (miRNA) cargo that get into peripheral blood, which may facilitate tumor progression and cancer aggressiveness. These circulating exosomal miRNA can serve as minimally invasive biomarkers of disease and provide prognostic information. The objectives of this research were (1) to isolate and characterize CMT exosomes and their miRNA profiles *in vitro*; (2) profile circulating serum miRNA from clinical CMT patients and determine their diagnostic utility, and; (3) evaluate the association between differentially expressed circulating miRNA and histopathologic tumor characteristics and overall survival.

Cell-free conditioned media was harvested from normal and malignant canine mammary epithelial cells. Transmission electron microscopy (TEM) and dynamic light scattering (DLS) identified that this media contained numerous irregularly round, 150-200 nm diameter, “cup-shaped” vesicles. Western blot for CD9 confirmed these vesicles were exosomes. Exosomal miRNA was submitted for RNA deep-sequencing (RNAseq) and found hundreds of differentially expressed miRNA between CMT and normal mammary cells. Among the significantly up-regulated miRNA were miR-18a, miR-19a,

and miR-181a, which were validated by qRT-PCR. *In silico* bioinformatic analysis found that the CMT exosomal miRNA profile was predicted to regulate a number of cell proliferation, apoptosis, and hormone receptor pathways, including the estrogen receptor (ESR1) and tumor suppressor PTEN.

Next, serum was collected from 10 dogs with histologically-confirmed malignant CMT and 10 healthy female control dogs (5 intact and 5 spayed). RNAseq revealed 65 differentially expressed circulating miRNA. A subset of seven miRNA were validated by digital droplet PCR (dPCR). Serum miR-19a and miR-125a showed good diagnostic performance in discriminating CMT patients from controls. This population of serum miRNA showed overlap with the in vitro exosomal miRNA, and were predicted to regulate a number of important tumor suppressors, pathways relevant to metastasis, and chemoresistance.

Finally, circulating miRNA were analyzed for their relationship to clinical and pathological characteristics. Serum miR-18a by RNAseq was significantly higher in patients with evidence lymphatic invasion (metastasis), and nearly significant for CMT patients with high-grade (Grade III) versus low-grade (Grade I/II) tumors. No miRNA correlated with survival times. *In situ* hybridization (ISH) revealed neoplastic epithelial cells expressed pre-miR-18a, pre-miR-19b, and pre-miR-34c, indicating those specific tumor cells represent one likely source of the circulating serum miRNA (as opposed to stromal cells, inflammatory cells, adnexa, or other tissues). This research is the first to characterize CMT exosomes and circulating miRNA, identified miR-19b and miR-18a as candidate diagnostic and prognostic biomarkers (respectively), and informs future research on serum miRNA for CMT.

Acknowledgments

This research was made possible by the hard work, intellectual contributions, and support of many people besides myself. First, I would like to thank my Major Professor, Dr. R. Curtis Bird. He inspired me to study microRNA at a time when the field was in its infancy and there was little guidance available to junior researchers. I greatly appreciate his flexibility and patience in working with a combined resident-graduate student (and later faculty member) who frequently had to balance numerous other time demands. Furthermore, the guidance of my PhD Committee, including Dr. Pete Christopherson, Dr. Annette Smith, and Dr. Russell Cattley, was invaluable in shaping the trajectory of this project. Dr. Rusty Arnold deserves mention for volunteering his time as University Reader of this dissertation and attending my subsequent PhD defense.

Portions of this work have already been published as a peer-reviewed manuscript, and other aspects comprise manuscripts in preparation for imminent submission. My co-authors on these papers deserve special mention for their expertise and hard work, including Patricia DeInnocentes, Dr. Gisela Romero-Martinez, Dr. Jey Koehler, Dr. Tony Moss, Dr. Nripesh Prasad, Dr. Kris Irizarry and Connor Ellis. Dr. James Gillespie provided invaluable advice regarding liposome/exosome biology and assay techniques. Dr. Maninder Sandey advised on digital PCR. Karen Wolfe assisted with electron microscopy.

The generous financial support of the Scott-Ritchey Research Center and the American College of Veterinary Internal Medicine (ACVIM) Foundation allowed this project to flourish in a way that would not have been possible otherwise. This funding paid for the RNA deep-sequencing provided through a partnership with Hudson-Alpha that is the cornerstone of this dissertation. Additionally, the Auburn University College of Veterinary Medicine provided resources and a stipend through the combined residency-graduate program that allowed me freedom from the pressure for my lab to support my salary through extramural funding. Furthermore, my friends, colleagues and fellow house officers at AUCVM are too numerous to mention individually, and all left an indelible impression on my time here.

Dr. Pedro Diniz at Western University deserves special acknowledgment as my first research mentor. He took me on as a naïve and unskilled veterinary student and shaped the future researcher I would become. Dr. Diniz instilled in me a rigorous work ethic, strong benchtop technical skills, and taught me the value of determination, resourcefulness, and striving to get as close to perfection as possible, as well as the sheer joy in scientific discovery.

I especially want to thank my parents, Dennis and Jane, for always pushing me to work hard and do my best, and being proud of everything I've ever done in life. My brother Ryan has been a confidante and friend throughout the challenges of my professional career as a veterinarian, pathologist, and scientist. Finally, I owe the deepest gratitude to my amazing wife, Dr. Lenore Bacek. She provided constant support and encouragement throughout the ups and downs of graduate school. There were more than a few moments where the way forward looked hopeless and I considered leaving my

studies, but her unwavering love and steadfast belief in me sustained me through these moments of doubt and despair. Without her, this dissertation would have been left unfinished.

Dedication

My research and doctoral dissertation are dedicated to the memory of my late aunt Roxanne Hocko, who lost her fight against breast and ovarian cancer ten years ago. Despite the grueling doldrums of her treatment, she was always full of laughter, optimism, and wisdom. Roxanne was a bold and free-spirited person who touched the lives of everyone around her, especially mine, and was instrumental in encouraging my pursuit of a non-traditional career in science and writing. Breast cancer treatment continues to advance leaps and bounds based on the incremental research findings of thousands of scientists, and my hope is that I contributed one small piece to the puzzle of diagnosing and treating breast cancer in women like Roxanne and our canine companions alike.

Table of Contents

List of Tables

List of Figures

List of Abbreviations

3’/5’-UTR	3 or 5-prime Untranslated Region(s) of mRNA
ACVP	American College of Veterinary Pathology
AFIP	Armed Forces Institute of Pathology
ASO	Antisense oligonucleotide
BC	Breast Cancer (Human)
CDK	Cyclin Dependent Kinase
CI	Confidence Interval
CMEC	Canine Mammary Epithelial Cell
CMT	Canine Mammary Tumor
CNV	Copy Number Variation
CpG (Island)	Methylated regions of adjacent cytosine and guanosine residues
CNV	Copy Number Variation
Cq	Quantification Cycles (qPCR)
DapB	Dihydrodipicolinate reductase (bacterial gene)
dPCR	Digital (droplet) Polymerase Chain Reaction
DEPC	Diethyl pyrocarbonate
DLS	Dynamic Light Scattering
ER/ESR1	Estrogen Receptor (1α)
EGFR/ErbB	Epidermal growth factor receptor

eIF4E	Eukaryotic Translation Initiation Factor 4E
EMT	Epithelial-to-Mesenchymal Transition
EVs	Extracellular Vesicles
FFPE	Formalin-Fixed Paraffin Embedded (tissue)
HDAC	Histone Deacetylase
HF1-5	Healthy Female (subjects in Chapters 3 and 4)
H3K9Ac	Acetylation of Histone 3 at Lysine residue 9
H3K4Me2	Dimethylation of Histone 3 at Lysine residue 4
HS1-5	Healthy Spayed (subjects in Chapters 3 and 4)
IACUC	Institutional Animal Care and Use Committee
IHC	Immunohistochemistry
ISH	In Situ Hybridization
MC1-10	Mammary Carcinoma (subjects in Chapters 3 and 4)
MET	Mesenchymal-to-Epithelial Transition
mRNA	Messenger RNA
miRNA	microRNA
MVBs	Multivesicular Bodies
ncRNA	non-coding RNA
OE/OHE	Ovariectomy / Ovariohysterectomy
PCA	Principal Component Analysis
PCR	Polymerase Chain Reaction
Pol II/III	(RNA) Polymerase II / III
Poly(A)	Polyadenylation / Polyadenylated

PBS	Phosphate Buffered Saline
PPIB	Peptidyl-prolyl cis-trans isomerase B
PR	Progesterone Receptor
PTEN	Phosphatase and tensin homolog
qRT-PCR	Quantiative Reverse-Transcription Polymerase Chain Reaction
RISC	RNA-Induced Silencing Complex
RNAse	Ribonuclease
RNAseq	RNA (deep) sequencing
RPM	Reads per Million
SE	Standard Error
snoRNA	Small nucleolar RNA
TEM	Transmission Electron Microscopy
TNM	Tumor, Node, Metastasis Classification of Malignant Tumors
UNG	Uracil-DNA N-glycosylase
WHO	World Health Organization
WSAVA	World Small Animal Veterinary Association

Chapter 1: Literature Review

Section 1.1. Canine Mammary Tumors: Epidemiology, Classification, and Molecular Pathogenesis.

1.1.1. Epidemiology and Risk Factors

Canine mammary tumors (CMT) are the most common tumor in intact female dogs, comprising at least half of all neoplasms in this demographic (Sorenmo et al., 2013). In a large research colony of Beagles, 476/672 (71%) of females were diagnosed with one or more CMT (included benign and malignant tumors) (Benjamin et al., 1999). The exact prevalence of CMT varies widely between studies based on geographic location, age and breed of study population, and methodology (i.e. data pulled from pet insurance claims versus tumor databases or hospital medical records). Additionally, CMTs have a broad range of clinical behavior, with approximately half being benign and half being malignant (Perez Alenza et al., 2000). Survey data of intact female dogs in northern California found an incidence of 257.7 mammary carcinomas per 100,000 (Dorn et al., 1968). Mammary tumors were the most frequent tumor in female dogs according to a large Italian tumor registry, with malignant CMTs having an incidence of 476 per 100,000 dog years at risk (Baioni et al., 2017). An epidemiologic survey of insured dogs in Sweden found the incidence of CMT ranged from 111-154 per 10,000 dog years at risk based on longitudinal cohorts (Egenvall et al., 2005). The overall mortality rate ranges from 4.5% to 6% for malignant CMT (Egenvall et al., 2005; Benjamin et al., 1999).

The two greatest risk factors for CMT are age and degree and duration of exposure to estrogen (and to a lesser extent progesterone) (Sorenmo et al., 2013). As with

the vast majority of cancers in human and veterinary oncology, older canine patients are at higher risk for CMT because they have more time to be exposed to hormone cycles and environmental triggers of mutations (Schneider, 1970). The average age for developing CMT in one Norwegian cohort was 7.8-8.8 years, depending on breed (Moe, 2001). In one large cohort of 80,000 insured Swedish dogs, the incidence of CMT increased exponentially from 1% at six years old to 6% at eight years old, then nearly doubling again to 13% at ten years of age (Egenvall et al., 2005).

Physiologic concentrations of estrogen and progesterone contribute to normal mammary gland development during sexual maturation (Lamote et al., 2004). These sex hormones can also lead to mammary hyperplasia and carcinogenesis in both women and dogs, whether endogenous from the ovaries or exogenously administered (such as progestins given to stop estrus behavior in dogs) (Queiroga et al., 2011; Block et al., 1975). As would be expected for this hormonal dependence, ovariectomy (OE) or ovariohysterectomy (OHE) has a preventive effect on the development canine mammary tumors (CMT) (Schneider et al., 1969; Dorn et al., 1968). According to one of these seminal studies, females receiving OE/OHE before their first estrus cycle have an approximate lifetime risk of developing CMT of ~0.5%, whereas the risk increases when performed after each additional estrus cycle until a lifetime risk of ≥25% when OE/OHE is completed after the third estrus cycle (Schneider et al., 1969). It should be noted that a recent systematic review considered the Schneider et al (1969) study and many of the others (that were 30-40 years old) establishing the decreased risk of CMT with early OE/OHE to be flawed, and the quality of evidence weaker than previously acknowledged (Beauvais et al., 2012). However strong the evidence, there is clearly some link between

hormonal exposure and CMT development, and the debate about reproductive surgery in dogs will continue to rage on because it is complex and impacted as much by the question of cancer reduction as by social mores and public safety concerns.

Another major risk factor for BC and CMT is shared by many cancers: obesity. While the mechanisms for the obesity-cancer link are numerous and incompletely understood, there is epidemiologic evidence in both human and veterinary medicine to support it. Women with a BMI >25 have a 1.3-1.5-fold higher risk of BC than women with BMI ≤24 (Calle & Kaaks, 2004). Likewise, dogs that were obese at one year of age were reported to be significantly more likely to develop CMT than those who were in lean body condition at a young age (Perez Alenza et al., 1998). Some of the hypotheses to explain the link include dysregulated aromatase expression, insulin resistance and excess levels of insulin/IGF-1, increased oxidative stress, and excess acute phase inflammatory cytokines like IL-1, TNF-α, and COX-2 (Bhardwaj et al., 2019). Obesity may also increase circulating estrogen concentrations by down-regulating sex hormone chaperone proteins, which can increase risk for BC in women (Tymchuk et al., 2000; Hankinson et al., 1998).

There does appear to be a breed-associated risk for CMT in dogs that mirrors ethnic susceptibility to BC (such as the overrepresentation of African-American women in overall BC incidence and mortality (DeSantis et al., 2019)). Pure-bred dogs, including Boxers, Cocker Spaniels, Dobermans, German Shepherd dogs, English Springer Spaniels, and others seem to develop CMT at higher rates than other breeds and mixed-breed dogs (Egenvall et al., 2005; Moe, 2001; Dorn et al.,, 1968). Some of this may be an artifact of breed popularity and thus statistical overrepresentation, but some breed relationships do

suggest genetic links. English Springer Spaniels with BRCA1/2 mutations have a nearly four-fold rate of developing CMT and may represent a model to BRCA-related hereditary breast cancer in women (Rivera et al., 2009). However, such mutations appear to only account for a minority of cases in the overall dog population, as such mutations are likely to have been removed from the breeding pool by selective pressure.

1.1.2. Translational Relevance

The use of dogs as models of human carcinogenesis has a number of advantages over cell culture systems or mouse models. Cell culture systems lack the heterogeneity of complex three-dimensional tumors, do not typically allow studying stromal interactions, lack an immune system, and cannot replicate whole-animal drug pharmaokinetics (Masters, 2002; Johnson et al., 2001). Other issues with cell line instability, mislabeling or cross-contamination can lead to confounding study results (MacLeod et al, 1999). Laboratory rodent studies can remedy some of these deficiencies intrinsic to a simple *in vitro* system, but many of these mouse and rat strains are highly inbred, also lack intact immune systems (such as athymic nude mice), and may yield results that don't translate to human oncology (Schuh, 2004). In addition, the very small size and blood volume of rodents creates issues with repeated laboratory testing and tissue sampling (Poitout-Belissent et al., 2016). Dogs, however, are genetically diverse (and have a well-annotated genome), have intact immune systems, frequently share an environment (and thus some cancer risk factors) with humans, and have a larger size that facilitates serial blood and tissue collection (Khanna et al., 2006; Vail & McEwen, 2000).

More specifically to mammary neoplasia, human breast cancer and spontaneous CMT share similar epidemiologic features and common links at the molecular level with similar mutations in genes such as PI3K, KRAS, WNT-beta, ER-alpha, PTEN and p53 (Pinho et al 2012; Schneider, 1970). A number of other mutations contribute to CMT development. Loss of tumor suppressor genes that repair DNA and/or induce apoptosis in irreparably damaged cells are particularly important for mammary neoplasia. CMT lesions can have frequent Copy Number Variations (CNV), including loss of critical tumor suppressor PTEN and gain of Myc loci (Borge et al., 2015). As previously mentioned, BRCA1/2 mutations contribute to hereditary breast cancer in women and familial risk for CMT in English Springer Spaniel dogs (Mahdavi et al., 2019; Rivera et al., 2009). SNPs in RAD51 have been associated with risk of CMT development (Canadas et al., 2018). Activating mutations in proto-oncogenes such as c-Met and STK11 are associated with mammary carcinoma in dogs (Chen et al., 2018; Canadas et al., 2018).

A number of prognostic factors are relevant in human medicine, including clinical stage, histologic grade, proliferation index, molecular subtype (estrogen receptor, progesterone receptor, and HER-2 status), and the presence or absence of metastatic disease (Sochor et al 2014; Redig et al 2013). Similar features—especially tumor size, grade, and stage—have been shown to be prognostic in canine patients with mammary neoplasia (see section 1.1.3), however there is considerably less research on the impact of hormone receptor status in this population (Sorenmo et al 2013; Chang et al 2005).

These clinical, epidemiologic, and genetic similarities make the use of canine mammary tumor cells and patients as a translational research model for human breast cancer appealing.

1.1.3. CMT Classification Systems

The gold standard for CMT diagnosis and subtyping, like most tumors in veterinary oncology, is tissue biopsy and histopathology. The histologic and molecular classification of human breast cancer and CMT in dogs is complex and has undergone frequent revision over the past few decades, including one in 1974 by the World Health Organization (WHO), another in 1999 through the combined efforts of the WHO and the Armed Forces Institute of Pathology (AFIP), and finally, an international consensus classification based on 2011 updates to the WHO human breast cancer parameters that was endorsed by the World Small Animal Veterinary Association (WSAVA) and the American College of Veterinary Pathologists (ACVP) (Hampe et al., 1974; Misdorp et al., 1999; Goldschmidt et al Vet Pathol 2011). The 2011 ACVP/WSAVA system provides numerous criteria for substratification into many individual tumor subtypes, but in essence the system tries to separate benign from malignant lesions and identify the tissue of origin (epithelial, glandular versus myoepithelial, basal, mesenchymal, etc). The surgical pathology criteria of malignancy are based on histologic growth pattern, cellular and nuclear pleomorphism, mitotic activity, necrosis, invasion into local tissue and vasculature, and regional or distant metastasis (Goldschmidt et al., 2011).

CMT can also be diagnosed on cytology, but the diagnostic accuracy of discriminating benign from malignant lesions is questionable in various published studies with many false positives and negatives owing to complex tissue architecture, benign lesions with significant atypia, cytologically well-differentiated lesions that behave aggressively, and frequent concurrent inflammation and necrosis (Simon et al., 2009; Cassali et al., 2007). Thus, mammary cytology should be interpreted cautiously and remains most useful for confirming metastatic lesions in patients with previously diagnosed CMT.

Once a histopathologic determination of malignancy has been reached, mammary carcinomas can be sub-stratified based on the architectural structures these lesions form including carcinoma in situ (in which the malignant neoplasm has not yet breached through adjacent basement membranes or vessels), simple carcinomas (such as tubular, tubulopapillary, and cystic-papillary), solid carcinoma, micropapillary invasive carcinoma, comedocarcinoma, anaplastic carcinoma, a malignant tumor that develops in an area of a benign adenoma or mixed mammary tumor, complex carcinoma (contains benign myoepithelium), carcinoma and malignant myoepithelioma (both elements are malignant), malignant mixed carcinoma, ductal carcinoma, intraductal papillary carcinoma, and carcinosarcoma (Goldschmidt et al., 2011). There are exception subtypes of epithelial malignancies including squamous cell and adenosquamous carcinomas, among others. It bears mentioning that the commonly used term “inflammatory (mammary) carcinoma” is not a specific histologic entity, but a clinical label based on finding rapid spread through lymphatics with prominent edema; this unique form of CMT has an aggressive disease course and a grave prognosis. There is evidence that complex

carcinomas resulted in better outcomes than simple carcinomas, and within simple carcinoma the prognosis from best to worst appears to be: Simple carcinomas in situ, simple tubulopapillary carcinomas, simple solid carcinomas, and lastly, simple anaplastic carcinomas (Pena et al., 2012).

While determination of benign versus malignant CMT and histologic subtyping are critically important, further prognostication of mammary carcinomas requires tumor grading and staging. The primary grading system for CMT is a modification of the human breast cancer Nottingham Prognostic Index, aka the Elston and Ellis score (Pena et al., 2012). The Pena grading system evaluates degree of tubule formation (a marker of differentiation), nuclear atypia, and mitotic index. These scores are summed and used to generate a grade from I to III (with I being the lowest and III being the highest). This grading system was evaluated prospectively in 68 dogs with malignant CMT and found that grading was statistically significantly associated with stage, metastasis, and shortened survival (Pena et al., 2013).

In addition to grading, staging of CMT employs the human "TNM" system, whereby tumors without evidence of metastasis are classified based on size: <3 cm are Stage I, 3-5 cm are Stage II, and >5 cm without metastasis are Stage III. Patients with local lymph node metastasis only are classified as Stage IV, and any patient with distant metastases are Stage V. Generally, patients with lower stage disease are more likely to be cured with mastectomy alone than require systemic therapy, although this grading system cannot be applied to patients with mammary sarcomas or inflammatory mammary carcinoma (Sorenmo et al., 2013).

1.1.4. Molecular Pathogenesis

Human breast pathology still incorporates elements of these anatomic classifications, but due to overlapping biological behavior, attempts were made to combine anatomy with molecular biology to better determine prognosis and response to therapy. One of the foundations of this new classification system was that the primary malignant cell in the vast majority of breast cancers was either a luminal cell or a basal/myoepithelial cell, and that these would likely express distinct cytokeratin and hormone receptor profiles. Beginning in 2000 (Perou et al.) and 2001 (Sorlie et al.), a series of breast cancer tissue RNA microarray expression studies confirmed that myriad different breast cancer samples could be clustered into one of only a few molecular subtypes based on RNA expression. These are Luminal A (Estrogen Receptor and/or Progesterone Receptor positive, HER-2 negative), Luminal B (same as Luminal A, but with HER-2 overexpression), basal-like (no expression for ER, PR, and HER-2, aka "triple negative"), and HER-2/Ne/ErbB-2 overexpressing without expression of ER or PR (aka "HER-2+ breast cancer") (Table 1). Extended phenotypes evaluating Epidermal Growth Factor Receptor (EGFR), ErbB-3, and ErbB-4 have been evaluated, but are less routinely used. Thus far, there has been limited adoption of the extended molecular phenotype classification in veterinary medicine, although one study classified patient-derived CMT cell lines according to these parameters using qPCR (Kabir et al., 2017).

Table 1: Molecular classification of BC/CMT based on hormone receptor expression. For Luminal A and B tumors, at least *one* of the hormone receptors ER and PR *must* be positive. ER and PR can also be simultaneously expressed in Luminal A/B tumors.

Molecular Subtype	**Estrogen Receptor (ER)**	**Progesterone Receptor (PR)**	**HER-2/Neu**
Luminal A	+ or -	+ or -	-
Luminal B	+ or -	+ or -	+
HER-2+	-	-	+
Triple-negative/basal-like	-	-	-

The estrogen and progesterone receptors ER/PR differ from the EGFR (ErbB-1) and HER-2 (ErbB-2) receptors in both cellular localization and mechanism of action. Briefly, both the ER and PR are classified as "nuclear steroid receptors" and are found within the cytoplasm (Girgert, et al., 2019). Their respective lipid-soluble hormone ligands (such as 17 beta-estradiol, aka E2 for ER) must first pass through the cell plasma membrane to interact with their target receptor (Siersbæk et al., 2018). The ER/PR binds its appropriate target, becomes phosphorylated and dimerizes, then enters the nucleus, where the complex induces transcription of downstream gene elements, including positive cell cycle regulators such as Cyclin D2 and CDK4/6 the (Siersbæk et al., 2018; Grimm et al., 2016). There are also non-canonical effects of the ER and PR receptors

mediated through PI3K/Akt and MAPK cytosolic signaling pathways, Src kinase activation, and others that are still being elucidated (Girgert, et al., 2019). Finally, estrogens may also have cellular effects through interaction with the G-protein coupled estrogen receptor (GPER/ GPR30) (Hsu et al., 2019).

Initially, natural hormone levels facilitate mammary tumor development and carcinogenesis. Over time, CMTs may become independent of hormone signaling. Several studies have demonstrated this fact. Nieto et al. (2000) evaluated 89 CMT lesions for Estrogen Receptor 1α (ER) expression and found that ER expression was negatively correlated with grade, stage, size, metastasis, and positively correlated with survival. Chang et al. (2009) evaluated 113 mammary gland lesions for ER/PR expression. All benign tumors were PR+ while 23/24 were ER+. In contrast, only ~72% of malignant tumors were PR+ and ~50% were ER+. CMT lesions with positive ER and/or PR status were more likely to be low grade, low stage, and patients with malignant CMTs positive for both ER and PR had significantly prolonged survival times. PR+ positivity was an independently significant positive prognostic variable, while ER+ alone was not.

In contrast to ER/PR expression, HER-2 does not have a ligand and is often over-expressed in human breast cancer, allowing constitutive signaling to drive growth and proliferation (Cho et al., 2003). Studies in veterinary medicine have found less of a clear association between HER-2 expression, tumor aggressiveness, and prognosis (Pena et al., 2013). EGFR expression studies are even fewer than HER-2 in CMT, and there is no consensus on the role expression plays in CMT.

Section 1.2. Exosomes in Canine and Human Cancer.

1.2.1. Formation and Secretion of Exosomes

Cells can actively and passively shed a number of subcellular particles or extracellular vesicles (EVs), including apoptotic bodies, exosomes, and microvesicles. These EVs can overlap in size, leading to some authors using the terms interchangeably (and creating confusion in the literature). However, these EVs do vary in surface antigen profiles and mechanism of formation and secretion.

Exosomes are vesicles derived from multivesicular bodies (MVBs) and late endosomes in the cytoplasm and can be secreted (exocytosis) by the parent cell as well as taken up by recipient cells via receptor-mediated endocytosis (Wu et al., 2017; Simon & Raposo, 2009). Exosomes are not a homogeneous particle, rather they can vary in size, morphology and antigen expression between cell culture and serum, incubation time, and parent cell lineage (Aguilera-Rojas et al., 2018).

Exosomes range in size from 40-150 nm in size (Zha et al., 2017; Melo et al., 2014). Common surface antigens in most papers that have characterized exosomes/extracellular vesicles/MVBs include endosomal tetraspanin proteins such as Alix, Tsg101, CD9, CD63, and CD81 (Thery et al., 2002). These extracellular vesicles contain a cargo of miRNA and other ncRNA, mRNA, and proteins/peptides.

In contrast, microvesicles bud directly from the plasma membrane, vary in size from 50-1,000 nm, and express cytoplasmic antigens rather than proteins originating from MVBs/endosomes (Zha et al., 2017). Apoptotic bodies are the largest of these EVs; while they can be as small as 50 nm, they are more commonly in the range of 1-5 µm

(Zha et al., 2017; Wu et al., 2017). These cellular fragments are sloughed from cells undergoing programmed death and express phosphatidylserine, the so-called "find-me, eat me" signal that triggers macrophage clearance (Baxter et al., 2019).

The formation and secretion of exosomes is controlled by a number of factors in the cell and tissue microenvironment. In general, cellular stressors increase release of exosomes. Acidosis, hypoxia, and induction of tumor suppressor p53 all lead to higher exosome production (King et al., 2012; Parolini et al,. 2009; Yu et al., 2006). For some tissues, specific stimulatory ligands such as Epidermal Growth Factor (EGF) may also induce exosome production and release (Ciravolo et al., 2011).

1.2.2. Isolation and Analysis of EVs

There are a number of different ways to isolate EVs from conditioned media *in vitro* and biofluids *in vivo*. One of the most traditional methods is ultracentrifugation. As most EVs are extremely small in size, they have a very low density and require speeds of 100,000 x g or more for several hours (Thery, 2006). An alternative to ultracentrifugation uses commercially available kits with high-density solutions (usually polyeythlene glycol (PEG)-based) to precipitate exosomes at a lower speed. Head-to-head comparison of multiple of these proprietary commercial exosome precipitation kits suggests significant differences in exosome yield, composition, and quality between each, highlighting the importance of carefully analyzing the materials & methods of studies when interpreting or attempting to replicate findings (Macias et al., 2019). Both ultracentrifugation and precipitation kits may result in contamination with various proteins and non-specific

debris (Zhang et al., 2019). Size-based filtration techniques may allow for a purer recovery of EVs, and can separate exosomes from other EVs and apoptotic bodies, though may also result in some EV loss (Woo et al., 2017). EVs can also be concentrated and analyzed by high-throughput methods such as flow cytometry or Magnetic-activated cell sorting (MACS) (Koliha et al., 2016; Pospichalova et al., 2015)

Because of the subtle differences in size and molecular cargo between these EVs, it is important to analyze these particles by multiple methods to properly characterize them. Numerous techniques, including electron microscopy (both scanning and transmission), immunogold-labeling electron microscopy, western blot, dynamic light scattering (DLS), nanotracking analysis (NTA), atomic force spectroscopy, and more novel techniques are described every year (Gurunathan et al., 2019). On Transmission Electron Microscopy (TEM), these particles on EM are typically round and have a characteristic "cup-shaped" morphology with negative staining (i.e. uranyl acetate) (Thery et al., 2006). DLS and NTA analyze particle sized based on the Brownian motion of the structures in the solvent, and vary whether it is light scatter (DLS) and image-analysis (NTA) used for calculations (Gurunathan et al., 2019).

As the nascent field of EV/exosome biology evolves, expert opinion on minimum requirements for defining extracellular vesicle studies recommends assaying particle size and morphology by at least two distinct methods (Lötvall et al., 2014). Exosomal tetraspanin proteins such as CD9, CD63, and CD81 should be assessed by western blot, flow cytometry, proteomics, or a combination of approaches (Lötvall et al., 2014). Finally, downstream functional analysis confirms the identity and utility of the various EVs isolated (Lötvall et al., 2014).

Once a population of exosomes has been isolated and characterized, they are suitable for downstream applications, such as profiling their mRNA and miRNA by PCR and/or RNAseq. Proper preservation of exosomes is critical, as their size and molecular cargo are sensitive to temperature, handling, and length of storage (Lee et al., 2016). Isolated exosomes should either be used immediately for analysis/experiments, or split into aliquots, stored at -80°C, and thawed once each (Lee et al., 2016).

1.2.3. Exosomes in Cancer

There is compelling evidence that the exosomes secreted by cancer cells are not inert cellular byproducts, but rather are functional and biologically relevant. Exosomes are shed into plasma and serum of human patients with breast cancer, ovarian cancer, and pancreatic adenocarcinoma (Gonzalez-Villasana et al., 2019; Ciravolo et al., 201; Taylor et al., 2008; He et al., 2014). In some patient populations, the absolute number of exosomes increases linearly with tumor stage (Taylor et al., 2008). One study found that the concentration and molecular content of exosomes correlated with the cancer cachexia phenotype in pancreatic adenocarcinoma patients (He et al., 2014).

For breast cancer specifically, the "triple-negative" breast cancer line Hs578T was shown to secrete high levels of CD63+/Tsg101+ exosomes, and the transfer of exosome-rich conditioned media to less aggressive breast cancer cell lines increased the proliferation rate and invasiveness of the "recipient" cells (O'Brien et al., 2013). HER-2+ breast cancer cells secrete exosomes in vitro and into patient sera that can bind to and

reduce the efficacy of the anti-Her-2/neu monoclonal anti-body trastuzumab (Herceptin) (Ciravolo et al., 2011).

Breast cancer cell exosomes contain pre-miRNA and Dicer, and generate mature miRNA when cultured independent of parent cells (Melo et al., 2014). Exosomal miRNA is shielded from RNAse activity, which may facilitate them circulating through peripheral blood and having effects on distant tissue targets (Cheng L et al., 2014). A number of breast cancer studies indicate that exosomal miRNA drive changes in cell behavior (Santos et al., 2016). Le et al. (2014) found that human and mouse breast cancer cell lines secreted exosomes enriched in miR-200a/b/c, and that transfer of these exosomes to naïve cells induced the EMT and promoted a metastatic phenotype. Exosomes from MDA-MB-231 breast cancer cells were enriched in miR-10b, and incubating normal mammary cells with those exosomes increased pre-malignant changes by regulating genes involved in the EMT such as KL4 and of HOXD10 (Singh et al., 2014).

Section 1.3. microRNA as Cancer Biomarkers.

1.3.1. microRNA Biogenesis and Evolution

As discussed above, exosomes contain numerous biologically active molecules, including microRNA. miRNA are ancient regulatory non-coding RNA molecules shared throughout Eukaryota, from plants to nematodes to mammals (Berezikov, 2011). In the early 1990s to 2000, multiple research groups discovered novel short non-coding RNA molecules lin-14 and let-7 that regulated the sequence of developmental events in *Caenorhabditis elegans* larvae (Lee et al., 1993; Reinhart et al., 2000). While lin-14

appeared to be unique to *C. elegans*, subsequent research found that the let-7 nucleotide sequence was conserved across species as diverse as the fruit fly *Drosophila melanogaster*, zebrafish *Danio rerio* and *Homo sapiens*, suggesting primitive evolutionary origins and importance (Pasquinelli et al., 2000). Interestingly, it is worth noting that while a few miRNA-like molecules have been found in yeast and fungi, many of those species lack key proteins such as Argonaute and Dicer (Chen et al., 2014).

In addition to the ancient and conserved nature of some miRNA, the number of validated miRNA genes appears to increase with organism complexity throughout the Bilaterian phylogenetic tree, which implies these molecules play a role in directing advanced tissue structures (Grimson et al., 2008). Some of the earliest known miRNA conserved across species include miR-100, miR-125 and miR-375, and these appear to regulate primordial functions such as digestive tube development, among other functions (Christodoulou et al., 2010). Finally, the fact that miRNA biogenesis enzyme Dicer knockout mutations in mice are embryonic lethal reinforces the powerful role miRNA have in organism development and homeostasis (Bernstein et al., 2003).

The advent of next-generation sequencing techniques has allowed researchers to identify both known and novel miRNA and compare the distribution across species over evolutionary time. The number of known miRNA is a continually moving target as new studies are published that cause the number to be revised, but as of this writing, the number of miRNA genes in humans is approximately 2,000 (Hammond, 2015). The latest number of canine miRNA include 720 well-annotated loci and 91 novel miRNA that await verification (Penso-Dolfin et al., 2016). Though the number of known miRNA genes is continually expanding through deep-sequencing, not all of these sequences have

been validated as real miRNA, and many of the predicted target genes have not been functionally validated in an experimental setting (Lee et al., 2015).

Mature miRNA originate as long, non-coding RNA transcription products of RNA Polymerase II (less frequently RNA Pol III) in the nucleus called primary microRNA or pri-miRNA that may be hundreds of nucleotides to over 2,000 bases in length, and have 5' caps and poly(A) tails (Bartel, 2004; Williams, 2008; Berezikov, 2011). As illustrated in Figure 1, an RNAse called Drosha works with its partner DGCR8 (aka Pasha) to form the microprocessor complex and edit the unwieldy pri-miRNA to a smaller 60-70 nucleotide precursor microRNA (pre-miRNA) by cleaving near the stem loop that ultimately becomes one strand of the final miRNA molecule (Bartel, 2004). The pre-miRNA leaves the nucleus through an active GTPase channel called Exportin-5 (Figure 1) (Lund et al, 2004). Once in the cytoplasm, another enzyme with RNAse III activity called Dicer (that also functions to generate siRNA and in defense against viral RNA) trims the pre-miRNA to a double-stranded 18-23 nt mature miRNA by cutting near the 3' overhang left by Drosha (Figure 1) (Grishok et al., 2001).

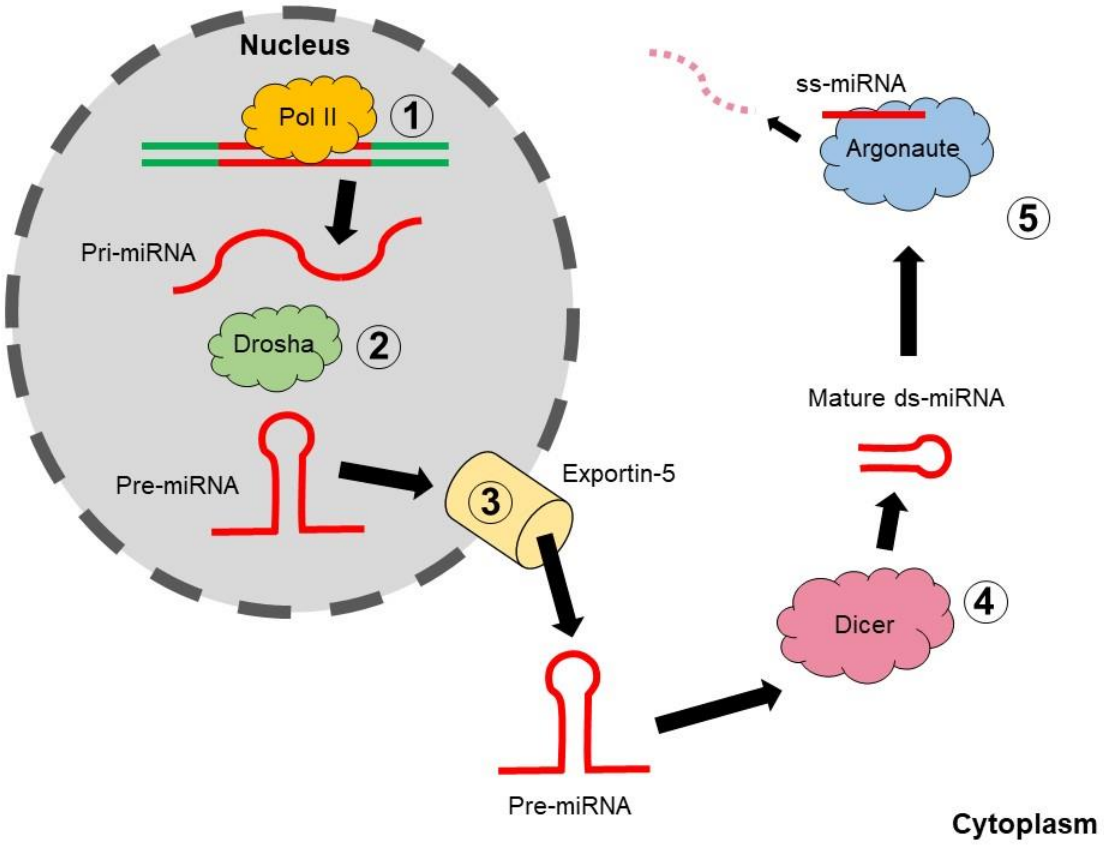

Figure 1. Schematic illustration of microRNA biogenesis. 1) RNA Polymerase II transcribes DNA sequences (green) that contain a long primary microRNA transcript (pri-miRNA; shown in red). 2) The RNAse III endonuclease Drosha trims the pri-miRNA to a shorter pre-miRNA that contains a stem-loop and flanking sequences. 3) The pre-miRNA exits the nucleus through Exportin-5. 4) A cytoplasmic RNAse, Dicer, cleaves the pre-miRNA to the final 18-22 nt double-stranded mature miRNA (ds-miRNA) sequence. 5) The mature miRNA binds with Argonaute and other proteins to form the microRNA-RNA-induced silencing complex (miRISC), one strand of the miRNA is released and degraded, while a single-strand of the miRNA (ss-miRNA) remains complexed to the miRISC that can down-regulate target mRNA.

Any DNA sequence that can be transcribed by RNA Pol II/III to transcripts of appropriate length and secondary structure capable of recognition by Drosha and Dicer has the potential to generate miRNA. Not surprisingly, one of the major sources of new miRNA in a given species' genome is miRNA loci duplication (Hertel et al., 2006). This can result in identical miRNA loci on different chromosomes, or when these sequences undergo subsequent mutation, they can result in related miRNA "families" with similar sequence that may regulate similar targets (Hertel et al., 2006). miRNA also frequently reside within intronic sequences that are normally spliced out during exon processing of mRNA (Rodriguez et al., 2004). These areas may be particularly ripe for evolution of miRNA as they are actively transcribed by the associated gene promoter yet under minimal sequence selection pressure (Campo-Paysaa et al., 2011). Non-intronic miRNA must develop their own promoters to be transcribed (Ozsolak et al., 2008). Up to half of human miRNA reside in introns, and these tend to be specific to *Homo sapiens* (Campo-Paysaa et al., 2011). miRNA may also be generated from insertion and mutation of transposon segments (Piriyapongsa et al., 2007). Finally, miRNA sequences can evolve spontaneously over time anywhere in the genome (Lu et al., 2008).

Interestingly, most miRNA in dogs are intergenic (497/720, 69%), whereas a minority (267/720, 37%) are located in introns (Penso-Dolfin et al., 2016). The few remaining miRNA are identified in the UTR or actual gene coding sequence (Penso-Dolfin et al., 2016). This could indicate that dogs have a smaller number of species-specific, recently-evolved miRNA than humans, or possibly that many intronic miRNA have yet to be documented in *Canis lupus familiaris*.

As described below in section 1.3.4, a number of miRNA are expressed at similar levels in the same tissues and disease states between women and intact female dogs. This makes sense as the high degree of sequence similarity between specific miRNA over eukaryotic taxa (often 100%) means a greater likelihood of matching results between pre-clinical models such as dogs with CMT and women with BC. Thus, miRNA have greater potential as translational biomarkers than less conserved gene sequences (such as human-specific BRCA1/2 mutations) or peptide/protein sequences (such as serum MUC-1 and Carcinoembryonic antigen (CEA) protein levels) (Gam, 2012).

1.3.2. miRNA Regulation of Gene Expression

miRNA do not code for peptides or proteins, yet they exert a powerful effect on tissue gene expression through (largely negative) post-transcriptional regulation of target mRNA (Stroynowska-Czerwinska et al., 2014). miRNA do not accomplish this alone, but through binding to multiple ribonucleoprotein partners to form the miRNA-RNA Induced Silencing Complex (miRISC) (Hammond et al., 2000). The miRISC is assembled primarily from the mature miRNA species binding to one of the Argonaute (Ago) family of proteins as well as several chaperones and co-activators, such as heatshock protein 90 (HSP90) and TRBP (Meister, 2013; Carthew & Sontheimer, 2009). When a mature miRNA is loaded into the miRISC it is double-stranded, but one of the two strands is broken down while the other remains bound and functional (Yang et al., 2013). Research suggests which strand is inactivated and released is stochastic, and may be irrelevant, as both the 5’ and 3’ strands are complementary sequences able to target regions of the 3’

Untranslated Region (UTR) of a given mRNA (Yang et al., 2013; Griffiths-Jones et al., 2011).

The miRISC is capable of regulating gene expression through several canonical and non-canonical mechanisms that either directly degrade the mRNA or interfere with ribosomal translation (Stroynowska-Czerwinska et al., 2014). Mature miRNA contain a "seed sequence" complementary to a 7 or 8 nucleotide motif in the 3' UTR of the target mRNA (or less commonly the 5' UTR or other transcript elements) through partial or complete Watson-Crick base-pairing (Iorio, 2012; Carthew & Sontheimer, 2009; Lewis et al., 2003). Nearly two-thirds of mammalian genes are predicted to have one or more miRNA binding sites, although prediction algorithms may overestimate the proportion of targets that are regulated at biologically relevant levels *in vivo* (Pinzón et al., 2017). Somewhat paradoxically, miRNA with *more* 3' UTR mRNA binding site matches may be *less* effective at repressing translation for any one of its target genes due to a dilution effect (Garcia et al., 2011). However, multiple adjacent miRNA binding sites in a 3' UTR may enhance the down-regulation of that mRNA (Sætrom et al., 2007).

The way in which a given miRNA prevents mRNA translation depends largely on how homologous the miRNA seed sequence is to its target mRNA(s) (Yates, 2013). A complete match between the miRNA seed sequence and 3' UTR mRNA sequence usually results in direct cleavage of the mRNA transcript by the miRISC complex (Zeng et al., 2003; Hutvagner & Zamore, 2002). This "slicing" mechanism may be the predominant pathway in plants (Jones-Rhoades et al., 2006).

On the other hand, a partial seed sequence match tends to impair translation of the mRNA through several processes (Iorio, 2012). An imperfect match between miRNA

seed sequence and 3' UTR site can trigger deadenylation by the miRISC (Wu et al., 2010; Wu et al., 2006). mRNA that have lost their poly(A) tails are inherently unstable and become degraded by cellular P-body organelles (Zheng et al., 2008). Another mechanism of translational repression is blocking initiation of translation by preventing eukaryotic initiation factor 4E (eIF4E) from guiding the mRNA 5'cap to the ribosome (Humphreys et al., 2005). Still other possibilities for miRNA repression exist, including the miRISC physically associating with polyribosomes and impairing translation (Nottrott et al., 2006).

1.3.3. microRNA Expression in Cancer

By the late 1990s, miRNA were well-known for their role guiding embryogenesis and development. However, in the early 2000s, researchers began to discover miRNA expression was altered in a variety of disease states, particularly cancer. One of the first studies to associate miRNA with a role in cancer found that almost 70% of B-cell chronic lymphocytic leukemia (CLL) cases had down-regulation or deletion or miR-15 and miR-16 (Calin et al., 2002). A follow-up study by the same group found that those two miRNA regulated the anti-apoptotic oncogene BCL2, which was over-expressed in the CLL patients with loss of miR-15 and miR-16 (Cimmino et al., 2005). Shortly thereafter, down-regulation of different miRNA, miR-143 and miR-145, was documented in colorectal cancer tissues (Michael et al., 2003). A large scale study of 20 cancers found that miRNA profiles clustered hierarchically and could classify tumor types more robustly then their associated mRNA profiles (Lu et al., 2005). A few years after the initial studies showing that loss of miRNA expression was common in cancer it was

observed that miR-34a, which is lost in many tumors, could be *induced* by tumor suppressor p53, and actually mediated many of its effects, including apoptosis (Chang et al., 2007). This suggested a complex, reciprocal interplay between oncogenes and tumor suppressor genes and their associated miRNA.

But why are miRNA dysregulated at all in cancer? The simple answer is that cancer is fundamentally a genetic disease whereby the progressive acquisition of selectively advantageous mutations allows neoplastic cells to outcompete normal host cells for survival (Kinzler & Vogelstein, 1996; Hahn et al., 1999). The stepwise process of neoplastic transformation confers a number of functional and structural changes to the tumor cell genome that leads to excessive oncogene expression and/or loss of tumor suppressor genes, causing perpetual cell division, the ability to survive cytostatic signals and apoptosis, and acquisition of the ability to spread to distant tissues (Hanahan & Weinberg, 2011). In fact, one of the emerging "hallmarks" of cancer is genomic instability (Hanahan & Weinberg, 2011). Because pri-miRNA arise from RNA Pol II/III transcription products, any local or global forces that increase or decrease gene expression can impact miRNA expression (Suzuki et al., 2013).

Physical changes to the genome directly affect gene expression. Cancer cells are well-known to have copy number alterations, which may result from chromosomal rearrangement and gene fusion, deletion of small or large loci (Korkola & Gray, 2010). Recurrent breast cancer mutations in women include the tumor suppressors BRCA1/2, p53, p16/INK4A, and CHEK1, and the oncogene PIK3CA (Pinho et al., 2012) Some of these genes, such as p53, directly alter downstream miRNA expression, such as induction of miR-34a (He et al., 2007).

Besides physical changes to DNA sequences, epigenetic changes such as CpG island hypermethylation, and histone modifications (i.e. acetylation or methylation at specific lysine resides) can have profound effects on gene expression by altering chromatin states that facilitate or preclude access by the cell's transcription machinery (Croce, 2009). Methylated CpG DNA generally prevents normal transcription, functionally silencing that region. One study used methyl-CpG and chromatin immunoprecipitation followed by microarray analysis to screen for methylation sensitive miRNA promoters, and found 128 miRNA had altered methylation (Baer et al, 2012). Interestingly, there were roughly twice as many hypomethylated promoters as hypermethylated; loss of methylation would lead to overexpression, while increased CpG methylation would lead to down-regulation (Baer et al, 2012). This hypothesis was elegantly validated when a variety of human cancer cell lines were treated *in vitro* with a de-methylating agent and 17 miRNA increased by more than three-fold compared to controls (Saito et al., 2006). One of these miRNA in particular, miR-127, resided in a hypermethylated CpG island and was shown to have tumor suppressor type effects by down-regulating the oncogene BCL6 (Saito et al., 2006).

Histone deacetylases (HDAC) can remove acetyl-groups from histone proteins to induce heterochromatin and decrease gene transcription in those areas (Patra et al., 2019). HDAC1-3 are up-regulated in chronic lymphocytic leukemia, resulting in a decrease in histone acetylation H3K9Ac/H3K4me2, and subsequent loss of expression of miR-15, miR-16, and miR-29b (Sampath et al., 2012). These miRNA expression changes induced by histone deacetylation are reversible with HDAC-inhibitors, validating this pathway (Sampath et al., 2012; Saito et al., 2006). These studies raise the possibility that some

tumors (i.e. CLL) use DNA methylation and histone deacetylation to epigenetically silence a tumor suppressive miRNA, and are reminiscent of the link between loss of miR-15/miR-16 and gain of BCL2 expression in CLL described earlier (Saito et al., 2006; Cimmino et al., 2005; Calin et al., 2002).

Because miRNA impair translation of a given message, they tend to have the opposite effect of their target gene when considering gain of function or loss of function changes. In the specific context of cancer, a miRNA that normally suppresses an oncogene such as c-Myc essentially functions as a "tumor suppressor miRNA" (sometimes termed a ts-miR), and a loss of function change (through deletion, hypermethylation, etc) would promote neoplastic transformation. On the other hand, a miRNA that reduced expression of a tumor suppressor such as p53 would be considered an "onco-miRNA," and gain of function through promoter hypomethylation, loci duplication, or generalized increase in euchromatin, would lead to neoplasia.

miRNA can also have more complex phenotypic effects that defy simple classification as a ts-miRNA or an oncomiR. The Epithelial-to-Mesenchymal Transition (EMT)—and its reverse phenomenon, the Mesenchymal-to-Epithelial Transition (MET)—is an important process whereby epithelial cells lose their adhesion to each other and their basement membranes by downregulating E-cadherin and other tight junction proteins, becoming phenotypically more like connective tissue mesenchymal cells (Musavi Shenas et al., 2018). The EMT is fundamental to tissue/organ development during embryogenesis, as well as wound healing and fibrotic diseases. However, the EMT has a darker side: It confers traits such as increased motility and invasiveness that enable cancer cells to spread throughout the body (Hanahan & Weinberg, 2011). Many

miRNA, such as miR-129-5p, miR-148a, and miR-200b/c, indirectly regulate EMT-inducers such as TGF-β/SMAD signaling to promote metastasis (Zare et al., 2017). Others, like the miR-1, miR-34, and miR-200 families, directly regulate transcription factors that mediate EMT effects, such as ZEB1/2, Snail, Slug, and Twist1 (Musavi Shenas et al., 2018; Rhodes et al., 2015; Agostini & Knight, 2014).

The EMT may also impart a number of other traits to cancer cells that make them resistant to treatment, including chemoresistance, immunosuppression, metabolic shifts, and induction of stem-like cells (Lu & Kang, 2019; van Staalduinen et al., 2018).

1.3.4. The Role of miRNA in Breast Cancer and CMT

miR-19b is overexpressed in both breast cancer tumor samples and cell lines, correlates with higher stage and metastasis, and was shown to regulate the pro-proliferative PI3K/AKT pathway (Li et al., 2018). miR-19a also appears to correlate with Estrogen Receptor 1-α (ESR1α) gene expression (aka ER+), as it is expressed at higher levels in ER- MDA-MB-231 breast cancer cells than in less aggressive and ER+ MCF7 cells (Wu et al., 2015). miR-19a and miR-181a have been shown to mediate chemotherapy resistance in human MCF7 and TNBC breast cancer cells by down-regulating tumor suppressors PTEN and BAX (respectively) (Liang et al., 2011; Niu et al., 2016). Over-expression of miR-29b also inhibits PTEN and promotes invasive metastatic behavior in MDA-MB-231 breast cancer cells (Wang et al., 2011).

Serum/plasma microRNA have recently been shown to add diagnostic and prognostic value to the work-up of women with breast cancer. miR-200c levels in blood had high diagnostic sensitivity for breast cancer patients, and increasing expression was associated with shortened progression-free interval and risk of death (Antolin et al, 2015). Serum miR-19a, miR-15, and miR-181a have been shown to be proxy markers for global patient tumor burden and allow treatment monitoring (Sochor et al., 2014). In one study, a panel of five of circulating microRNA (miR-21, miR-23b, miR-190, miR-200b, miR-200c) were associated with poor clinical outcome (Papadaki et al., 2018). In another study, miR-331 and miR-195 were found to accurately discriminate patients with metastatic breast cancer versus those with only local disease (McAnena et al., 2019). Serum miR-19a and miR-205 were increased in patients with Luminal A breast cancer that was chemoresistant to epirubicin and paclitaxel (Li et al., 2014). Some miRNA show different trends between tumor tissue and serum levels in women with breast cancer, but others appear more stably up-regulated in both, including miR-18a, miR-19a, miR-20a, miR-30a, miR-103b, miR-126, miR-192, miR-1287 (Guo et al., 2013).

While there are far fewer studies of microRNA in CMT, those that exist demonstrate similar trends, with the ability to discriminate benign from malignant types, as well as identifying correlations between histologic and molecular subtypes. One study of miRNA expression in canine mammary cancer versus normal mammary tissue found significantly increased miR-21 and miR-29b in mammary carcinoma versus non-cancerous tissue, and miR-181b was specifically upregulated in the tubulopapillary carcinoma subtype (Boggs et al., 2008). qRT-PCR microarray analysis of multiple distinct CMT cell lines found a number of miRNA are consistently dysregulated in CMT

cells including miR-18a, miR-19a, miR-29b, miR-34c, and miR-181a (Kabir et al., 2017; Kabir et al., 2015).

However, the real promise of miRNA research goes beyond mere diagnosis and into providing functional information and mechanistic insight into the drivers of malignancy. *In silico* analysis predicts that a number of miRs dysregulated in CMT also directly control ESR1a, Progesterone Receptor (PR), PTEN, and other pathways. Kabir et al (2015) previously showed that CMT cells can over-express miR-141 to escape apoptosis from tumor suppressor p16/INK4A.

Section 1.4. Project Justification

Clearly, miRNA play an important role in development and progression of a variety of human cancers, including breast cancer and CMT. A deeper insight into the molecular regulatory pathways of CMT could allow a "personalized medicine" approach to prevention, detection, and treatment of dogs with mammary cancer. miRNA can also be inhibited by RNA antisense oligonucleotides (ASO), raising the possibility that key miRNA may represent therapeutic targets.

Furthermore, exosomal and circulating miRNA represent promising minimally invasive diagnostic biomarkers in human oncology that may provide prognostic information about molecular subtypes, such as hormone receptor status, grade, and presence of occult metastasis. With detailed molecular and prognostic knowledge based on serum miRNA levels, veterinarians and owners could make a more informed choice about how aggressive to be with surgery and systemic chemotherapy.

While a few published studies have profiled miRNA in CMT cell lines and tumor tissue, much remains unknown: Do CMT cells secrete exosomes? If so, do their exosomes contain miRNA, and how does that profile compare to those of the parent cells? Can circulating serum miRNA distinguish dogs with CMT from controls? What are the predicted targets of this exosomal and circulating miRNA network? Do these miRNA correlate with any pathologic or clinical parameters? Within tumor tissues, which cells specifically express these miRNA?

This project seeks to answer these questions in the hope that they play a small part in advancing diagnostics for CMT and breast cancer, improve understanding of disease pathogenesis, and some day distantly may represent promising new therapeutic targets.

Chapter 2: Malignant canine mammary epithelial cells shed exosomes containing differentially expressed microRNA that regulate oncogenic networks

Section 2.1. Introduction

Canine mammary tumors (CMT) represent the most frequent tumor in hormonally intact (non-ovariohysterectomizd) female dogs, and CMT have similar incidence and comparable distribution of malignant potential to breast cancer (BC) in women (Rasotto et al., 2017; Sorenmo et al., 2013; Merlo et al., 2008). Some forms of CMT may represent a useful translational model for human BC as it shares risk factors such as age, hormone exposure, and obesity, although there are some differences in subtypes that limit direct comparison (Lim et al., 2015; Egenvall et al., 2005; Perez Alenza et al., 2000). Furthermore, CMT and BC share similar genetic alterations, including downregulation of tumor suppressors p16/INK4A, PTEN, BRCA1, and p53, as well as upregulation of oncogenes KRAS, PI3K/AKT, and MAPK (Lutful Kabir et al., 2015; Pinho et al., 2012; Uva et al., 2009). Recently, CMT has been shown to be classifiable into human molecular subtypes luminal A, luminal B, HER-2, and triple-negative/basal-like according to estrogen receptor alpha (ESR1α), progesterone receptor, and HER-2/ErbB-2 expression by immunohistochemistry in patient tumor tissue and by qRT-PCR in a cohort of well-characterized cell lines (Lutful Kabir et al., 2017; Shinoda et al., 2014). In addition, CMT, like human BC, shows a negative correlation between estrogen hormone receptor ESR1 expression and increasing tumor grade (Shinoda et al., 2014; Chang et al., 2009).

Currently, as in women with BC, definitive classification of benign versus malignant CMT, as well as tumor grading, requires histopathology. This is problematic because collecting those samples requires invasive surgery. Current less invasive alternatives such as fine-needle aspirate cytology vary from 67.5-81% accuracy (Simon et al., 2009; Cassali et al., 2007). Another significant prognostic factor for CMT is advanced stage, with shortened survival times for dogs with large tumors (>3 cm) and/or metastasis, highlighting the importance of early detection (Chang et al., 2005; Philibert et al., 2003). An accurate, minimally invasive, biomarker for CMT diagnosis and malignant potential could improve outcomes through intervention at a lower stage of disease.

One such potential class of biomarker is microRNAs (miRNAs, miRs), a type of small (18-22 nucleotides), non-coding RNA that are highly conserved across species and play crucial roles in the negative, post-transcriptional regulation of gene expression in both health and disease (Yates, 2013). Each miRNA recognizes numerous gene targets through hybridization with a complementary "seed sequence" in the 3' untranslated region (UTR) of mRNA resulting in either degradation of the transcript or inhibition of ribosomal translation (Iorio & Croce, 2012). Dysregulation of miRNAs is particularly prevalent in cancer, where genetic instability of tumors leads to altered miRNA expression profiles that promote oncogenesis (Suzuki et al., 2013). Numerous studies demonstrate miRNA are differentially expressed in women with BC in tissue, exosomes, and serum/plasma, (Wu et al., 2015; Antolín et al., 2015; Li et al., 2014; Sochor et al., 2014).

Multiple miRNAs are already known to be altered in CMT, though the data are complex and sometimes conflicting, particularly depending on the RNA source (cells,

exosomes, tumor tissues, serum/plasma, etc), microRNA profiling technique(s), and normalizing strategies. One early study of miRNA expression between CMT and normal mammary gland tissue using a small set of individual qRT-PCR assays found miR-29b and miR-21 were significantly upregulated in neoplastic versus normal tissue, while miR-181b and let-7f were specifically upregulated in tubulopapillary carcinoma (Boggs et al., 2008). In another, miR-141 specifically was demonstrated to be upregulated in several well-characterized CMT cell-lines and experimentally validated to down-regulate tumor suppressor p16/INK4a (Lutful Kabir et al., 2015). This same study also identified a number of other differentially expressed miRs by qRT-PCR microarray in CMT that were also altered in human BC, including miR-21, miR-155, miR-9, miR-34a, miR-143/145, and miR-31 (Lutful Kabir et al., 2015). A separate research group established a CMT line (labeled "SNP") from a primary patient mammary tumor and compared its miRNA expression to normal mammary tissue through miRNA hybridization arrays and found the microRNAs with the greatest increase and decrease were miR-143 and miR-138a, respectively (Osaki et al., 2016). A separate study of various primary and metastatic canine mammary tumor tissues using qRT-PCR found up-regulated miR-210 in neoplastic versus normal tissue, higher miR-21 in malignant mammary carcinomas (but not benign tumors), and that the metastatic tumors had altered miR-29b, miR-101, mir-125a, miR-143 (von Deetzen et al., 2014). Another study evaluated primary versus metastatic mammary carcinomas using RNA hybridization arrays and qRT-PCR, and found a distinct signature of microRNA expression in metastatic canine mammary carcinoma, although the expression of these candidate metastasis markers were not statistically different in peripheral blood (Bulkowska et al., 2017). Finally, a recent study

evaluating circulating microRNA in blood by qRT-PCR for multiple different types of cancer found miR-214 and miR-126 were significantly up-regulated in serum from dogs with mammary carcinoma (along with numerous other tumor types) (Heishima et al., 2017). Of note, most of these studies performed no or limited *in silico* bioinformatics analysis for these miRNA, and only the study of miR-141 and p16/INK4a experimentally validated the annotated targets (Lutful Kabir et al., 2015).

miRNAs make particularly good biomarkers because they can be secreted in biofluids such as serum, urine and breast milk, and protected from endogenous RNases by packaging in exosomes and/or binding to proteins such as Argonaute (Yates, 2013; Iorio & Croce, 2012). Exosomes are 30-200 nm in diameter round vesicles with a lipid membrane, and are secreted by cellular organelles called multivesicular bodies. There is some evidence to indicate that exosomes are actively secreted by tumor cells to facilitate cell-to-cell communication to distant cells and tissues (Taylor et al., 2008). These tumor exosomes and their cargo of miRs, mRNA, and proteins may also modulate the behavior of local stromal and immune cells (Penfornis et al., 2016). One such study provided data that tumor exosomes derived from human patients with lung and pancreatic carcinomas were able to induce myotube apoptosis through miR-21 and TLR7 signaling, recapitulating the cancer cachexia phenotype in an in vitro model (He et al., 2013).

The aims of the current study were to isolate and characterize exosomes shed by normal canine mammary epithelial cells (CMEC) and CMT cells in vitro, analyze the miRNA profile of these exosomes, and to perform *in silico* bioinformatic annotation of this miRNA signature. We hypothesized that both CMEC and CMT cells grown in serum-free media would shed exosome-like microvesicles containing abundant miRNAs,

and that the miRNA signature of the CMT extracellular vesicles would be enriched in a subpopulation of miRs predicted to regulate important molecular targets in CMT.

Section 2.2. Materials and Methods

2.2.1. Cell culture

The following cell lines were used: Three normal canine mammary epithelial cell cultures independently derived from separate canine patients without mammary pathology (CMEC1, CMEC2, CMEC3), and five stable and highly transformed cell lines derived from canine patients with histopathology-confirmed mammary carcinoma including CMT12 (formerly CMT2), CMT27 (formerly CMT4) and CMT28 (formerly CMT5) as well as 2 more recently derived lines including CMT47 (derived from a mammary adenocarcinoma from a pure-bred Miniature Schnauzer) and CMT119 (derived from a mammary carcinoma from a Golden Retriever) (Lutful Kabir et al., 2017; Lutful Kabir et al., 2015). The CMT cells used are the product of our laboratory group in collaboration with Dr. Lauren Wolfe (retired). They were all derived/rescued from surplus biopsy specimens recovered following standard of care surgery of canine mammary cancer patients. Each biopsy specimen to be cultured was divided in two at the time of collection: one for epithelial cells to be sorted by flow cytometry and grown in culture, and one placed in formalin to be processed for routine histopathology and reviewed by a board-certified pathologist to identify the cell type and confirm malignancy. All CMT cell lines in this study were confirmed to be derived from mammary carcinoma/adenocarcinoma tumors on histopathology, but tissues were not further classified into mammary tumor histologic subtypes (i.e. simple, complex,

micropapillary, etc). All owners of such animals sign a general informed consent that notes that biopsy specimens recovered in this manner may be used for research. No IACUC approval is required for such specimens. All CMEC samples were recovered from normal geriatric female dogs in the breeding colony housed and managed under IACUC PRN 2015-2688. All such specimens were recovered post-mortem following euthanasia performed in the normal management of the colony. In no case were any of these animals euthanized for the current study. All cell lines are routinely analyzed using canine-specific RT-PCR assays for Canine Mammaglobin-A (unpublished data) to ensure the species source.

CMT and CMEC cells were grown in 75 cm^2 flasks in synthetic Xerum-free® media + DMEM media supplemented with 2X penicillin/streptomycin antibiotics at 37ºC until 70-80% confluence. Media from the first 24 hours of culture was discarded and conditioned media from the second 48 hours was harvested on day 3 of growth prior to trypsinization and subculture.

2.2.2. Exosome isolation

Exosomes and exosomal proteins were isolated by progressive centrifugation and ultracentrifugation. Briefly, 5-10 mL conditioned cell culture media were progressively centrifuged at 4°C at 300x g for 10 minutes, 2,000 x g for 10 minutes, and 10,000 x g for 30 minutes, each time discarding the pellet and retaining the supernatant, to remove cells and debris. The processed supernatants were then centrifuged at 100,000 x g at 4°C for 70 minutes, and the resulting supernatant was subjected to another cycle of centrifugation

at 100,000 x g at 4°C for 70 minutes. The final pellet was resuspended in 50 uL PBS (Thery et al., 2006).

2.2.3. Dynamic light scattering

The size distribution of vesicles in the cell-free conditioned media diluted 1:5 to 1:20 (depending on particle count rate) in 1x DEPC-treated PBS was measured by intensity-weighted dynamic light scattering using a Malvern ZetaSizer ZS90 (Malvern instruments, Ltd., Worcestershire, UK) according to the manufacturer's instructions.

2.2.4. Transmission electron microscopy

Cell-free conditioned media from both CMEC and CMT cells, prepared by progressive centrifugation and ultracentrifugation as previously described, was loaded onto copper-formvar grids treated with 1% Alcian blue (to increase hydrophobicity) and negatively stained with 1% uranyl acetate (Thery et al., 2006). Grids were loaded into a Zeiss EM10 transmission electron microscope (Carl Zeiss Microscopy, LLC, Thornwood, NY, USA) and imaged at 20,000x to 63,000x magnification with an accelerating voltage of 60 kV (2 second exposure).

2.2.5. Western blot

Protein from ultracentrifuge-precipitated exosomes was quantified by nanospectrophotometry and/or Qubit protein assay. Two micrograms of native exosomal protein from pooled CMEC and CMT samples was mixed with 4x Laemmli buffer heated at 95^{O}C for 15 minutes. Proteins were resolved by SDS-PAGE on 4-20% precast

polyacrylamide gels (Bio-Rad, Hercules, CA, USA) using the Precision Plus Protein Western C standards (Bio-Rad, Hercules, CA, USA) to determine the sizes of the bands, and then transferred to a nitrocellulose blotting membrane (LI-COR Biosciences, Lincoln, NE, USA). After electrophoresis, the fractions were electro-transferred to nitrocellulose membrane (Bio-Rad, Hercules, CA, USA) and blocked for 1 hour with Odyssey Blocking Buffer (LI-COR Biosciences, Lincoln, NE, USA). Membranes were incubated overnight at room temperature with 1:200 primary antibody CD9 Mouse-anti-Human (clone MM2/57, Bio-Rad AbD Serotec Inc, Hercules, CA, USA) in Odyssey Blocking Buffer (LI-COR Biosciences, Lincoln, NE, USA). Next the membranes were washed 3X for 10 minutes in 1X PBS in 0.1% Tween 20 (Sigma-Aldrich Corp., St. Louis, MO, USA). Next, secondary antibody IRDye Goat-anti-Mouse (LI-COR Biosciences, Lincoln, NE, USA) 1:10,000 dilution was incubated in Blocking Buffer (LI-COR Biosciences, Lincoln, NE, USA) for 1 hour at 4^{o}C. Membranes were washed 3 times at room temperature with 1X PBS in 0.1% Tween 20 for 10 minutes. Fluorescent bands were visualized with Odyssey Near-Infrared Western Blot detection system in Image Studio (LI-COR Biosciences, Lincoln, NE, USA).

2.2.6. RNA extraction & microRNA deep-sequencing

RNA was extracted from 5 mL of cell-free, serum-free conditioned media using the Norgen Biotek Urine/Cell Culture Exosomal RNA Isolation kit (Norgen Biotek, Thorold, ON, Canada) according to manufacturer instructions. After the lysis step, 10 pM final concentration synthetic miRVana cel-miR-39-3p mimic (Thermo Fisher Scientific, Waltham, MA, USA) was spiked into samples as an external control for technical

variation. Extracted RNA was stored at -80°C until being shipped on dry ice to the Genomic Services Laboratory at the Hudson Alpha Institute for Biotechnology. Small RNA libraries were prepared for sequencing from total RNA from each sample using a NEBNext Small RNA Library Prep Set for Illumina (New England BioLabs Inc., Ipswich, MA, USA) according to the manufacturer's protocol. Briefly, 3' adapters were ligated to total input RNA followed by hybridization of multiplex SR RT primers and ligation of multiplex 5' SR adapters. Reverse transcription (RT) was performed using ProtoScript II RT for 1 hour at 50°C. Immediately after the RT reaction, PCR amplification was performed for 15 cycles using LongAmp Taq 2X Master Mix. Illumina indexed primers were added to uniquely barcode each sample. Post-PCR material was purified using a QIAquick PCR purification kit (Qiagen Inc., Valencia, CA, USA). Post-PCR yield and concentration of the prepared libraries were assessed using a Qubit 2.0 Fluorometer (Invitrogen, Carlsbad, California, USA) and DNA 1000 chip on an Agilent 2100 Bioanalyzer (Applied Biosystems, Carlsbad, CA, USA), respectively. Size selection of small RNA was done using 3% dye free agarose gel cassettes on a Pippin Prep instrument (Sage Science Inc., Beverly, MA, USA). Post-size selection yield and concentration of the libraries were assessed using Qubit 2.0 Fluorometer and DNA High sensitivity chip on Agilent 2100 Bioanalyzer, respectively. Accurate quantification for sequencing applications was performed using the qPCR-based KAPA Biosystems Library Quantification kit (Kapa Biosystems, Inc., Woburn, MA, USA). Each library was diluted to a final concentration of 1.25 nM and pooled in equimolar ratios prior to clustering. Single End (SE) sequencing (50 bp) was performed to generate at least 15

million reads per sample on an Illumina HiSeq2500 sequencer (Illumina, Inc., San Diego, CA, USA).

Post processing of the sequencing reads from RNA-seq experiments from each sample was performed as per the Genomic Services Laboratory unique in-house pipeline. Briefly, quality control checks on raw sequence data from each sample was performed using FastQC (Babraham Bioinformatics, London, UK). Raw reads were imported on a commercial data analysis platform (AvadisNGS, Strand Scientifics, CA, USA). Adapter trimming was done to remove ligated adapter from 3' ends of the sequenced reads with only one mismatch allowed, poorly aligned 3' ends were also trimmed. Sequences shorter than 15 nucleotides length were excluded from further analysis. Trimmed reads with low qualities (base quality score less than 30, alignment score less than 95, mapping quality less than 40) were also removed. Filtered reads were then used to extract and count the small RNAs which were annotated using microRNAs from the miRBase release 20 database (http://www.mirbase.org/). Samples were subjected to quantification and active region quantification (AvadisNGS, Strand Scientifics, CA, USA). The quantification operation carries out measurement at both the gene level and at the active region level. Active region quantification considers only reads whose 5' end matches the 5' end of the mature miRNA annotation. Samples were then grouped by identifiers and the differential expression of each miRNA was calculated based on the fold change observed between different groups.

2.2.7. qRT-PCR and data analysis

RNAseq results were validated by stem-loop quantitative RT-PCR (qPCR) for selected miRNA targets (selection process discussed in detail below). cDNA was created for each miRNA with a unique TaqMan™ stem-loop primer (Thermo Fisher Scientific, Waltham, MA, USA) with 1 ng RNA input using the TaqMan™ MicroRNA Reverse Transcription Kit (Thermo Fisher Scientific, Waltham, MA, USA) according to manufacturer instructions. A 1 µL cDNA product from the RT reaction was used as input for the qPCR reaction with TaqMan Universal Master Mix II no UNG (Thermo Fisher Scientific, Waltham, MA, USA), a specific 20X TaqMan microRNA assay for each target (Thermo Fisher Scientific, Waltham, MA, USA) and run in a BioRad CFX96 thermocycler (Bio-Rad, Hercules, CA, USA) according to the manufacturer protocol. Internal reference target miR-16 and external spike-in cel-miR-39 were used as control genes for normalization. Cq data was normalized using the $^{2\text{-}\Delta\Delta Cq}$ Livak method and presented as both log10 relative quantity for individual samples and fold change for the CMT group relative to the CMEC group (Livak & Schmittgen, 2001). miRNA that did not amplify were assigned a Cq number of 40 to allow calculation of normalized Cq values. These qPCR validation experiments were performed in triplicate and results were averaged and presented as mean ± SD.

2.2.8. Selection of initial set of miRNAs

miRNAs of interest were selected from the set of differentially expressed genes. An initial set of 16 miRNAs were selected based on their expression profile and association with published studies in human and/or canine mammary neoplasia (cfa-miR-

18a, cfa-miR-19a, cfa-miR-29c, cfa-miR-31, cfa-miR-34c, cfa-miR-105a, cfa-miR-181a, cfa-miR-206, cfa-miR-215, cfa-miR-345, cfa-miR-371, cfa-miR-495, cfa-miR-504, cfa-miR-615, cfa-miR-676, cfa-miR-1841). These were used for downstream bioinformatics analysis to identify putative gene targets for which enriched gene ontology terms and enriched biological pathways were identified.

2.2.9. Gene target predictions

Target prediction for each miRNA was accomplished using the miRDB online resource and analysis platform (http://www.mirdb.org/). This tool was created in 2008 and was comprehensively updated recently when the complete set of miRNA sequences from the miR Base repository were downloaded along with the complete set of 3'UTR sequences contained in the NCBI RefSeq database. Furthermore, the miRDB target prediction algorithm, MirTarget, which was developed using support vector analysis of high throughput expression data, is capable of predicting conserved and non-conserved target genes via weighting target site conservation as a high priority, but not as an absolute requirement. miRDB scores predicted targets in a range from 50 to 100, with a higher score indicating a greater statistical confidence in the prediction. According to the FAQ on the miRDB website, "a predicted target with a score > 80 is most likely to be real." Subsequently, target gene prediction was performed and scores greater than 80 were considered as representing the most confident gene predictions (Wong & Wang, 2015). Gene targets for the complete set of 16 miRNAs were generated by selecting all gene targets having scores greater than 80 for each of the 16 miRNAs. The resulting set

of all gene targets was filtered to remove redundant gene targets (i.e. gene targets that were associated with two or more different miRNAs).

2.2.10. Gene ontology and KEGG pathway enrichment

The DAVID database for annotation, visualization and integrated discovery (version 6.8) was used to perform gene ontology enrichment analysis on sets of target genes using the gene symbol produced by the target prediction algorithm in miRDB. Canine gene symbols were uploaded into the DAVID database and the resulting sets of enriched gene ontology terms or KEGG pathways were identified (Dennis et al., 2003).

2.2.11. Statistical Analysis

qRT-PCR relative quantity data were assessed for normality by visual inspection and Shapiro-Wilk test. Non-directional, non-parametric Mann-Whitney statistical testing was performed based on data that were not normally distributed. $P < 0.05$ was considered statistically significant for both RNAseq and qRT-PCR expression comparisons between groups. The DAVID gene ontology software provides both raw and Benjamini-corrected p-values, and a crude threshold of $p < 0.06$ was selected to screen for potentially relevant pathways (Irizarry et al., 2016).

Section 2.3. Results

2.3.1. Characterization of extracellular vesicles

Ultrastructural evaluation of exosome-enriched supernatants using transmission electron microscopy confirmed the presence of variable numbers of irregularly round, occasionally cup-shaped vesicles ranging in size from approximately 60-120 nm in diameter (Figure 2). These vesicles occasionally formed variably-dense accumulations.

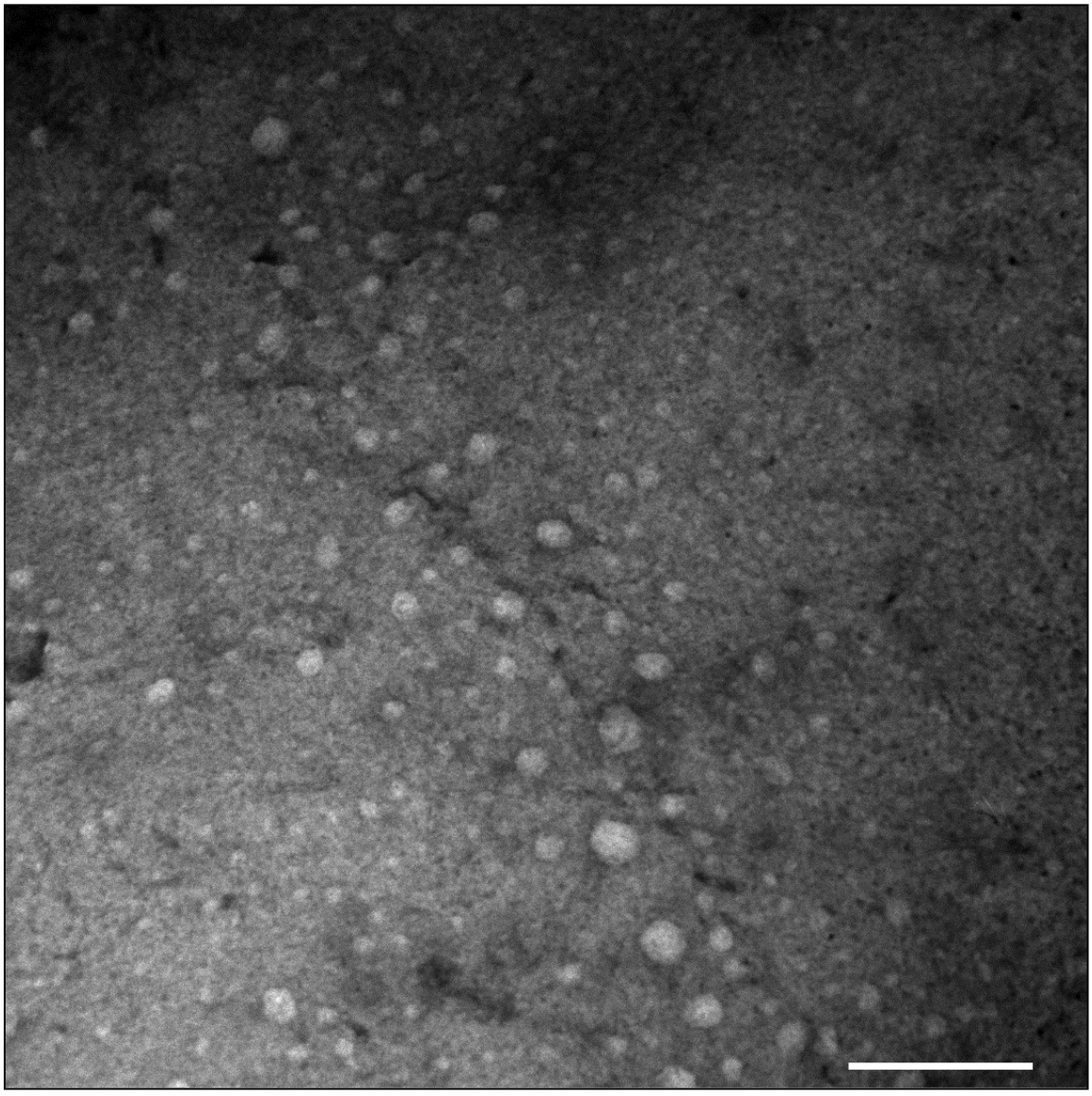

Figure 2. Transmission electron microscopy (TEM) of putative exosomes. Representative transmission electron micrograph (TEM) from ultracentrifuge-purified extracellular vesicles. Extracellular vesicles were irregularly round and varied widely in diameter from approximately 50-100 nm. Scale bar = 250 nm.

Dynamic light scattering of this cell-free fraction showed a broad distribution of particle sizes with an average diameter of approximately 150 to 200 nm (Figure 3). The average protein concentrations in these cell-free fractions was 0.13 to 0.6 µg/µL. Putative exosome marker CD9 was detected in cell-free media from both CMEC and CMT cell lines by Western blotting (Figure 4). Our findings were consistent with having isolated exosome-like extracellular vesicles.

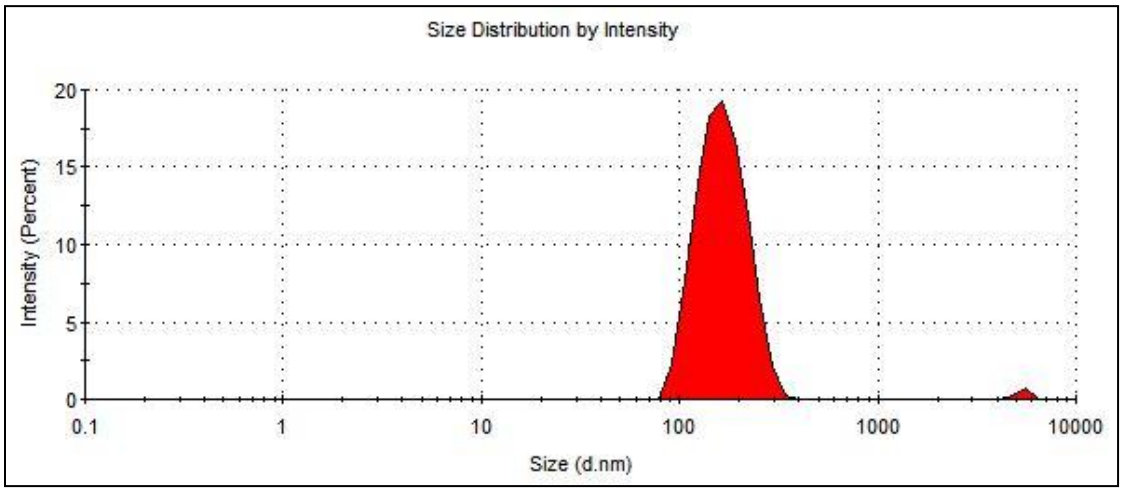

Figure 3. Dynamic light scattering curve for extracellular vesicle fractions. The mean intensity-weighted diameter of EVs varied from approximately 150-200 nm. The small peak between 1,000 and 10,000 nm likely represents large polydisperse aggregates of particles.

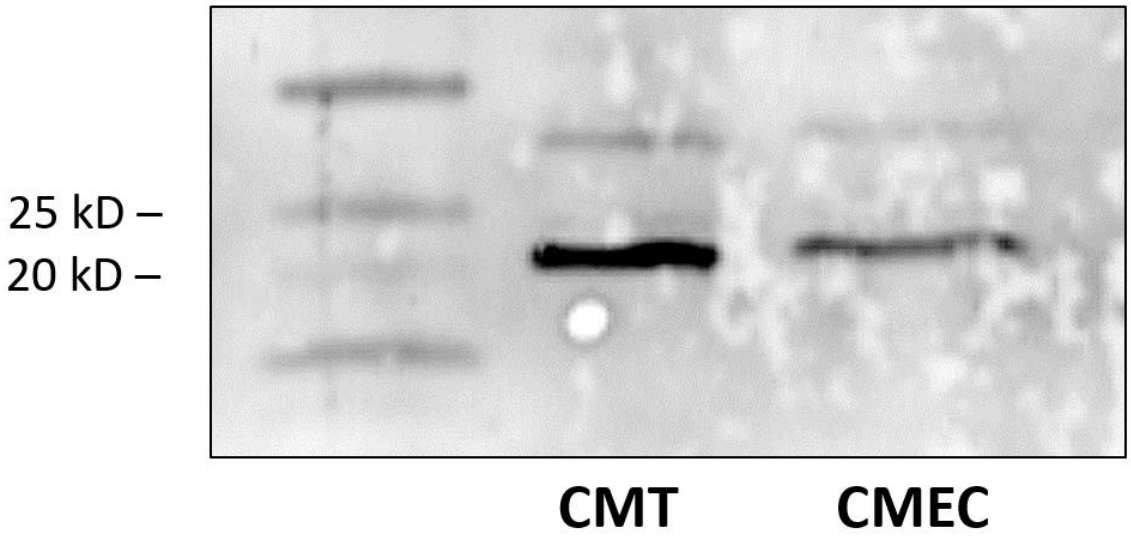

Figure 4. Western blot of CD9 protein. Western blot demonstrated both CMT and CMEC samples are positively immunoreactive for a protein approximately 20-25 kD in size. The CMT sample was more intensely positive despite the same total protein input, suggesting higher exosomal content in the CMT conditioned media.

2.3.2. microRNA profiling by small RNA deep-sequencing and qRT-PCR validation

The RNA bioanalyzer profiles were typical of exosomal samples, skewing heavily towards small RNA (~20-200 nucleotides), with minimal detection of rRNA (Figure 5). Three hundred thirty-eight unique miRs were detected in the cell-free RNA fractions from CMEC and CMT samples.

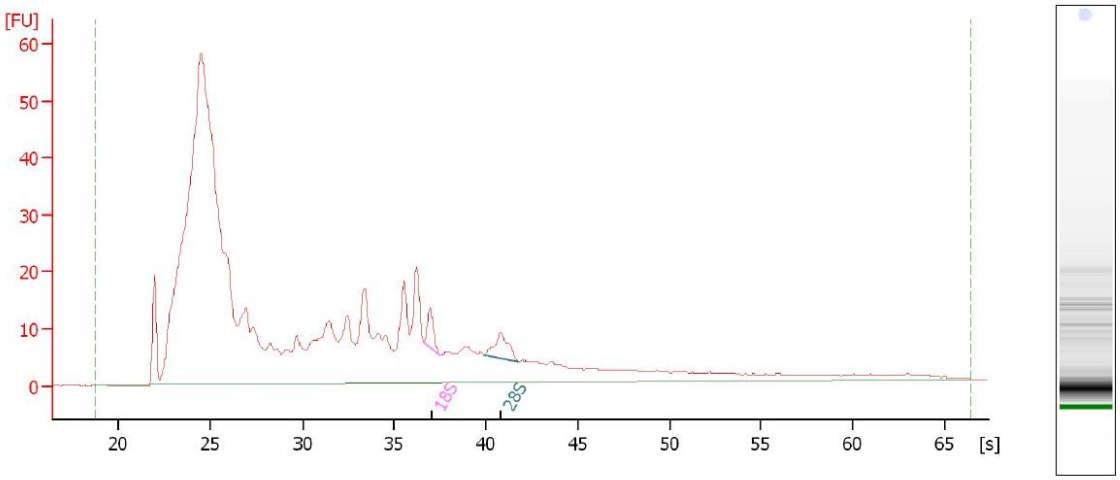

Figure 5. RNA bioanalyzer fluorogram from CMT cell-free conditioned media. A large proportion of the RNA is small in size (range likely to contain microRNAs). 18S and 28S markings denote location typical of rRNA peaks.

In a principal component analysis of the miRNA from all eight samples the CMEC and CMT samples clustered into two separate groups, although the CMT group had two significant outliers (Figure 6).

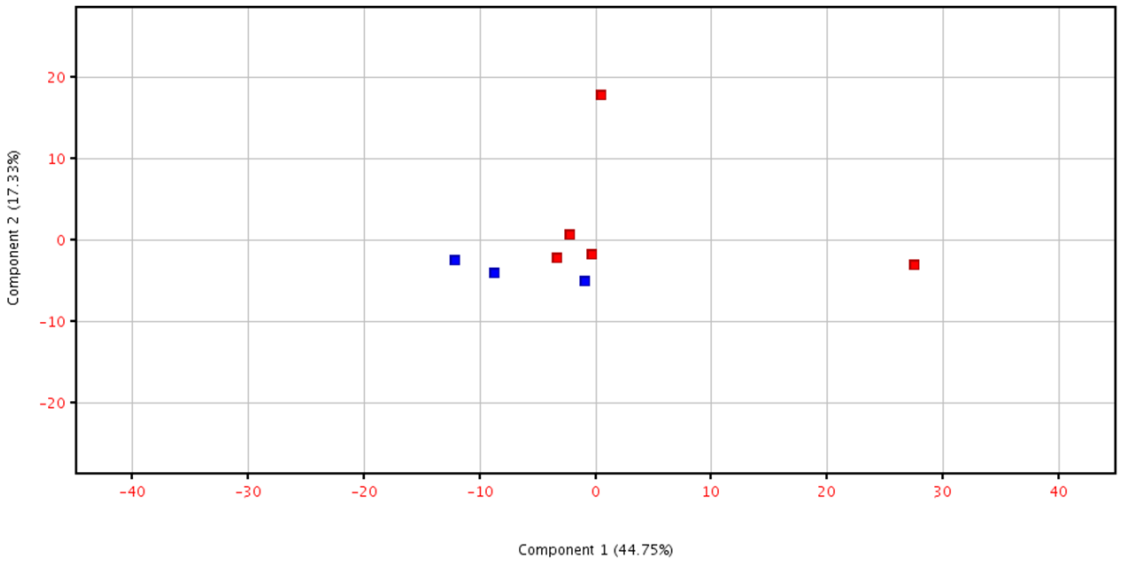

Figure 6. Principal Component Analysis (PCA) plot for exosomal microRNA. Distinct clustering of the of the microRNA by RNAseq was observed between CMT (red) and CMEC (blue) group biological replicates.

Volcano plot analysis illustrate that numerous miRs were significantly over- and under-expressed by CMT exosomes relative to CMEC (Figure 7). Using criteria of $p < 0.05$ and a fold-change $\geq \pm$ 1.5-fold change, there were 170 differentially expressed miRs between CMT and CMEC groups (Appendix 1). Removing isoform miRs from different chromosomal locations yielded 145 unique differentially expressed miRs, with 118 miRs upregulated and 27 miRs downregulated in CMT as compared to CMEC.

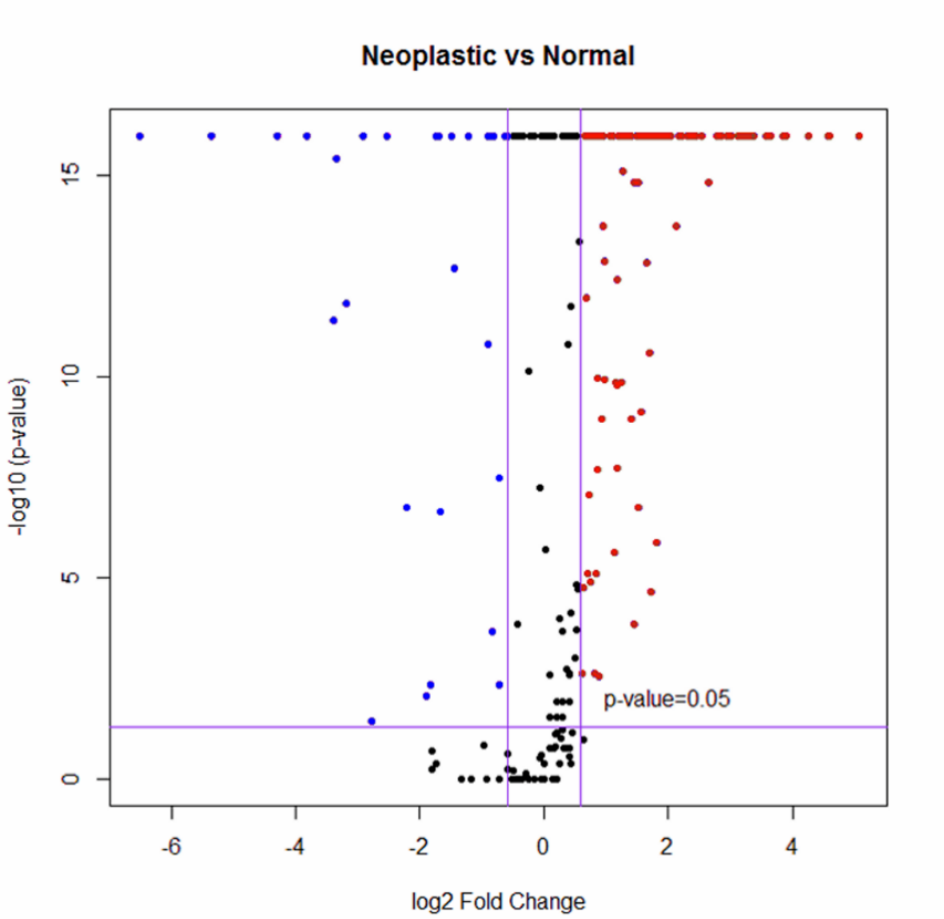

Figure 7. Differential exosomal miRNA expression volcano plot. This graph shows up-regulated and down-regulated miRs. miRNAs in the upper right and upper left quadrants were statistically different between CMT and CMEC groups ($p < 0.05$). miRs identified in red were >1.5-fold up-regulated in the CMT group relative to CMEC; miRs identified in blue were >1.5-fold down-regulated in the CMT group relative to CMEC.

Three of the significantly upregulated miRs (miR-18a, miR-19a, and miR-181a) were selected for qRT-PCR validation. The average relative quantities (log10 $2^{\wedge -\Delta Cq}$) for cfa-miR-18a, cfa-miR-19a, and cfa-miR-181a for CMEC and CMT groups were

significantly higher in the CMT group compared to CMEC (Figures 8A-C). Each of these three miRs showed very similar fold-change between CMT and CMEC for both small RNA deep-sequencing and qRT-PCR assays (Figure 9). Table 2 compares fold-change and p-values for RNAseq and qRT-PCR data.

A

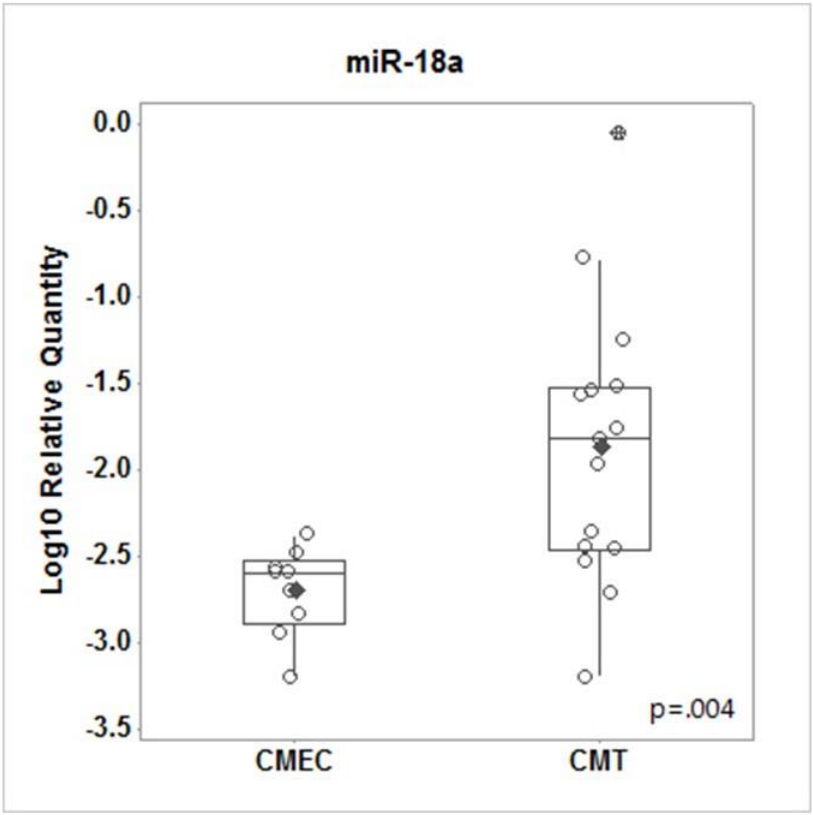

B

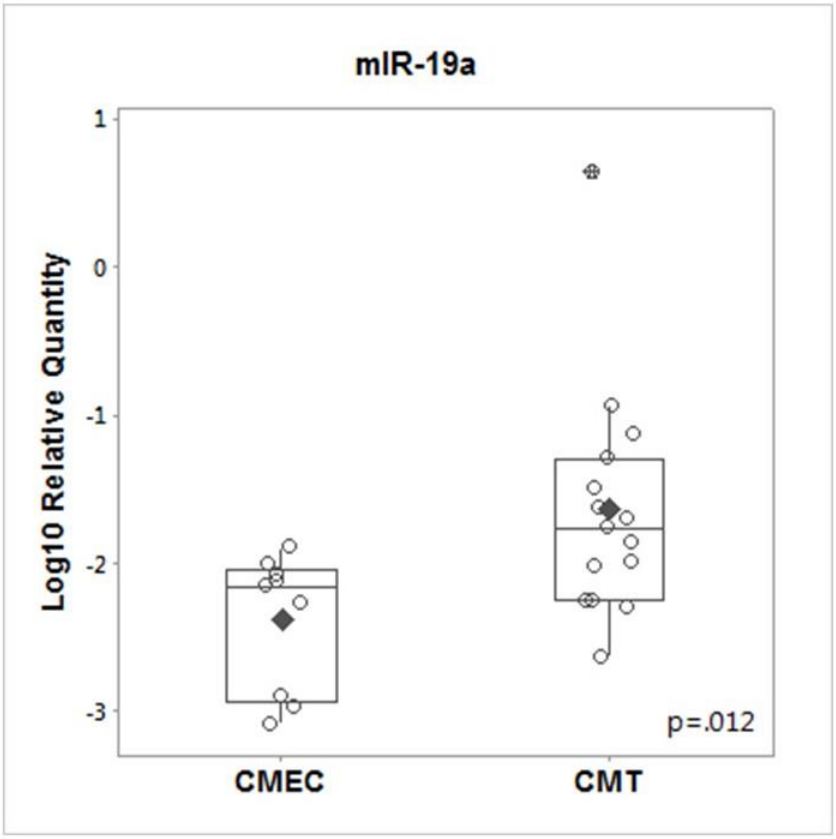

C

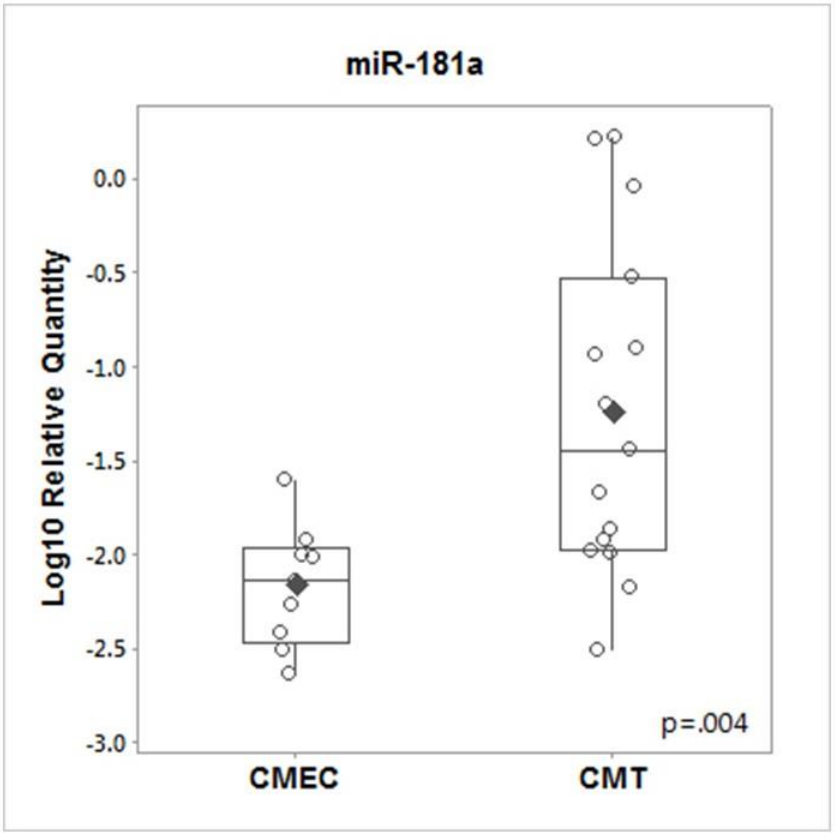

Figure 8. qRT-PCR validation of exosomal RNAseq data. A-C. Relative quantification (log10) for selected validation targets miR-18a (7A), miR-19a (7B), and miR-181a (7C). Relative quantification was calculated for each biological replicate according to the equation $2^{-\Delta Cq}$, with cel-miR-39 as spike-in exogenous control and miR-16 as an endogenous control; experiments were performed in triplicate from cell culture to RNA extraction, cDNA synthesis and qRT-PCR. Data were not normally distributed and compared by non-parametric, non-directional Mann-Whitney test. P <0.05 was considered statistically significant. The black horizontal line represents the group mean and the vertical "whiskers" represent ±1 SD.

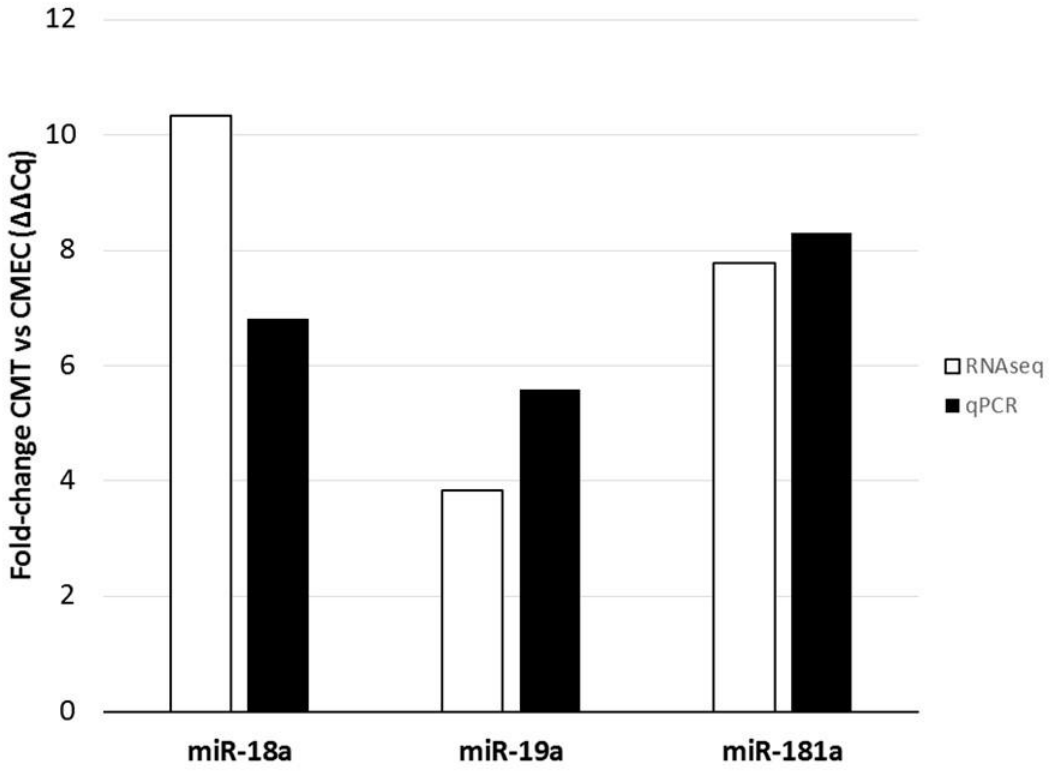

Figure 9. Comparison of fold-change between exosomal microRNA deep-sequencing and manual stem-loop qRT-PCR assays. Data were normalized using the 2-ΔΔCq method. The average group Cq for cfa-miR-16 (endogenous control) and cel-miR-39 (exogenous spike-in control) were used as housekeeping genes for normalization. White bars represent relative fold-change for RNAseq data, black bars represent fold-change for qRT-PCR (3 experimental replicates).

Table 2: Comparison of exosomal microRNA expression by RNAseq and qRT-PCR.

	RNAseq		**qRT-PCR**	
microRNA	**Fold-change**	**p-value**	**Fold-change**	**p-value**
miR-18a	10.34	0	6.82	0.004
miR-19a	3.84	0	5.58	0.012
miR-181a	7.70	0	8.30	0.004

2.3.3. In silico analysis of microRNA targets

A set of sixteen differentially expressed miRNAs from this data set were selected for *in silico* analysis of canine predicted miR targets (Figure 10). The number of predicted genes identified per miRNA ranged from 124 to 751 genes for total predictions and from 24 to 300 genes for predictions having a score greater than 80 (Table 3). To gain an appreciation for the types of biological processes associated with these 16 miRNAs, the complete set of gene targets for all 16 miRNAs was used for a gene ontology biological process enrichment analysis.

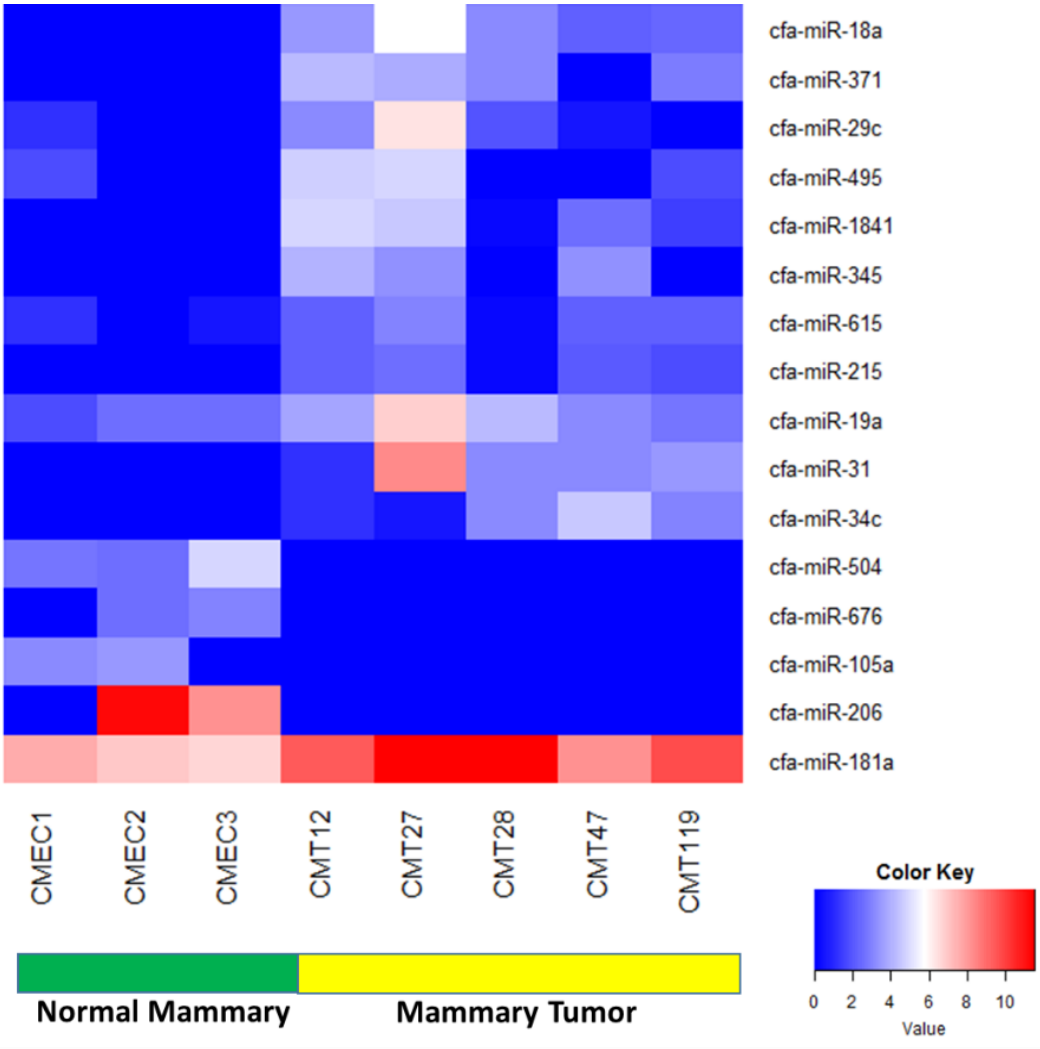

Figure 10. Supervised absolute expression heat map for sixteen canine miRNAs in CMEC vs. CMT exosomal RNA samples. Three biological replicates (CMEC1, CMEC2, and CMEC3) corresponding to normal mammary tissue exhibit relatively low levels of expression for the first eleven miRNAs while the last five miRNAs exhibit considerably higher levels of expression. The pattern is reversed in the mammary tumor samples (CMT12, CMT27, CMT28, CMT47, and CMT119) as visualized in the right side of the heat map. Because of the dichotomous pattern of expression across the control and mammary samples, these miRNAs may represent valuable candidates for clinically relevant biomarkers.

Table 3: Number of Predicted Gene Targets for selected miRNAs of biological interest.

miRNA	**Total Targets Predicted**	**Targets with Score > 80**
cfa-miR-18a	181	55
cfa-miR-19a	646	300
cfa-miR-29c	536	208
cfa-miR-31	359	98
cfa-miR-34c	420	154
cfa-miR-105a	362	105
cfa-miR-181a	694	274
cfa-miR-206	358	133
cfa-miR-215	124	24
cfa-miR-345	215	58
cfa-miR-371	550	164
cfa-miR-495	729	263
cfa-miR-504	176	43
cfa-miR-615	163	39
cfa-miR-676	552	182
cfa-miR-1841	751	219

The complete set of all 2,323 miRNA target genes with scores greater than 80 were selected. Following removal of redundant target genes in the list, we identified a set of 1,849 unique target genes. The filtered list was used in the DAVID database and, of

the 1,849 gene symbols uploaded, 1,819 were successfully mapped to canine genes using the DAVID gene list manager. In contrast, the gene list manager identified 1,737 of the 1,849 gene symbols as human genes.

2.3.4. Gene Ontology Enrichment Across All Gene Targets

A total of 145 gene ontology terms were identified as enriched, with 85 having p-values less than or equal to 0.06. Although we considered GO annotations with p-value < 0.06, we focused on those with p-value <0.05 (Table 4). A set of 34 enriched terms are also included (Table 4). These terms provide some insight into the cellular role of the 16 miRNAs.

Table 4: Enriched gene ontology (GO) biological process enriched terms associated with combined set of predicted target genes.

GO biological process term	**N**	**%**	**P-Value**	**Benjamini**
positive regulation of transcription from RNA polymerase II promoter	87	4.8	5.10E-05	1.60E-01
ubiquitin-dependent protein catabolic process	23	1.3	5.70E-04	6.30E-01
G1/S transition of mitotic cell cycle	13	0.7	8.50E-04	6.20E-01
positive regulation of glucose import in response to insulin stimulus	6	0.3	4.10E-03	8.70E-01
negative regulation of canonical Wnt signaling pathway	18	1	5.30E-03	9.00E-01
regulation of establishment of cell polarity	6	0.3	6.40E-03	9.10E-01
regulation of cell morphogenesis	7	0.4	7.30E-03	8.80E-01
protein autophosphorylation	22	1.2	7.70E-03	8.70E-01
vesicle fusion	12	0.7	7.90E-03	8.60E-01
negative regulation of apoptotic process	35	1.9	8.90E-03	8.70E-01
regulation of small GTPase mediated signal transduction	6	0.3	9.50E-03	8.70E-01
regulation of mRNA stability	6	0.3	9.50E-03	8.70E-01
TOR signaling	6	0.3	9.50E-03	8.70E-01
intrinsic apoptotic signaling pathway by p53 class mediator	7	0.4	9.90E-03	8.70E-01

negative regulation of extrinsic apoptotic signaling pathway	9	0.5	1.10E-02	8.60E-01
histone ubiquitination	5	0.3	1.10E-02	8.40E-01
neuronal stem cell population maintenance	7	0.4	1.30E-02	8.40E-01
chromatin remodeling	12	0.7	1.50E-02	8.60E-01
response to hypoxia	15	0.8	1.60E-02	8.70E-01
mRNA splice site selection	5	0.3	1.80E-02	8.70E-01
miRNA mediated inhibition of translation	5	0.3	1.80E-02	8.70E-01
regulation of gene expression	14	0.8	2.20E-02	8.80E-01
positive regulation of cell-substrate adhesion	8	0.4	2.80E-02	9.00E-01
histone H3-K9 trimethylation	3	0.2	3.30E-02	9.20E-01
histone H2A ubiquitination	3	0.2	3.30E-02	9.20E-01
polarized epithelial cell differentiation	3	0.2	3.30E-02	9.20E-01
regulation of blood coagulation	5	0.3	3.50E-02	9.20E-01
positive regulation of cell proliferation	34	1.9	3.80E-02	9.30E-01
positive regulation of erythrocyte differentiation	6	0.3	4.00E-02	9.30E-01
negative regulation of cell migration	13	0.7	4.30E-02	9.40E-01
histone H3-K4 trimethylation	5	0.3	4.60E-02	9.50E-01
positive regulation of apoptotic process	21	1.2	4.60E-02	9.40E-01
stem cell population maintenance	9	0.5	5.00E-02	9.50E-01
cell migration	19	1.0	5.32E-02	9.50E-01

Among the enriched biological processes are a number implicated in cell division including: G1/S transition of mitotic cell cycle; negative regulation of apoptotic process; intrinsic apoptotic signaling pathway by p53 class mediator; positive regulation of cell proliferation and positive regulation of apoptotic process. Additional terms, associated with specific cellular processes involved in development and differentiation were also identified such as: regulation of establishment of cell polarity; regulation of cell morphogenesis; neuronal stem cell population maintenance; polarized epithelial cell differentiation; positive regulation of erythrocyte differentiation; and positive regulation of cell-substrate adhesion. Finally, terms associated with chromatin remodeling were present including: histone ubiquitination; chromatin remodeling; histone H3-K9 trimethylation; histone H2A ubiquitination; and histone H3-K4 trimethylation.

2.3.5. Small Subset of miRNAs having potential for clinical biomarker relevance

Based on the initial gene ontology enrichment analysis of all target genes associated with the set of 16 miRNAs, a choice was made to select a relatively small subset that might be suitable candidates for downstream clinical biomarker applications. The overarching goal in selecting the miRNA subset was focused upon (1) maximizing the representation of target genes associated with the set of enriched gene ontology terms while simultaneously (2) minimizing the number of miRNAs selected. Analysis of target gene representation associated with enriched gene ontology terms identified three miRNAs: cfa-miR-18a, cfa-miR-19a, and cfa-miR-181a. Together, these three miRNAs contain target genes for all but one enriched gene ontology term listed in Table 4 (histone H3-K9 trimethylation). Moreover, the overlap of target genes between these miRNAs was less than 7% (Figure 11).

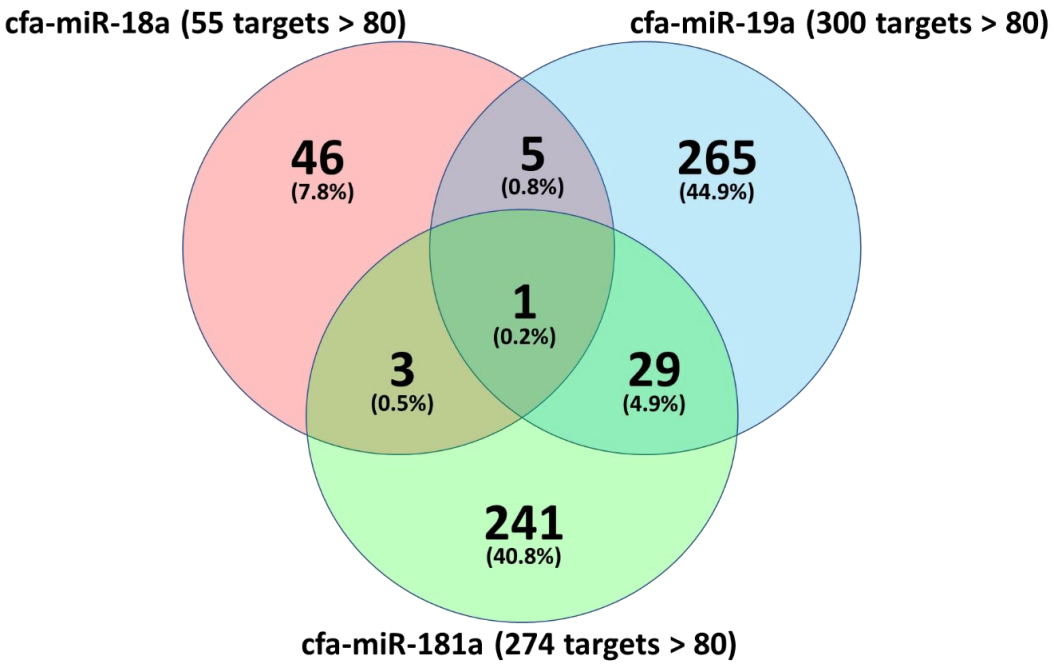

Figure 11. Overlap of target genes in the miRNA subset. A miRNA subset was selected from among the 16 miRNAs (Figure 9). Overlap of target genes is indicated by both numbers of target genes and percentage of total genes (sum of each miRNA's target gene set). Cfa-miR-18a represents an miRNA with relatively low expression in normal mammary tissue and higher expression in mammary tumor samples. Similarly, cfa-miR-19a also exhibits low expression in normal mammary samples and higher expression in mammary tumor samples. In contrast, cfa-miR-181a exhibits considerably higher expression in the normal mammary tissue compared to 18a and 19a. Additionally, 181a expression in mammary tumor samples is greater than any other miRNA among the 16 miRNAs represented in Figure 9.

2.3.7. *Functional Annotation of miRNAs cfa-miR-18a, cfa-miR-19a, and cfa-miR-181a*

The target genes predicted for cfa-miR-18a were used to generate functional annotation using the DAVID database. The set of 53 predicted target genes were submitted to the DAVID database to identify relevant functional annotation. Upon submission, 52 genes were successfully mapped. Gene enrichment analysis was performed using the biological process terms (GOTERM_BP_ALL) (Table 4). "Epithelial development" was identified as being enriched with p-value=0.0192 in association with the ESR1, FRS2, HIF1A, and PDE4D genes. The terms "mammary gland lobule development" and "mammary gland alveolus development" were both associated with the ESR1 gene and the HIF1A gene (p-value = 0.052). The pathway "proteoglycans in cancer" was identified as an enriched KEGG pathway with p-value=0.010. The genes associated with this pathway were ESR1, HIF1A, FRS2, SDC4. Analysis of cfa-miR-19a was based on the set of 300 predicted target genes, 299 of which were successfully mapped to canine genes using the DAVID gene list manager. Gene ontology biological process terms enriched included endothelial cell apoptotic process associated with BMPR2 and HIPK1 (p-value=0.052). Additionally, the term cell proliferation was associated with E2F8, LRP2, MDM4, APPL1, and ANXA7 (p-value=0.060). Enriched pathways obtained from KEGG pathway enrichment analysis included: renal cell carcinoma associated with RAP1A, RAP1B, PAK6, PIK3CB and PIK3R3 (p-value=0.011); cGMP-PKG signaling pathway with ATF2, CACNA1C, MEF2A, NFATC2, PIK3CB, PDE5, PIK3R3, and SLC25A6 (p-value=0.002); MAPK signaling pathway in association with RAP1A, RAP1B, RAPGEF2, TAOK1, ATF2, CACNA1C, MAPK8, MAP3K12 and RPS6KA5 (p-value=0.017); FoxO signaling

pathway through an association with FBXo32, CCND2, PIK3CB, PIK3R3, and S1PR1 (p-value= 0.003); and colorectal cancer with the genes APPL1, MAPK8, PIK3CB, and PIK3R3 (p-value=0.060).

Similar analysis of the 274 gene targets of cfa-miR-181a resulted in the successful mapping of 261 canine genes in the DAVID database. The analysis identified enriched gene ontology biological process terms: Microtubule Anchoring in association with FOPNL, GCC2 and CLASP1 (p-value=0.014); Positive Regulation of Transcription from RNA Polymerase II Promoter in association with DDX3, INO80, KLF15, LMO1, RORA, TAF9B, ATXN7, CDON, CCNK, HMGB2, IL1A, KMT2A, PROX1, RPS6KA3, and THRB (p-value=0.053). KEGG pathway enrichment analysis identified Protein Processing in Endoplasmic Reticulum with DNAJC3, SEC24A, SEC24C, SEL1, ATXN3, HSP90B1, and MBTPS2 (p-value=0.017); Glycerophospholipid Metabolism in association with DGKQ, ETNK1, GPD1L, LCLAT1, and MBOAT1 (p-value=0.026); and Phosphatidylinositol Signaling System in association with DGKQ, PPIP5K2, INPP4A, PI4K2B, and PLCB1 (p-value=0.031). A full list of gene ontology processes predicted to be targeted by miR-18a, miR-19a and miR-181a is provided (Table 5).

Table 5: Predicted target genes in representative set of enriched gene ontology biological process terms. See Appendix 3 for full gene IDs.

Enriched Term	Gene Ontology Id	Target Genes (within all 16 miRNAs)	Targets in 3 miRNA Subset
G1/S transition of mitotic cell cycle	GO:0000082	CCNE2, ACVR1B, EIF4E, CACUL1, CAMK2G, CAMK2D, USP37, RANBP1, RPS6KB1, PPP3CA, PHF8, LATS2, RBBP8	19a: CACUL1, RBBP81 181a: RPS6KB1

regulation of establishment of cell polarity	GO:2000114	ROCK1, GATA3, KRIT1, RICTOR, ARFGEF1, KANK1	19a: ARFGEF1 181: KANK1
negative regulation of apoptotic process	GO:0043066	FKBP8, TAF9B, NAA15, FOXO1, TP63, CITED2, SETX, PTK2, CASP3, DAB2, PRKAA1, RARB, HSPA5, AGO4, DNAJC3, KLHL20, CDK1, PDCD10, ADAMTS20, ZNF830, CBL, ASIC2, IGF1, RHBDD1, UBE2B, ASCL1, HSP90B1, GSK3B, HIPK3, VEGFA, ARF4, MAPK8, MDM4, APBB2, CAMK1D	19a: HIPK3*, MDM4, MAPK8, ADAMTS20, KLHL20 181a: HIPK3*, HSP90B1, UBE2B, TAF9B, DNAJC3
establishment of cell polarity	GO:0030010	RAB11FIP2, UST, RICTOR, WEE1, EPHB1, MARK1, KIF26B	19a: WEE1 181a: RAB11FIP2, MARK1
intrinsic apoptotic signaling pathway by p53 class mediator	GO:0072332	ZMAT1, ZMAT4, ZMAT3, PPP1R13B, ZNF385B, DDX5, ZNF346	19a: ZNF385B
negative regulation of extrinsic apoptotic signaling pathway	GO:2001237	PHIP, ZMYND11, NRP1, ITGA6, IGF1, PSME3, RPS6KB1, SGMS1, GCLM	19a: ZMYND11 181a: GCLM, RPS6KB1
histone ubiquitination	GO:0016574	SUZ12, UBE2A, HUWE1, UBE2B, PHC1	19a: UBE2A, SUZ12 181a: UBE2B
neuronal stem cell population maintenance	GO:0097150	NOTCH1, FOXO1, DLL1, FOXO3, CDH2, PROX1, MMP24	181a: PROX1
chromatin remodeling	GO:0006338	ATRX, TOP1, RSF1, HNF1A, GATA3, MORF4L2, INO80, CHD1, TP63, ARID1B, SMARCA2, RERE	19a: INO80*, SMARCA2, ATRX 181a: INO80*
positive regulation of cell-substrate adhesion	GO:0010811	PPM1F, SMOC2, CCDC80, JAK2, NID1, EDIL3, PRKCE, ABI3BP	19a: SMOC2 181a: ABI3BP

histone H3-K9 trimethylation	GO:0036124	BEND3, ARID4A, ARID4B	
histone H2A ubiquitination	GO:0033522	UBE2A, UBR2, UBE2B	19a: UBE2A 181a: UBE2B
positive regulation of cell proliferation	GO:0008284	KMT2D, CNBP, CACUL1, ESM1, IL34, CNOT7, CNOT6, TGFB2, PTK2, S1PR1, KRAS, CNOT6L, RARB, LOC488215, INSR, ACER3, UBE2A, PDCD10, KLB, SLC25A5, MECP2, ROGDI, IGF1, DLL1, TET1, SUZ12, ADM, HIPK1, HDAC1, VEGFA, HBEGF, MAB21L1, CARM1, EIF5A2	18a: KLB 19a: S1PR1*, CNOT7, CACUL1, CNOT6, UBE2A, ROGDI, HIPK1, SUZ12 181a: S1PR1*, ESM1, CARM1, ADM
negative regulation of cell migration	GO:0030336	PTPRJ, RAP2A, ADARB1, RAP2C, OSBPL8, ABHD2, KANK1, THY1, SFRP1, ROBO1, RRAS, TP53INP1, SRGAP2	19a: RAP2C 181a: KANK1, OSBPL8, ADARB1
histone H3-K4 trimethylation	GO:0080182	TET3, BEND3, ARID4A, KMT2A, CTR9	181a: KMT2A
stem cell population maintenance	GO:0019827	PHF19, EIF4E, NIPBL, MED28, MTF2, EOMES, KLF4, DDX6, CTR9	18a: PHF19 19a: DDX6
cell migration	GO:0016477	CCDC88A, AVL9, CDH2, VAV2, EPHB3, SDC4, TGFB2, SDC1, SORBS2, GSK3B, ARF4, CDC42BPA, JAK2, LIMD1, LAMC1, CSK, KCTD13, NFATC2, USP33	18a: SDC4, SORBS2 19a: USP33*, NFATC2, CCDC88A, SDC1, EPHB3 181a: USP33*, AVL9, CDC42BPA

NOTE: gene symbols with asterisk (*) in last column denote gene targets associated with more than one miRNA

Section 2.4. Discussion

To the authors' knowledge, this is the first study reporting secretion of exosome-like extracellular vesicles by canine mammary epithelial cells *in vitro*. Similar to previous reports of canine exosomes found in urine and serum/plasma, the vesicles were irregularly rounded, occasionally "cup-shaped," and immunopositive for the transmembrane tetraspanin protein CD9, known to regulate the progression of cancer (Ichii et al., 2017; Yang et al., 2017; Charrin et al., 2014). These findings strongly support these vesicles being exosomes, the small subcellular particles 50-200 nm in diameter that are actively shed from multivesicular bodies of parent cells. Exosomes contain proteins, peptides, mRNA, and microRNA, have been shown to be taken up by distinct cells through endocytosis, and they may play a role in distant cell-to-cell communication, especially in the context of neoplasia (Ichii et al., 2017; Yang et al., 2017).

As expected, the cell-free conditioned media that contained these exosomes was highly enriched in hundreds of distinct microRNAs. The microRNA profile of normal and malignant canine mammary exosomes was distinct, and yielded a number of significantly up-regulated and down-regulated miRs that may represent putative biomarkers of mammary neoplasia. These findings largely corroborate previous studies on miRNA in canine mammary neoplasia. Several studies of miRNA expression in canine mammary tumor tissue and CMT cells versus normal mammary tissue found significantly increased miR-29b, which was also significantly upregulated in the CMT exosomal RNA in the present study (along with the closely related miR-29c) (Osaki et

al., 2016; Boggs et al., 2008). One of those studies also found miR-181b was significantly upregulated in the tubulopapillary carcinoma subtype (Boggs et al., 2008).

Interestingly, our results differ substantially from those of von Deetzen et al. (2014), although it should be pointed out that in that study, the authors used miR-181b and miR-155 as housekeeping controls for qRT-PCR normalization, and both of those miRs appear to be upregulated in our data and previous studies of CMT (von Deetzen et al., 2014; Lutful Kabir, 2014; Boggs et al., 2008). Our results also diverge from Bulkowska et al. (2017), where several relevant up-regulated miRNA in the present study (such as miR-19a, miR-29b/c, and miR-181a) were shown to be down-regulated in malignant mammary carcinomas with metastasis (Bulkowska et al., 2017). This could be explained by the dramatic changes in tumor cell phenotype and gene expression in metastatic lesions compared to their matched primary tumor, such as occurs in the epithelial-to-mesenchymal transition (EMT) that has been documented in metastatic canine mammary carcinoma (Raposo-Ferreira et a., 2018).

miR-126 was previously identified as a circulating biomarker of multiple canine cancers including mammary carcinoma, and it is up-regulated in our CMT exosomal RNA (Heishima et al., 2017). This would fit with the hypothesis that canine mammary carcinoma cells secrete exosomes containing miR-126 (among other miRNA) into circulation. However, the other putative biomarker in that study, miR-214, was strongly down-regulated in our CMT exosomal RNA. One possibility for this mismatch could include secretion of miR-214 by other cells than mammary carcinoma cells (i.e. cells of the immune system, stroma, or other organs). Another possibility is a mismatch between tumor cell, exosomal, and circulating microRNA profiles. Supporting this hypothesis,

previous cell culture work in our lab has shown a complex relationship between exosomal miRNA profiles and the miRNA profile of the parent cell lines. Several miRs, including miR-18a, miR-19a, miR-29c, miR-181a, miR-215, miR-345, miR-371, and miR-1841, are up-regulated in both CMT parent cells and their exosomes (Lutful Kabir et al., 2015; Lutful Kabir, 2014). However, miR-31 and miR-34c had mixed expression patterns in the parent cells despite being uniformly upregulated in exosomes, and miR-495 was strongly down-regulated in all CMT parent cells while being up-regulated in the exosomal RNA population (Lutful Kabir et al., 2015; Lutful Kabir, 2014). This preliminary finding may suggest there is an active selection or enrichment process of particular miRNA within exosomes, or a negative feedback loop with the targets they regulate.

Many of these exosomal miRNAs were predicted to target dozens or hundreds of individual gene targets. Of particular note, miR-18a, miR-18b and miR-22 were highly up-regulated in the CMT exosomal RNA group and predicted to have an extremely high likelihood of targeting to 3' UTR of the estrogen receptor ESR1α mRNA (miRDB score of 99 for miR-18a and miR-18b, and 87 for miR-22). A number of other additional miRNA, including miR-181a, miR-181b, miR-181c, miR-181d, miR-19a, miR-19b, miR-148b, miR-203, miR-323, miR-874, and miR-486 were also predicted to negatively regulate ESR1α, although with a lower probability than the >80 score threshold (Appendix 3). Although targets with score greater than 80 have a greater likelihood of being true targets, some targets with scores below 80 may also be real. While it has long been known that human and canine mammary neoplasms lose ESR1α expression along with increasing grade and stage, this finding may indicate that miRNA such as miR-18a

contribute to this loss of hormone receptor activity (Chang et al., 2009; Chang et al., 2005). If this is verified *in vivo* in clinical patients, it may suggest miR-18a and others represent a non-invasive marker of CMT hormone status and phenotype, and could provide one potential mechanism for the loss of ESR1α with increasing CMT grade.

For gene ontology and functional enrichment analysis, the DAVID resource provides both p-values and Benjamini corrected p-values to aid investigators in the analysis process. The higher stringency of Benjamini corrected p-values dramatically reduces the number of significant results. On the one hand, this is a valuable way to reduce false positives from the analysis. On the other hand, a bioinformatics analysis aimed at providing clues as to the biological roles of miRNAs exhibiting altered expression profiles in normal mammary samples versus mammary tumor samples benefits greatly from broader inclusion criteria. Therefore, both the p-value and Benjamini corrected p-value were reported, and inclusion criteria for enriched gene ontology terms was set with a threshold p-value less than or equal to 0.06. This approach parallels the method described in Irizarry et al. (2016) and allows for retrieval of relevant functional annotation occurring at (or near) the boundary of p-value significance (Irizarry et al., 2016).

This set of enriched biological processes is particularly interesting in the context of mammary tumorigenesis and progression. The cell cycle-associated processes clearly relate to accelerated proliferation that can contribute to malignant transformation. For example, the transition between G1/S is a critically regulated check point in the cell cycle (Malumbres & Barbacid, 2009). Aberrations in the control of G1/S transitions can contribute to aberrant cell division and undesirable cell proliferation (Malumbres &

Barbacid, 2009). Similarly, positive and negative regulation of apoptosis impacts which cells survive in the cellular population. Altered expression of pro-apoptotic and/or anti-apoptotic gene products may adversely contribute to increased susceptibility to tumorigenesis in mammary tissues.

Equally important are the biological processes associated with cellular differentiation, adhesion and stem cell maintenance. Molecular factors underlying cellular differentiation may contribute to altered genetic programs within the cell. Abnormal expression of these factors may alter cellular programs leading to dysregulation of the cell cycle. Likewise, altered levels of genes implicated in cell adhesion may contribute to metastatic phenotypes that shift the clinical status of tumors from benign to malignant.

Finally, biological processes regulating chromatin have tremendous potential to dramatically alter the long-term genetic programs associated with cells. Modification of histones through methylation, acetylation, deacetylation, and ubiquitination directly modulate which chromatin regions are accessible for gene expression (Nair & Kumar, 2012). Silenced regions encoding tumor suppressors may shift cells towards a more oncogenic potential (Nair & Kumar, 2012).

This study has a number of important limitations. First, the number of biological replicates was relatively small, which was a function of both the high cost of the RNAseq methodology, as well as the difficulty harvesting and maintaining normal canine mammary epithelial cells in culture. However, the RNAseq dataset identified hundreds of miRs, many of which were significantly different, and many of these miRs match other studies in the human and veterinary literature. Another limitation is that there is currently

no consensus as to the optimal way to normalize exosomal microRNA qRT-PCR data. This was dealt with through a commonly used approach of relative expression based on ΔΔ-Cq normalization to pooled endogenous (miR-16) and exogenous (cel-miR-39) controls, which yielded very similar fold-change between RNAseq and qRT-PCR (Figure 3D). Furthermore, the use of specific stem-loop primers and sequence-specific probes, rather than non-specific intercalating dye methods (i.e. SYBR green), increased the specificity and robustness of this data.

These data suggest that as in women with BC, CMT cells shed exosomes enriched in differentially expressed miRNA, especially miR-18a, miR-19a, and miR-181a. Preliminary *in silico* evidence suggests these miRNAs may modulate biological processes associated with, or contributing to, the balance between normal and neoplastic states. A miRNA population predicted to regulate so many aspects of cellular proliferation and hormone activity suggests that these miRs are not just inert cellular by-products, but may actually play an active part in neoplastic transformation and/or progression, and evidence that they are actively selected for secretion. Furthermore, the identification of these miRs in secreted exosomes raises the possibility that they may be shed into biofluids such as blood, urine, and breast milk, allowing their use as minimally-invasive biomarkers with mechanistic and prognostic relevance, and the similarity between canine and human breast cancer exosomal miRNA profiles may have significance for translational research, and future studies need to experimentally validate that these miRNAs regulate the predicted targets (such as miR-18a and ESR1α).

Chapter 3: Comparison of circulating microRNA expression between dogs with and without mammary carcinoma by deep sequencing and digital droplet PCR

Section 3.1. Introduction

We presented *in vitro* evidence in Chapter 2 that CMT cells shed exosome-like microvesicles enriched in miRs, and that the exosomal miRNA pattern is predicted to regulate the estrogen receptor (ESR1), key tumor suppressor PTEN, and other genes relevant to human and canine breast cancer. It is well known that miRNA levels in many types of tumor cells and tissues are frequently dysregulated, but their real value as potential biomarkers comes from the fact that they are frequently secreted into biofluids such as serum/plasma, urine, breast milk, and cerebrospinal fluid (Suzuki et al., 2013; Iorio & Croce, 2012). In contrast to most forms of RNA, including mRNA, circulating serum/plasma microRNA levels are relatively stable over time, a range of temperatures, multiple freeze-thaw cycles and other pre-analytical variables, making them practical to detect and analyze (Mitchell et al., 2009; Mall et al., 2013). Circulating microRNA may also be bound to proteins such as Argonaute and/or actively secreted into exosomes by tumor cells, immune cells, and other tissues (Turchinovich et al., 2011).

Numerous studies on women with breast cancer suggest circulating microRNA can be useful both diagnostically as well as to stratify patients according by prognosis. One prospective study of breast cancer patients identified a combination of serum miRNA (miR-21, miR-23b, miR-190, miR-200b, miR-200c) that predicted tumor recurrence and shorter survival; these miRNA increased the accuracy of the model beyond standard prognostic factors (Papadaki et al., 2018). Another study found that a

panel of serum miRNA, including miR-19a, miR-15, and miR-181a, correlated with patient tumor burden, decreased following surgical resection, and were found at greater concentrations in patients that had experienced relapse (Sochor et al., 2014). miR-331 and miR-195 were found to accurately discriminate patients with metastatic breast cancer versus those with only local disease (McAnena et al., 2019). miR-19a and miR-205 were also increased in patients with Luminal A breast cancer that was chemoresistant to epirubicin and paclitaxel (Li et al., 2014).

Research on circulating miRNA is a growing area of interest in veterinary oncology, although there are currently only a few published studies for serum/plasma miRNA in CMT. One such study evaluated plasma miR-126 and miR-214 in various epithelial and non-epithelial canine tumors, and both miRNA were significantly increased in dogs with mammary carcinoma (along with a number of other malignancies) relative to healthy controls (Heishima et al., 2017). Another study found that canine mammary carcinoma tissues from patients with metastasis had a different microRNA signature than those with only local disease, but the proposed miRNA of interest were not significantly different in plasma (Bulkowska et al., 2017).

Two unique challenges to measuring circulating microRNA are (1) their much lower concentrations in serum/plasma, and (2) a lack of consensus on the most appropriate normalization strategy (Stein et al., 2017). To address the low yield, various RNA extraction and reverse transcription (RT) protocols have been optimized for low input in the range of picograms per microliter. Methods such as RNAseq and the TaqMan Advanced microRNA assay systems include a pre-amplification step that increases analytical sensitivity, although this may also introduce bias (Chu & Nabity, 2019). The

challenge in typical qPCR normalization arises from the fact that normal "housekeeping" control genes that are abundant in cells and tissues, such as snoRNAs, are generally absent to minimally detectable in serum and plasma, making them unusable for serum exosome samples. As an alternative approach, some authors have recommended absolute quantification through a standard-curve calibrated to an exogenous spike-in miRNA such as cel-miR-39 (Dirksen et al., 2016). Others normalize qPCR to plasma input volume (Bailey et al., 2019). RNAseq allows relative and absolute quantification based on normalization across millions of all mapped reads (Chu & Nabity, 2019). dPCR provides absolute quantification without a normalization gene by measuring tens of thousands of PCR reactions in parallel and assaying against a standard curve for FAM fluorescence (Stein et al., 2017). One study comparing qPCR and dPCR for miRNA in lung cancer found high correlation between the assays, with dPCR having lower coefficient of variation and greater reliability (Campomenosi et al., 2016).

Based on the studies described above and weighing the considerations, we determined that the optimal combination of sensitivity and robust results for profiling circulating miRNA in dogs with and without mammary carcinoma was initial target identification by RNAseq validated by dPCR absolute quantification. Our hypothesis was that the serum miRs would be differentially expressed between healthy dogs and those with CMT with good diagnostic performance, that multiple assay methods (RNAseq and dPCR) would provide similar results, and that many of the significantly dysregulated miRNA would overlap with the previously identified set of putative exosomal microRNA biomarkers, including miR-18a/b, miR-19a/b, miR-29b/c, miR-34c, miR-155, and miR-181a/b/c.

Section 3.2. Methods

3.2.1. Patient Selection and Tumor Pathology

Healthy females (5 spayed and 5 intact) were prospectively recruited for the control group and 10 dogs with malignant canine mammary tumors (CMT) were included in the neoplastic group. Exclusion criteria for healthy females was any evidence of disease by a veterinarian's physical exam, or abnormalities on complete blood count (CBC) or serum biochemistry tests. The five healthy intact females varied by stage of estrus at the time of blood collection, and included three in estrus, one in diestrus, and one in anestrus.

Nine of the ten mammary carcinoma subjects were from a previous study on dendritic cell fusion vaccines for CMT; the tumor tissue and serum from all of these patients was collected prior to any treatments or interventions (Bird RC et al, 2019). One of the ten CMT dogs (MC10) was part of a breeding colony for research dogs at the Scott-Ritchey Research Center and was scheduled for euthanasia due to age and quality of life concerns; a large mammary tumor was discovered prior to euthanasia, and fresh whole blood, serum, and tumor tissue were collected from this patient immediately post-mortem.

Two blinded board-certified anatomic pathologists confirmed the malignant status of the CMT biopsy lesions (GM, JK). Tumors were subtyped histologically, graded, and assessed for the presence or absence of lymphatic/vascular invasion by one blinded pathologist (GM) as previously described (Rasotto et al, 2017).

3.2.2. RNA Extraction and microRNA deep-sequencing (RNAseq)

RNA was extracted from 200 uL of serum using the exoRNAeasy midi kit (Qiagen) according to manufacturer instructions. RNA yield was assessed by Qubit 2.0 RNA fluorometric assay. Purity and quality control was assessed through an Agilent 2100 bioanalyzer.

Extracted RNA was stored at -80°C until being shipped on dry ice to the Genomic Services Laboratory at the Hudson Alpha Institute for Biotechnology for deep-sequencing as described in Chapter 2, Section 2.2.6.: "RNA extraction & microRNA deep-sequencing."

3.2.3. Digital Droplet RT-PCR (dPCR)

Seven miRNA were selected for dPCR validation based on their serum RNAseq expression pattern, previous documentation of relevance to human and canine mammary neoplasia in the published literature, and potential target genes: cfa-miR-18a, cfa-miR-19b, cfa-miR-29b, cfa-miR-34c, cfa-miR-122, cfa-miR-125a, cfa-miR-181a. Serum RNA was converted to cDNA using the TaqMan™ Advanced miRNA cDNA Synthesis Kit (Thermo Fisher Scientific, Waltham, MA, USA) according to manufacturer instructions. For each 14.5 uL sample, 6 uL of pre-Amp cDNA template (1:10 dilution) was combined with 7.25 uL QuantStudio™ 3D Digital PCR Master Mix v2 (Thermo Fisher Scientific, Waltham, MA, USA), 0.725 uL of the appropriate custom 20x TaqMan® Assay (Thermo Fisher Scientific, Waltham, MA, USA), and 1.53 uL molecular grade water. Reaction tubes were gently vortexed and loaded into an individual QuantStudio™ 3D Digital PCR Chip v2 (Thermo Fisher Scientific, Waltham, MA, USA) using the QuantStudio™ 3D

Digital PCR Chip Loader (Thermo Fisher Scientific, Waltham, MA, USA) according to manufacturer directions. Chips were put into a ProFlex™ PCR System thermocycler (Thermo Fisher Scientific, Waltham, MA, USA) and run with the following protocol: 96°C for 10 minutes (one cycle), 60°C annealing/extension step for 2 minutes followed by 98°C melting step for 30 seconds (39 cycles), and a final stage of 60°C for 2 minutes followed by holding at 10°C. Chips were removed and stored in the dark at room temperature until being read on the QuantStudio™ 3D Digital PCR Instrument (Thermo Fisher Scientific, Waltham, MA, USA). Chip data was saved on a USB drive and uploaded to the QuantStudio™ 3D AnalysisSuite™ v3.1 (Thermo Fisher Scientific, Waltham, MA, USA). Absolute quantification was determined through the software algorithm after setting a FAM threshold based on the no template control (NTC) fluorescence histogram and scatterplot.

3.2.4. miRNA Gene Target Annotation

The top 10 over-expressed and under-expressed miRNA were searched in the canine database TargetScan 7.2. Predicted targets were sorted by aggregate probability of conserved targeting (Friedman et al., 2009), and probabilities >0.80 were considered highly likely targets.

3.2.5. Statistical Analysis

dPCR assay results were assessed for normality through visual inspection and Kolmorov-Smirnov tests with alpha = 0.010 using commercially available software (Analyse-it for Microsoft Excel v2.20, Analyse-it Software, Ltd). For normally-

distributed data, a two-tailed student's t-test was used to compare groups. Non-parametric data was compared via Wilcoxon-Mann Whitney tests. Receiver Operator Characteristic (ROC) curves were generated and sensitivity, specificity, and likelihood ratios were calculated. A p-value of <0.05 was considered statistically significant for all hypothesis testing.

Section 3.3. Results

3.3.1. Clinical Patient Characteristics

The median age of CMT dogs (10.5 years) was significantly higher than the healthy group (3 years) ($p=0.001$). For the CMT group, there was no strong breed predisposition, with two Labrador Retrievers, and one each of the following: Boston Terrier, Bullmastiff, Dachshund, German Shepherd, mixed breed, Rat Terrier, Samoyed, and Shih Tzu. For the healthy control group, all five intact females were Labrador Retrievers, while the spayed female cohort included three mixed breed dogs, one Boston Terrier, and one Jack Russell Terrier.

Patient tumor pathology characteristics are summarized in Table 6. Of the 10 dogs in the CMT group, 7 had a single tumor and 3 had two CMT tumors. The CMT histologic subtypes varied widely. Four dogs had Grade I tumors, three had Grade II, and three had Grade III. All three dogs with two tumors had the same grade CMT in each. Six dogs had tumor evidence of lymphatic invasion on their biopsies.

Table 6: CMT group tumor histopathologic subtype, grade, lymphatic invasion, and survival time

Case	**Histologic subtype**	**Grade**	**Lymphatic invasion**	**Inflammatory BC?**	**Survival (Days)**
MC1	Carcinoma-mixed type	Grade I	Yes--Lymphatic	No	183
MC2	Carcinoma--anaplastic	Grade III	Yes--Lymphatic	No	611
MC3	Carcinoma--cystic papillary; carcinoma--tubular	Grade I (both)	No	No	63
MC4	Carcinoma-micropapillary invasive	Grade II	Yes--Lymphatic	Yes	83
MC5	Carcinoma-spindle variant	Grade II	No	No	427
MC6	Carcinoma-mixed type; Carcinoma complex type	Grade I (both)	No	No	636
MC7	Carcinoma--solid; Carcinoma-micropapillary invasive	Grade II (both)	Yes--Lymphatics; LN+	Yes	85
MC8	Carcinoma in situ	Grade I	No	No	n/a

MC9	Carcinoma-anaplastic	Grade III	Yes--Lymphatics; LN+	Yes	42
MC10	Carcinoma--tubulopapillary/solid	Grade III	Yes--Lymphatics	No	n/a

3.3.2. microRNA Profiling by RNAseq

The average pre-amplification RNA concentration from serum was 6.72 ng/µL (range: 20 pg/µL – 129.84 ng/µL; standard deviation: 28.98 ng/ µL). RNA fluorograms indicated the samples were high quality and biased towards small RNA populations. 511 total microRNA were detected by RNAseq across the 20 serum RNA samples, with 452 unique miRs (59 miRs were duplicate isoforms from different gene loci). Principal component analysis (PCA) revealed that there was significant overlap in the overall serum miRNA profile between both intact and spayed healthy females, and partial overlap between the aggregate healthy group and the CMT group (Figure 12).

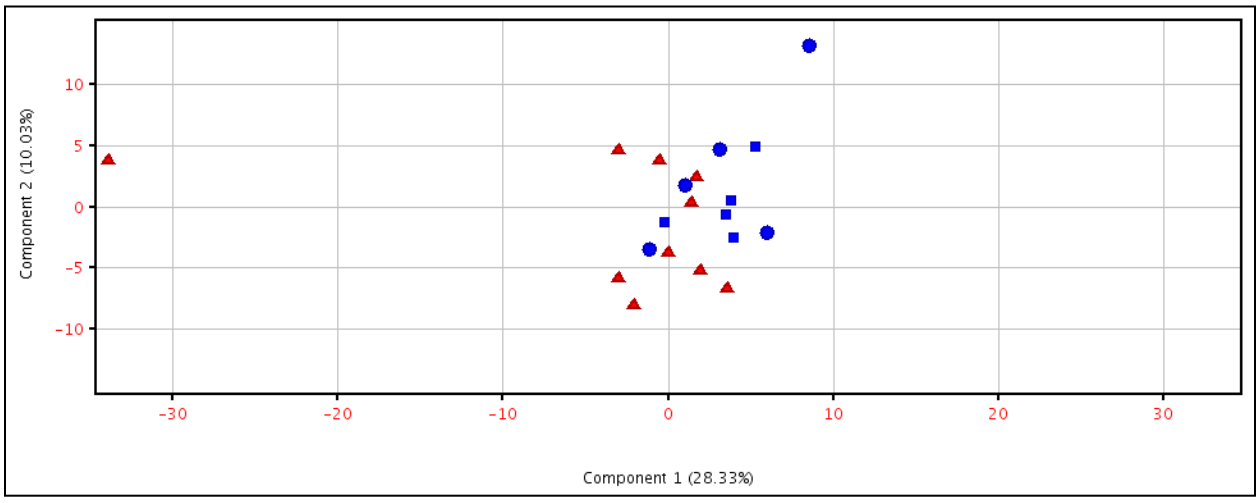

Figure 12. Principal Component Analysis (PCA) plot for circulating microRNA. Mammary carcinoma dogs are plotted in red, healthy control dogs are plotted in blue. Square data points represent sexually intact healthy females, while circles represent spayed healthy females. The intermixing between groups indicates significant overlap in the serum microRNA profile between CMT and healthy female dogs.

65 individual miRs were differentially expressed (>±1.5-fold) and statistically significant between healthy females and those with CMT. The volcano plot in Figure 13 graphically illustrates this differential miRNA expression between groups. Appendix 2 shows the significantly differentially expressed miRNAs in CMT samples compared to controls. Some of these up-regulated miRs have been previously identified as up-regulated in CMT exosomal RNA shed by cultured CMT cells in our lab, including miR-18a, miR-19b, miR-29b/c, miR-34c, miR-181c, miR-215, and miR-345 (See Chapter 2, Section 2.3. Results).

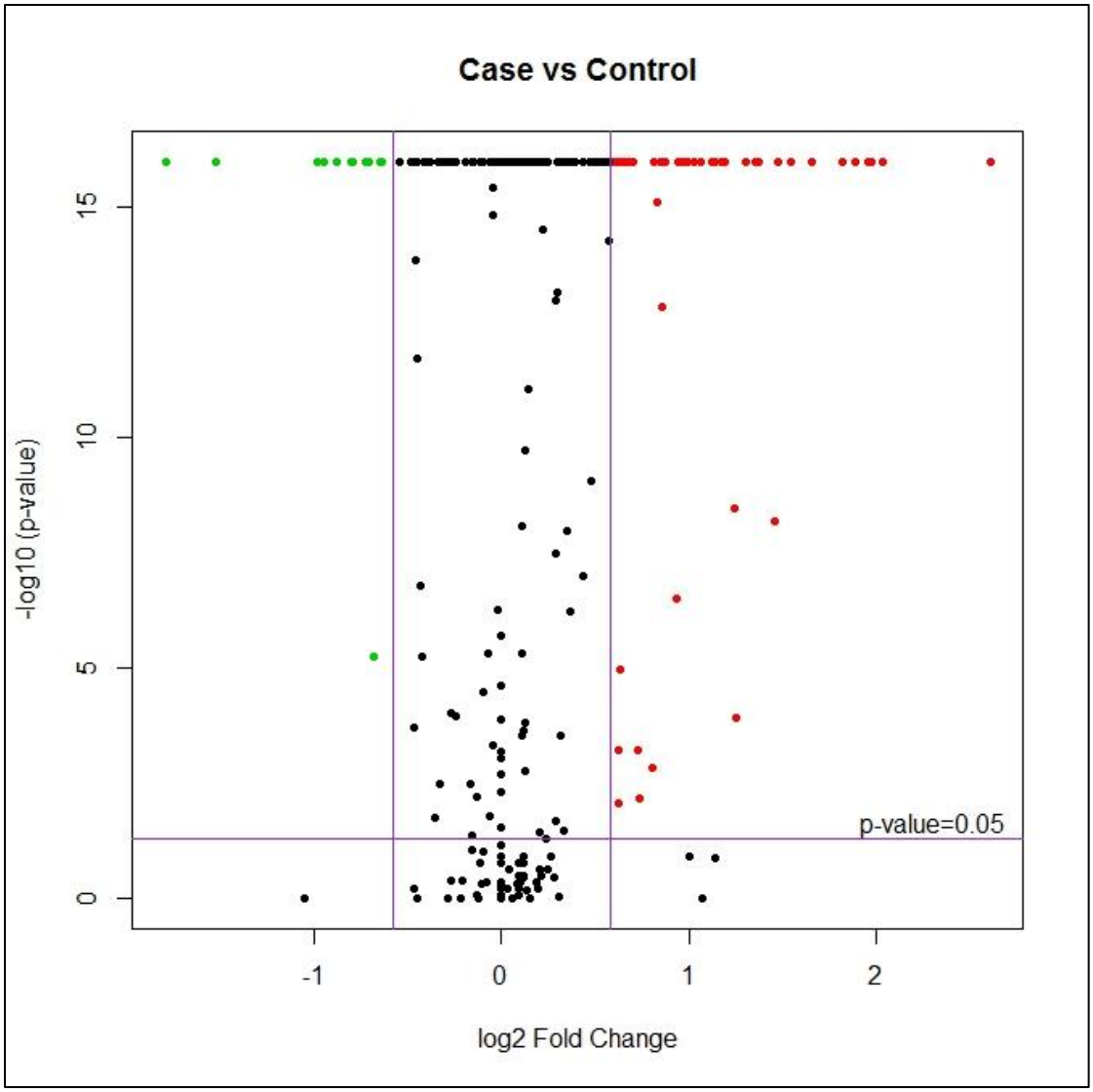

Figure 13. Volcano plot for serum microRNA expression by RNAseq. Red dots in the upper right are significantly up-regulated in the CMT group by >1.5-fold, while green dots in the upper left are significantly down-regulated >1.5-fold. Black dots were miRs that were expressed with a <± 1.5-fold difference and/or not statistically significantly different in expression between groups.

3.3.3. Absolute microRNA Expression by dPCR

Absolute miRNA expression data for cfa-miR-18a, cfa-miR-19b, cfa-miR-29b, cfa-miR-34c, cfa-miR-122, cfa-miR-125a, cfa-miR-181a are summarized in Table 7. miRNA cfa-miR-18a, cfa-miR-19b, and cfa-miR-181a were the most abundantly expressed miRs in the set tested by dPCR, with others having lower absolute expression. miR-34c and miR-125a had the largest magnitude relative fold-change between mammary carcinoma group and healthy control group (Figure 14). Both cfa-miR-19b and cfa-miR-125a were significantly higher in the mammary carcinoma group than among healthy control dogs by dPCR (Figure 15A & 15C). miR-34c was substantially higher in among dogs with mammary carcinoma than healthy subjects, although this difference narrowly missed statistical significance (Figure 15B, Table 8). One dog in the healthy control group (subject HS3) was an outlier with extremely high miR-19b expression (32,364 copies/µL). Clinical follow-up on this patient revealed that within one year of this sample collection, the patient developed widespread pulmonary metastasis from an unknown primary cancer and died shortly thereafter.

Table 7: Serum miRNA absolute expression by dPCR. P-values are for univariate statistical comparison between groups. An asterisk (*) indicates non-parametric data, medians compared by Wilcoxon rank-sum test. All other variables are normally distributed and means compared by two-tailed student's t-test. P <0.05 was considered statistically significant (statistically significant p-values highlighted in bold).

Mammary Carcinoma Group					Healthy Control Group				
microRNA	**Mean**	**Median**	**STD**	**Range**	**Mean**	**Median**	**STD**	**Range**	**p-value**
cfa-miR-18a	33397.4	28679.0	16977.7	10720 - 62271.0	26945.1	24270.0	16459.0	7381.4 - 60453.0	0.400
cfa-miR-19b*	18256.3	18073.0	6186.7	11635 - 31825.0	10357.4	8252.5	8249.4	2993.9 - 32364.0	**0.003**
cfa-miR-29b	3059.9	2921.0	1156.9	1707.4 - 5336.3	2276.1	1362.1	2555.8	284.95 - 8801.2	0.389
cfa-miR-34c*	1611.6	1023.9	1400.6	396.2 - 4410.4	614.0	584.3	363.9	110.22 - 1242.3	0.075
cfa-miR-122	284.6	254.5	181.3	48.9 - 635.6	186.0	132.8	164.6	36.7 - 559.0	0.219
cfa-miR-125a*	380.6	368.0	250.8	29.2 - 739.1	52.1	0.7	114.2	0.0 - 364.1	**0.000**
cfa-miR-181a	12503.2	10364.5	4765.0	8611.9 - 23296.0	10211.4	8396.3	5957.0	3564.7 - 19808.0	0.355

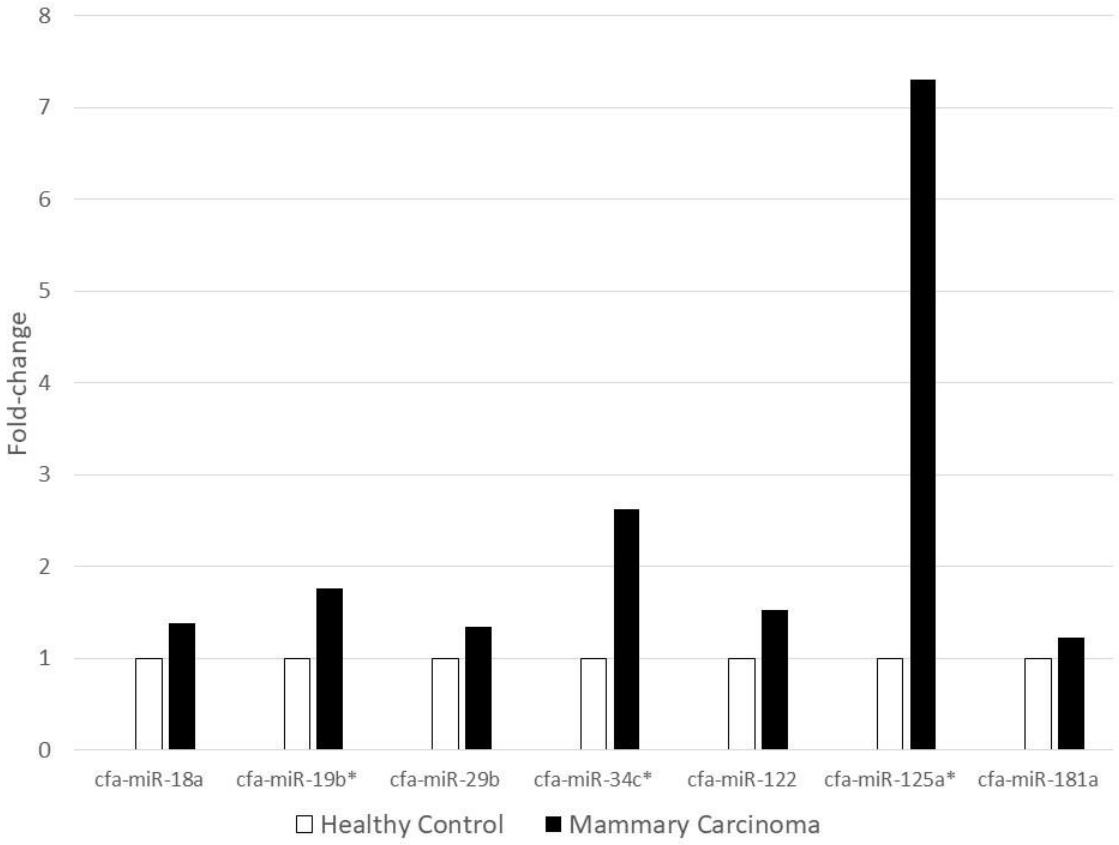

Figure 14. Serum miRNA dPCR relative expression histogram. Mean expression for each miRNA in copies/µL were compared (diving mammary carcinoma group values by healthy control group values, setting controls at 1.0 for each target). Black bars are fold-change for the mammary carcinoma group relative to the healthy controls (white bars).

A

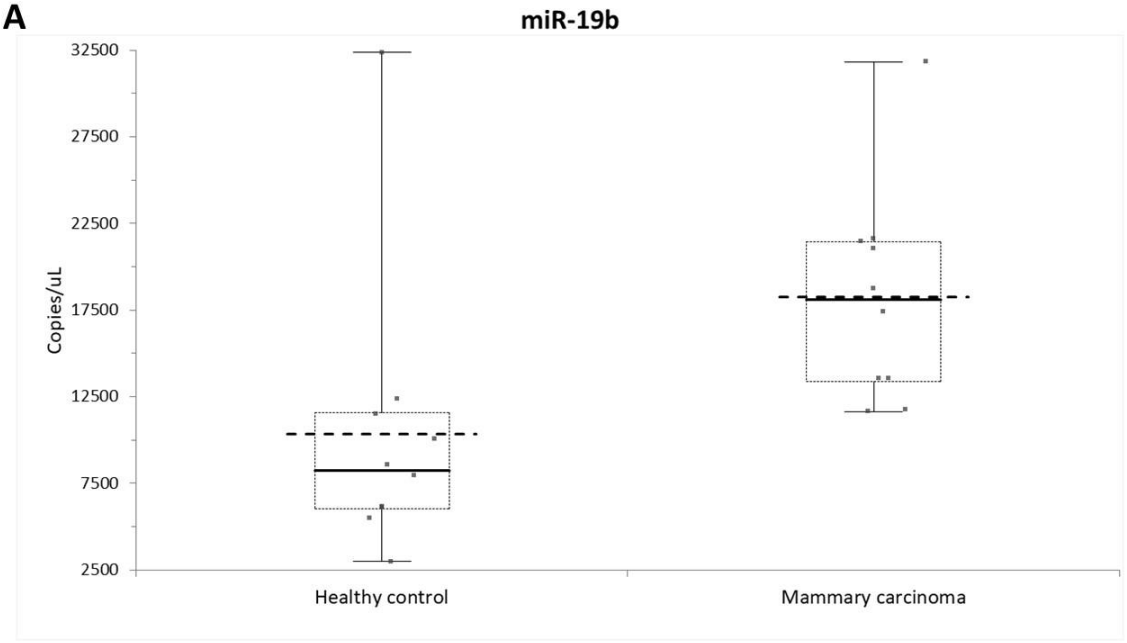
miR-19b
32500
27500
22500
17500
12500
7500
2500
Copies/uL
Healthy control
Mammary carcinoma

B

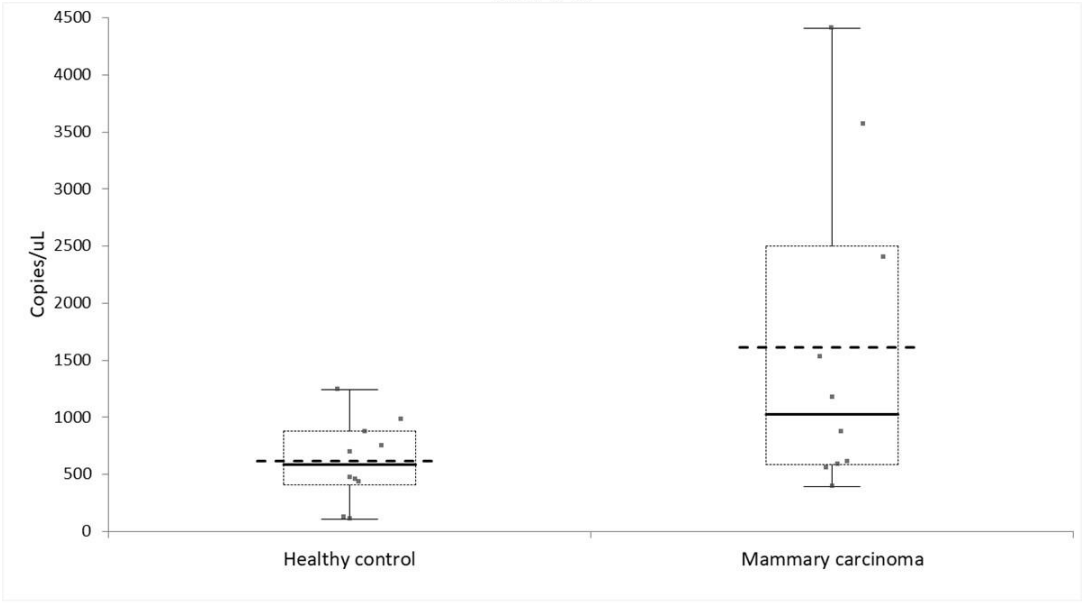
miR-34c
4500
4000
3500
3000
2500
2000
1500
1000
500
0
Copies/uL
Healthy control
Mammary carcinoma

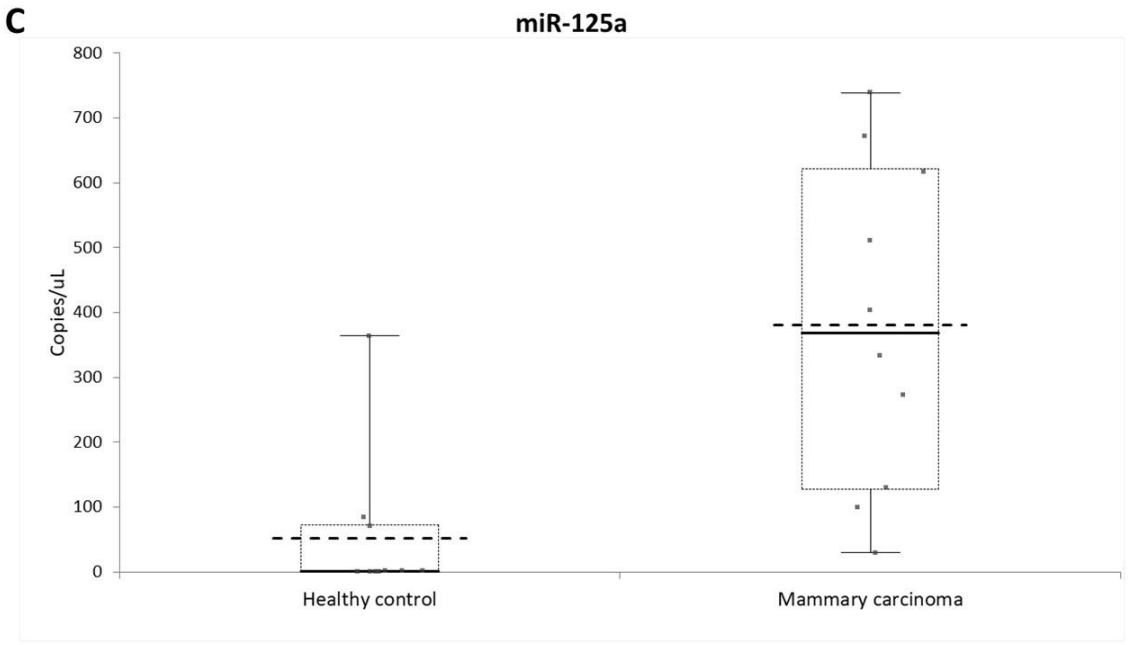

Figure 15. Box and whisker plots for absolute miRNA expression by dPCR. Bold horizontal lines are median values, dashed lines represent mean values, box and whiskers represent 95% confidence intervals. A. cfa-miR-19b. B. cfa-miR-34c. C. cfa-miR-125a.

RNAseq and dPCR assays were compared by assessing miRNA fold-change and statistical significance between the mammary carcinoma and healthy control groups, and this data is summarized in Table 8. Two of seven miRNA were significantly different by both methodologies (miR-19b and miR-125a). Results between the assays were largely similar in direction of fold-change, with the notable exception of miR-125a and miR-122, which were both increased by dPCR despite being down-regulated according to RNAseq. Six of seven miRNA had less-extreme fold-change by dPCR than RNAseq (with the

exception of miR-125a). miR-181a was abundantly expressed in both carcinoma and control cohorts, but did not vary statistically between groups by either RNAseq or dPCR.

Table 8: Comparison of dPCR and RNAseq results for select microRNA. Relative fold change in the mammary carcinoma group compared to the healthy control group. Significant p-values are bolded.

	RNAseq		dPCR	
microRNA	**Fold-change**	**p-value**	**Fold-change**	**p-value**
cfa-miR-18a	1.94	**0.000**	1.24	0.400
cfa-miR-19b	3.15	**0.000**	1.76	**0.003**
cfa-miR-29b	2.78	**0.000**	1.34	0.389
cfa-miR-34c	6.07	**0.000**	2.62	0.075
cfa-miR-122	-2.87	**0.000**	1.53	0.219
cfa-miR-125a	-3.46	**0.000**	7.31	**0.001**
cfa-miR-181a	1.02	0.500	1.22	0.355

3.3.4. miRNA Gene Target Annotation

504 unique genes were identified as significantly enriched among the predicted targets of the miRNA identified by RNAseq. The 20 most significantly enriched gene targets are shown in Figure 16. Table 9 shows the top 10 significantly up-regulated and down-regulated miRNA along with the number of high probability gene targets (P_{CT} >0.080) based on the TargetScan 7.2 database. The top five genes by P_{CT} are listed for each miRNA. The miR-19a/19b family had the highest number of probable gene targets in the up-regulated miRNA group at 610, while cfa-let-7b had the highest number of probable gene targets in the down-regulated group at 856. The canine estrogen receptor

ESR1 has two conserved seed-sequence sites predicted to have 0.79 - 0.83 aggregate probability of conserved targeting (PCT) for binding miR-19b (Figure 17).

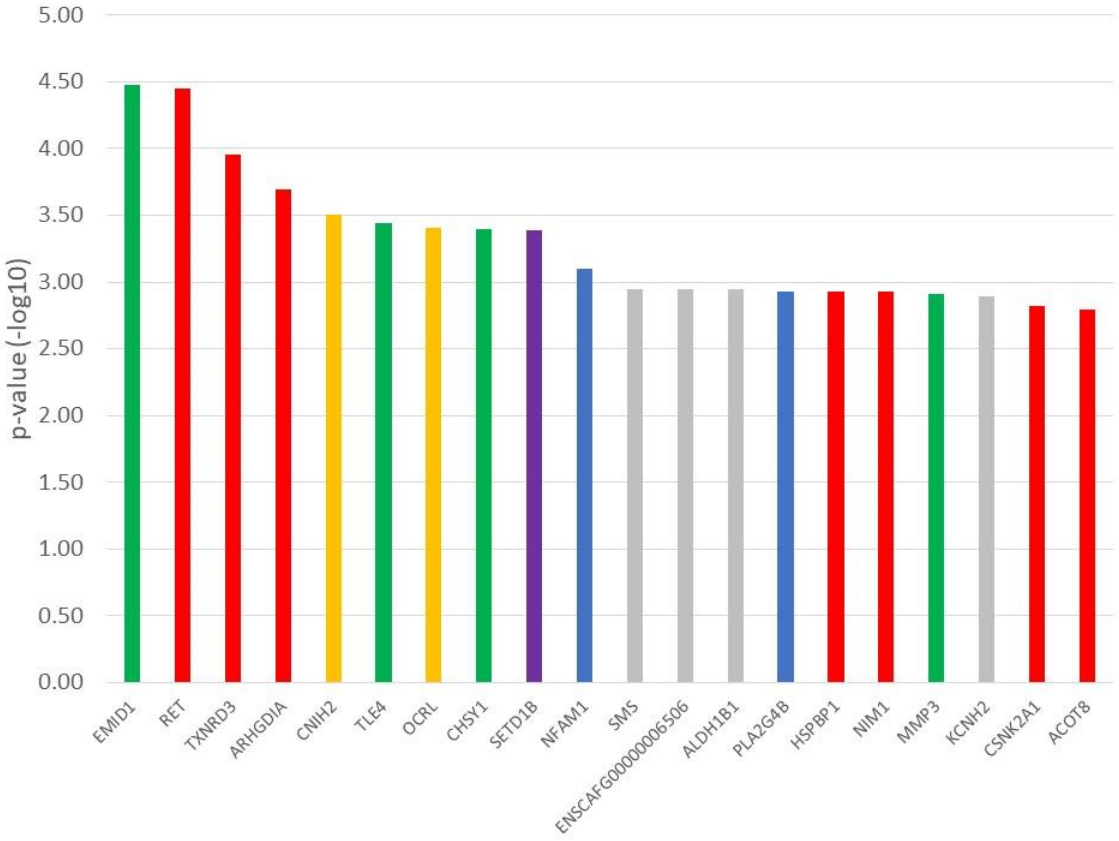

Figure 16. **Histogram of the genes most significantly enriched in miRNA targets among serum miRNA. The y-axis is the –log(10)-transformed p-value for each gene. Genes are color-coded by function: Green = Involved in cytoskeletal proteins, cell-cell adhesion, and/or the Epithelial-to-Mesenchymal Transition (EMT); Red = Oncogene/Proto-Oncogene; Yellow: Regulation of vesicle trafficking; Purple = Regulates chromatin remodeling; Blue = Regulator of inflammation / immune**

function. Bars in gray represent genes that either had no clear link to cancer or were novel genes without available annotation.

Table 9: List of the top 10 highest and lowest significantly different miRNA. These were miRNA in this patient population with the greatest significant fold change (positive and negative) with the number of genes predicted to be targeted with a high likelihood (aggregate probability of conserved targeting or P_{CT} >0.80). The five genes with the highest P_{CT} are listed. For miRNA with no targets that have a P_{CT} >0.80, they are listed as N/A with no genes are identified.

Up-regulated miRNA				
miRNA	**Fold-Change**	**p-value**	**# Targets (PCT >0.80)**	**Top 5 gene targets**
cfa-miR-34c	6.08	0	179	FAM76A, SYT1, FUT9, HCN3, PACS1
cfa-miR-135a-5p	4.08	0	250	SP3, KCNN3, CPLX1, CPLX2, SYT2
cfa-miR-199	3.93	0	134	SH3GLB1, PAK4, GNA12, ADAMTSL3, ITGB8
cfa-miR-182	3.93	0	143	ROCK1, BNC2, LPP, ADCY6, FRS2
cfa-miR-30b	3.69	0	594	PPARGC1B, CELSR3, MTDH, STOX2, DGKH

cfa-miR-19b	3.15	0	610	ZMYND11, PTEN, ATXN1, ZBTB20, AGO3
cfa-miR-23a	2.92	0	22	PDE7A, SESN3, KIAA1467, NR6A1, KLF3
cfa-miR-29b	2.78	0	279	COL1A1, TET1, TET3, PI15, COL1A2
cfa-miR-504	2.74	2.05E-09	0	N/A
cfa-miR-421	2.59	0	0	N/A

Down-regulated miRNA				
miRNA	**Fold-Change**	**p-value**	**# Targets (PCT >0.80)**	**Top 5 gene targets**
cfa-miR-125a	-3.46	0	416	BMF, ARID3B, ARID3A, NECAB3, PODXL
cfa-miR-122	-2.88	0	0	N/A
cfa-miR-375	-1.97	0	1	QKI
cfa-let-7b	-1.93	0	856	HMGA2, FIGN, LIN28B, NR6A1, TRIM71

cfa-miR-6529	-1.84	0	0	N/A
cfa-miR-10a	-1.74	0	20	CREB1, KPNA5, NR6A1, FIGN, RORA
cfa-miR-99b	-1.73	0	0	N/A
cfa-miR-423a	-1.65	0	0	N/A
cfa-miR-486	-1.64	0	0	N/A
cfa-miR-139	-1.60	2.22E-06	0	N/A

Figure 17. Conserved areas of canine ESR1 3' UTR targeted by cfa-miR-19b.

3.3.5. Diagnostic Performance

To evaluate the ability of these miRNA to discriminate case from control subjects, Receiver Operator Characteristic (ROC) plots were generated. The highest ROC Area-Under-the-Curve (AUC) was miR-125a at 0.930 (Figure 18A), indicating excellent ability to discriminate between patients with mammary carcinoma and healthy controls in this population. miR-19b also had a high ROC-AUC at 0.880 (Figure 18B). When excluding the outlier healthy control HS3 due to the possibility of occult neoplasia, the AUC-ROC for miR-19b increased to 0.978, which would indicate near perfect ability to discriminate groups. All other miRNA had fair to poor ROC-AUC (Table 10).

A

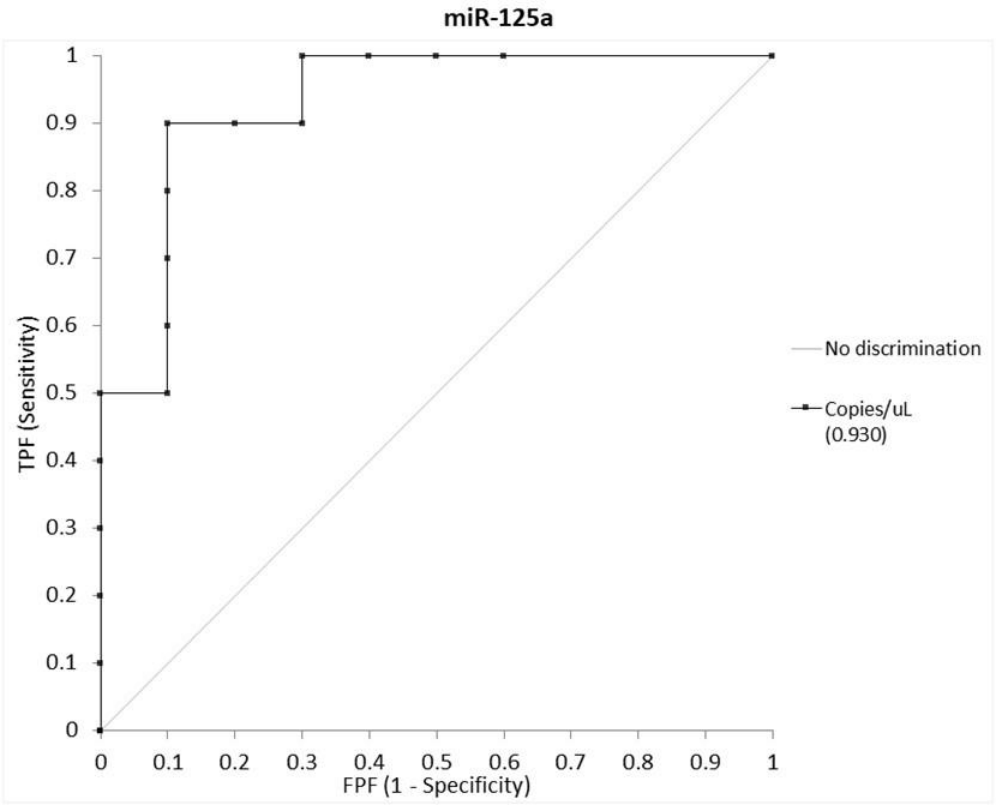
miR-125a
TPF (Sensitivity)
FPF (1 - Specificity)
0
0.1
0.2
0.3
0.4
0.5
0.6
0.7
0.8
0.9
1
No discrimination
Copies/uL
(0.930)

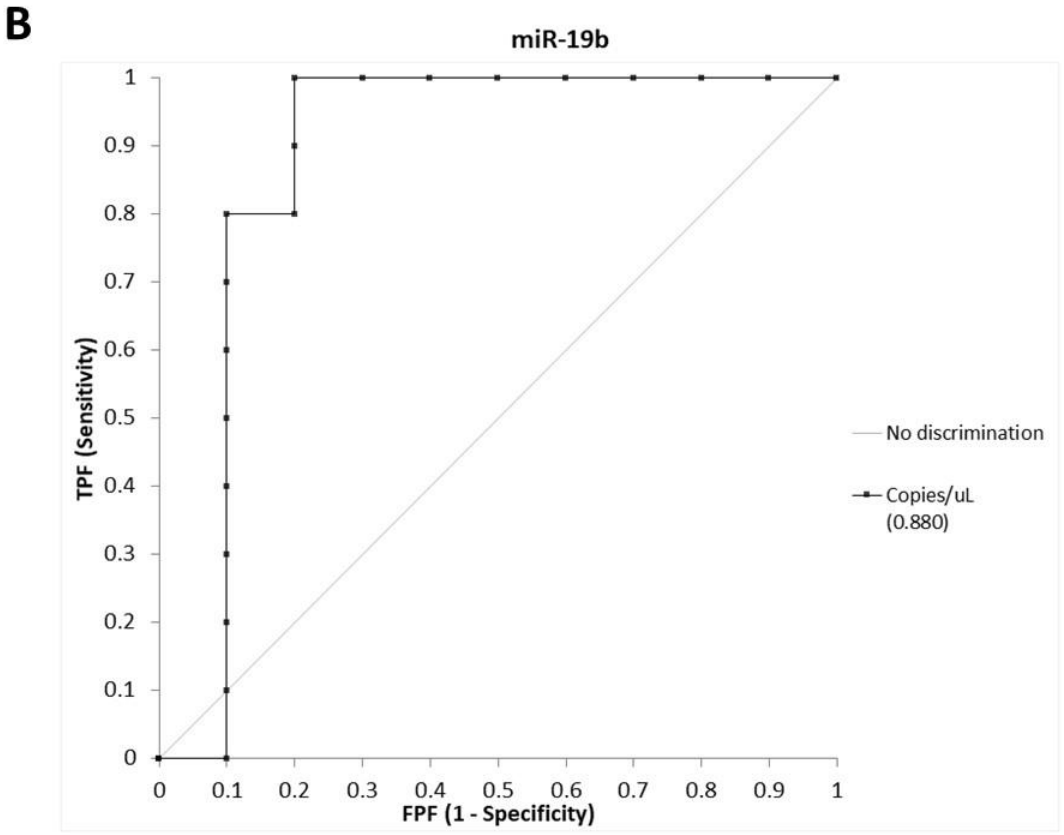

Figure 18. Receiver Operator Characteristic (ROC)- Area Under the Curve (AUC) plots for miR-125a (A) and miR-19b (B). The light gray line indicates an AUC of 0.0500 and no ability to discriminate diseases beyond chance. ROC-AUC provided in parentheses.

Table 10: ROC analysis for seven miRNA. These data include AUC, 95% Confidence Interval (CI), and Standard Error (SE).

microRNA	AUC	95% CI	SE
cfa-miR-18a	0.630	0.372 - 0.888	0.132
cfa-miR-19b	0.880	0.683 - 1.077	0.101
cfa-miR-29b	0.790	0.542 - 1.038	0.126
cfa-miR-34c	0.740	0.513 - 0.967	0.116
cfa-miR-122	0.690	0.430 - 0.950	0.132
cfa-miR-125a	0.930	0.816 - 1.044	0.058
cfa-miR-181a	0.650	0.380 - 0.920	0.138

Because of suitable biomarker characteristics for miR-19b (high absolute expression, strong up-regulation by the CMT group by RNAseq and dPCR, robust ROC-AUC), additional diagnostic test parameters were calculated for this miRNA. The diagnostic sensitivity and specificity of miR-19b varied by the selected cut-off, and whether patient HS3 was included or not. At 11,600 copies/uL and including HS3, miR-19b had a sensitivity of 100%, a specificity of 80%, and a positive likelihood ratio of 5.0 (95% CI: 1.96-17.64). At a cutoff of 13,000 copies/uL, the sensitivity decreased to 80% while specificity increased to 90%; the positive likelihood ratio increased to 8.0 (95% CI: 1.82-45.48), while the negative likelihood ratio was 0.22 (95% CI: 0.06-0.61). Excluding HS3 at 11,600 copies/uL, sensitivity was 100%, specificity 88.9%, and the positive likelihood ratio was 9.0 (95% CI: 2.30 – 50.27). Excluding HS3 at 13,000 copies/uL, sensitivity was 80%, specificity 100%, and negative likelihood ratio 0.20 (95% CI: 0.06 – 0.51).

Section 3.4. Discussion

This study demonstrates that serum from dogs with mammary carcinoma is enriched in hundreds of circulating microRNA. While the overall expression pattern between dogs with malignant CMT and healthy controls had significant overlap based on PCA, a number of individual microRNA were significantly up-regulated or down-regulated in the CMT group. Some of these, including miR-18a, miR-19b, miR-29b/c, miR-34c, miR-181c, miR-215, and miR-345, were previously selected as candidate CMT biomarkers from in vitro studies and bioinformatic analysis in our lab (See Chapter 2). Of these miRNA, miR-29b has previously been shown to be upregulated in malignant canine mammary tumors versus normal mammary tissue (Boggs et al., 2008). Circulating miR-

126 and miR-214 were both previously identified as increased in dogs with a variety of tumors, including mammary malignancy, however neither was among those significantly or differentially expressed between CMT and healthy dogs in this dataset (Heishima et al., 2017).

miR-19b was strongly and significantly up-regulated in the CMT group by both RNAseq and dPCR. Furthermore, ROC-AUC and sensitivity/specificity analysis indicated this particular miRNA had good ability to differentiate patients in the two groups. Although this is a small cohort of patients, and subjects with non-neoplastic mammary disease (i.e. mastitis) were not included, this suggests miR-19b may be a promising biomarker for canine mammary carcinoma. This agrees with prior studies that show circulating miR-19a (closely related to miR-19b) has prognostic significance in women with breast cancer (Li et al, 2014; Sochor et al, 2014).

Interestingly, one patient in the healthy spayed female cohort (HS3) had extremely high miR-19b expression, and went on to develop widespread metastasis from an unidentified primary cancer within twelve months of sample collection. While this patient did not show any outward evidence of occult malignancy on physical examination or laboratory testing, diagnostic imaging was not an inclusion criterion for the healthy controls and it is possible this patient had a small, unidentified tumor at the time of blood collection. However, the lack of post-mortem examination and/or tumor histopathology and immunohistochemistry limited the inferences that could be drawn from this outlier. Because of the possibility that this patient was actually not a false positive, but a rather patient with early malignancy that had not yet manifested itself obviously, AUC-ROC, sensitivity, specificity, and likelihood ratio analysis was run with and without this patient

included, and results for both were presented. However, this case could also represent a case where abnormal miRNA expression profiles predicted future clinical complications.

Similar to the bioinformatics results in Chapter 2, the circulating miRNA in this study were predicted to regulate numerous genes and pathways relevant to oncogenesis. Of the top 20 genes most significantly enriched in binding sites for these miRNA, 7/20 were oncogenes that promote cell proliferation, 4/20 were cytoskeletal proteins involved in cell-cell adhesion and the EMT (which promotes invasion and metastasis), and several others regulated inflammation/immune function, extracellular vesicle trafficking and chromatin remodeling (Figure 16). A few of the genes (such as spermine synthase and aldehyde dehydrogenase 1B1) were not obviously associated with cancer. Many of the genes with the highest P_{CT} for the most up-regulated and down-regulated miRNA in Table 10 involve the EMT/metastasis.

miR-19b specifically was predicted to target a number of important genes and pathways relevant to mammary tumorigenesis, such as ESR1 and the tumor suppressor PTEN. The conserved miR-19 family (which includes the highly similar miR-19a and miR-19b) has been proposed as a biomarker for multiple cancers in human oncology, including women with breast cancer. miR-19a was significantly associated with chemoresistance in patients with Luminal A breast cancer, and levels were greater than two-fold higher in chemoresistant compared to chemosensitive human breast cancer cases (Li et al., 2014).

miR-125a was significantly different between CMT and healthy groups by both RNAseq and dPCR, and also showed diagnostic promise based on AUC-ROC. However, the difference in fold-change between assays (down-regulated by RNAseq and up-

regulated by dPCR) raised concerns about the reliability of this miRNA as a biomarker and was not investigated in greater detail. RNAseq and dPCR generate relative and absolute quantification of genes through different methodologies, which could explain the mismatch. One potential source of discrepancy is the library preparation process required by RNAseq, but not dPCR (Chu & Nabity, 2019).

This study has a number of limitations. First, the small sample size may have been underpowered to detect modest but real group differences, especially for dPCR. Notably, absolute expression for miR-34c was prominently up-regulated in the mammary carcinoma group, but the p-value was slightly above the alpha 0.05 boundary of statistical significance for dPCR. However, despite the modest number of biological replicates, RNAseq identified millions of small RNA reads, and several target miRNA were validated by dPCR. In addition, both the mammary carcinoma and healthy control group subjects were robust, with the former having a variety of tumors of different histologic type and grade, and the latter including both OHE dogs and bitches in various stages of estrus. The diversity in histopathologic characteristics is especially important, and two important prognostic factors included high-grade tumors (Grade III) and tumors with lymphatic invasion (Rasotto et al, 2017). Second, this patient population did not include subjects with non-malignant mammary pathology such as mastitis or benign mammary tumors. This could be relevant as research evaluating microRNA in bovine and porcine milk has identified particular miRNA signature that increase with mastitis, including miR-21, miR-146a, miR-155, miR-222, and miR-383 (Lai et al., 2017). Fortunately, these miRNA are not among the most relevant potential biomarkers identified in this dataset.

Overall, this study identified a number of circulating miRNA that were significantly over- and/or under-expressed by dogs diagnosed with mammary carcinoma relative to healthy controls. These miRNA are predicted to regulate important tumor suppressor genes and endocrine pathways that promote mammary tumorigenesis. Some of these, such as miR-19b, have good diagnostic test performance, and may represent candidate biomarkers for CMT. Further prospective studies on a larger cohort of CMT patients are warranted to evaluate the diagnostic utility of circulating miR-19b.

Chapter 4: Association of Circulating microRNA with Clinical and Histopathologic Tumor Characteristics

Section 4.1. Introduction

We have shown in the preceding two chapters that normal and malignant canine mammary epithelial cells secrete exosomes enriched in miRNA *in vitro*, and that sera from dogs with CMT also contain differentially expressed circulating miRNA by RNAseq and dPCR. Several miRNA in particular, such as miR-18a, miR-19a/b, and the miR-181 family, among others, are upregulated in CMT tumor tissue, cell lines, exosomes, and serum. These findings suggest that those serum miRNA could be potential diagnostic biomarkers of CMT as they are in women with breast cancer (Bahmanpour et al., 2019). Additionally, these miRNA are predicted to regulate functionally relevant genes such as the Estrogen Receptor (ESR1, aka ER) and tumor suppressor PTEN, along with a number of oncogene and epithelial-to-mesenchymal (EMT)/metastasis pathways. This raises the real promise of circulating microRNA testing: that they may act as a "liquid biopsy" and act as non-invasive indicators of clinically relevant tumor prognostic variables beyond a simple binary output of cancer/not cancer.

Key prognostic factors for CMT include tumor subtype, grade, stage, and histologic evidence of lymphatic invasion. CMT histologic subtypes reported to have especially high mortality include anaplastic carcinoma, comedocarcinoma, carcinosarcoma, and micropapillary carcinoma (Canadas et al., 2019; Rasotto et al., 2017; Gamba et al., 2013). Dogs with Grade III tumors have significantly shortened survival compared with dogs that have Grade I or II CMT (Rasotto et al., 2017). CMT patients with tumor lymphatic invasion on their biopsies have a three-fold higher rate of tumor

recurrence and distant metastasis compared to CMT dogs where this is absent, and presence of lymphatic invasion is associated with a hazard ratio of mortality of 1.61 (Rasotto et al., 2017). Additionally, dogs that develop inflammatory mammary carcinoma have widespread metastasis and a very short survival time with a reported average survival of 25 days from diagnosis (Clemente et al., 2010; Perez Alenza et al., 2001). Other proxy markers for CMT aggressiveness include hormone receptor expression. Loss of estrogen and/or progesterone receptors correlates with aggressive phenotypes in women and dogs with mammary neoplasia (Mainenti et al., 2014; Chang et al., 2005).

There are numerous studies linking microRNA to these prognostic factors in women with breast cancer. Circulating miR-133a is significantly correlated with tumor grade in women with breast cancer (El-Mahdy et al., 2017). miR-331 and miR-195 predict metastasis in women with breast cancer (McAnena et al., 2019). microRNA are also dynamic markers of disease, changing over time as the tumor progresses. Dozens of microRNA in women with breast cancer are initially upregulated, but decrease over time in Grade III carcinomas relative to Grade I tumors (Dadiani et al., 2016). A study of dogs with CMT found miR-18a, miR-18b, miR-19b, and miR-181d were up-regulated in CMT samples from Grade III tumors, but down-regulated in lower grade tumors (Bulkowska et al., 2017).

One question that often arises in blood-based microRNA studies that identify candidate biomarkers is: What cells actually express and secrete these miRNA? CMTs are heterogeneous tissues composed of a mix of ductular and tubular epithelial cell types, myofibroblasts, stromal fibroblasts, inflammatory cells, and skin/adnexal cell types. Several studies have identified upregulation of miR-18a/b, miR-19a/b, miR-29b, and

miR-181a/b/d in CMT tumor tissues and cells (Bulkowska et al., 2017; Lutful Kabir., 2014; Boggs et al., 2008), but this expression data is based on homogenized cell/tissue lysate extractions and qPCR or microarray, and which specific cell types express a given miRNA is currently unknown.

We hypothesized that the circulating miRNA identified as candidate biomarkers in Chapter 3 would be significantly different among CMT dogs that had high grade tumors and lymphatic invasion on their biopsy, as well as between those that developed inflammatory mammary carcinoma and those that did not. We also predicted these miRNA would be significantly correlated with patient survival time. Finally, we hypothesized that precursor-microRNA for these mature circulating miRNA would be expressed by neoplastic epithelial cells and correlate with their serum counterparts.

Section 4.2. Methods

4.2.1. Patient selection and tumor pathology

Healthy females (5 spayed and 5 intact) were prospectively recruited for the control group and 10 dogs with malignant canine mammary tumors (CMT) were included in the neoplastic group. Exclusion criteria for healthy females was any evidence of disease by a veterinarian's physical exam, or abnormalities on complete blood count (CBC) or serum biochemistry tests. The five healthy intact females varied by stage of estrus at the time of blood collection, and included three in estrus, one in diestrus, and one in anestrus.

Nine of the ten mammary carcinoma subjects were from a previous study on dendritic cell fusion vaccines for CMT; the tumor tissue and serum from all of these patients were collected prior to any treatments or interventions (Bird et al., 2019). One of the ten CMT dogs (MC10) was part of a breeding colony for research dogs at the Scott-Ritchey Research Center and was scheduled for euthanasia due to age and quality of life concerns; a large mammary tumor was discovered prior to euthanasia, and fresh whole blood, serum, and tumor tissue were collected from this patient immediately post-mortem.

Two blinded board-certified anatomic pathologists confirmed the malignant status of the CMT biopsy lesions (GM, JK). Tumors were subtyped histologically, graded, and assessed for the presence or absence of lymphatic/vascular invasion by one blinded pathologist (GM) as previously described.

New slides were cut from the corresponding archived formalin-fixed paraffin embedded (FFPE) tissue block for each tumor specimen in the CMT group and submitted to the UC Davis Veterinary Histology Laboratory for Estrogen Receptor (ER) and Progesterone Receptor (PR) immunohistochemistry (IHC). Slides were shipped back and interpreted by three ACVP board-certified pathologists (EF, JK, GM).

4.2.2. Circulating microRNA Quantification

Serum miRNA were quantified by RNAseq and dPCR as presented in Chapter 3. miRNA absolute expression by RNAseq is in Reads per Million (RPM), while dPCR miRNA absolute expression is in copies/µL.

4.2.3. Tumor pre-microRNA in situ hybridization (ISH)

New slides were cut from the corresponding archived formalin-fixed paraffin embedded (FFPE) tissue block for each tumor specimen in the CMT group. In situ hybridization (ISH) was performed with the BaseScope™ Reagent Kit RED (Advanced Cell Diagnostics, Inc, Newark, CA, USA) according to manufacturer instructions. Custom probes for canine pre-miR-18a, pre-miR-19b, and pre-miR-34c were designed by Advanced Cell Diagnostics. Canine-specific PPIB was used as a positive control and the bacterial gene DapB was used as a negative control. The Advanced Cell Diagnostics HybEZ™ Oven (Newark, CA, USA) was used for all heating steps.

Briefly, unstained FFPE slides were baked for one hour at 60°C, followed by deparaffinization via standard xylene and 100% ethanol incubations. Blocking was performed by incubating RNAscope® Hydrogen Peroxide on slides for 10 minutes, followed by two washes in distilled water and antigen retrieval by incubation with 70 ml 10x Target Retrieval Reagent + 630 ml ddH2O at 98-102°C for 30 minutes. A hydrophobic barrier was drawn and slides dried overnight. Next, RNAscope® Protease III was incubated with slides at 40°C for 30 minutes. Probes for the target pre-microRNA, positive control, and negative control were incubated on slides for 2 hours at 40°C. Next, ZZ-linkers AMP1-6 were progressively incubated and washed (see manufacturer protocol for varying times and conditions). Approximately 120 µL of BaseScope™ Fast RED detection reagent were incubated with slides for 10 minutes at room temperature, then counterstained with 50% hematoxylin and coverslipped with Ecomount (Biocare Medical, LLC, Pacheco, CA, USA).

4.2.4. Image Analysis

Open source software Fiji for ImageJ v.2.0 (Schindelin et al., 2012) was used to analyze ISH results according to manufacturer recommendations (Technical Note TS 46-003, "Using ImageJ to analyze RNAscope and BaseScope Data," Advanced Cell Diagnostics, Newark, CA, USA).

To quantify pre-microRNA expression in probe dots per cell, three random 20x magnification fields of each tumor section were captured as .TIFF photomicrographs with an Olympus BX43 microscope and cellSens Entry software (Olympus Corporation of the Americas, Center Valley, PA, USA) and underwent color deconvolution based on region of interest (ROI) selections for representative nuclear, probe, and background staining patterns. Images then went through Otsu thresholding and the Analyze Particles function was used to count nuclei (filter settings: mean pixel area 600-infinite, circularity 0.3-1.0). The Trainable Weka Segmentation plug-in was used to count probe signal "dots". Briefly, a training set of five representative free-hand selections each for nuclear staining, probe, and background colors were used to segment the image, which went through thresholding as described above. The Analyze Particles function was used to count probe signals (filter settings: mean pixel area 40-500, circularity 0.35-1.0). Dots/cell was calculated by dividing the total number of nuclei counted by the total probes counted in each 20x field. Dots/cell results from the three fields for each tumor sample were then averaged.

4.2.5. Statistical analysis

RNAseq, dPCR, and BaseScope ISH assay results were assessed for normality through visual inspection of QQ plots and Kolmogorov-Smirnov tests with alpha = 0.010 using commercially available software (Analyse-it for Microsoft Excel v2.20, Analyse-it Software, Ltd). For normally-distributed data, a two-tailed student's t-test was used to compare groups. Non-parametric data was compared via Wilcoxon-Mann Whitney tests. Pearson's r was tested to evaluate correlation between patient survival time and pre-microRNA ISH results with circulating miRNA by RNAseq and dPCR. A p-value of <0.05 was considered statistically significant for all hypothesis testing.

Section 4.3. Results

4.3.1. Clinical patient characteristics

The median age of CMT dogs (10.5 years) was significantly higher than the healthy group (3 years) ($p=0.001$). For the CMT group, there was no strong breed predisposition, with two Labrador Retrievers, and one each of the following: Boston Terrier, Bullmastiff, Dachshund, German Shepherd, mixed breed, Rat Terrier, Samoyed, and Shih Tzu. For the healthy control group, all five intact females were Labrador Retrievers, while the spayed female cohort included three mixed breed dogs, one Boston Terrier, and one Jack Russell Terrier.

Patient tumor pathology characteristics are summarized in Table 6 in Chapter 3. Of the 10 dogs in the CMT group, 7 had a single tumor and 3 had two CMT tumors. The CMT histologic subtypes varied widely. Four dogs had Grade I tumors, three had Grade II, and three had Grade III. All three dogs with two tumors had the same grade CMT in

each. Six dogs had tumor evidence of lymphatic invasion on their biopsies. Three patients were treated with only surgical resection of their tumor and no adjunctive therapy (MC1, MC3, and MC8), while one dog received no treatment as the tumor was found after euthanasia and necropsy (MC10). The other 6/10 CMT dogs were treated with standard surgical resection of their tumor(s) followed by gemcitabine chemotherapy and an experimental CMT dendritic cell fusion vaccine (Bird et al., 2019).

4.3.2. Circulating miRNA association with Survival

Survival times from time of surgical resection to spontaneous death or euthanasia were available for 8 of 10 (80%) dogs in the CMT group. There were no statistically significant correlations between any of the seven circulating miRNA by RNAseq or dPCR and survival time in days (Table 11).

Table 11: Correlation between circulating miRNA expression and survival time.

Comparison	**Pearson's r**	**p-value**
Serum miR-18a (RNAseq) vs Survival (days)	0.011	0.980
Serum miR-18a (dPCR) vs Survival (days)	0.387	0.344
Serum miR-19b (RNAseq) vs Survival (days)	-0.103	0.809
Serum miR-19b (dPCR) vs Survival (days)	-0.110	0.796
Serum miR-29b (RNAseq) vs Survival (days)	-0.497	0.210
Serum miR-29b (dPCR) vs Survival (days)	0.186	0.660
Serum miR-34c (RNAseq) vs Survival (days)	-0.498	0.209
Serum miR-34c (dPCR) vs Survival (days)	-0.530	0.176

Serum miR-122 (RNAseq) vs Survival (days)	-0.017	0.969
Serum miR-122 (dPCR) vs Survival (days)	-0.293	0.481
Serum miR-125a (RNAseq) vs Survival (days)	-0.673	0.067
Serum miR-125a (dPCR) vs Survival (days)	-0.314	0.449
Serum miR-181a (RNAseq) vs Survival (days)	0.131	0.758
Serum miR-181a (dPCR) vs Survival (days)	-0.186	0.660

4.3.3. miRNA association with Histopathologic Characteristics

Circulating miRNA expression for these seven targets was compared between mammary carcinoma patients with grade III tumors (high grade) versus Grade I/II tumors (low grade), as well between mammary carcinoma patients with and without metastasis. miR-18a by RNAseq was significantly higher in the group with lymphatic invasion than without metastasis (2.82 vs 1.23 RPM, p=0.0281) (Figure 19A). miR-18a was also notably higher by RNAseq for the three dogs with Grade III tumors compared to all others (3.27 vs 1.72 RPM), though this was narrowly above the boundary of significance (p=0.051) (Figure 19B). No other serum miRNA by RNAseq or dPCR were significantly different between metastasis or grade groups. There was no significant difference between serum miRNA by RNAseq or dPCR between CMT dogs that developed inflammatory mammary carcinoma versus those that did not.

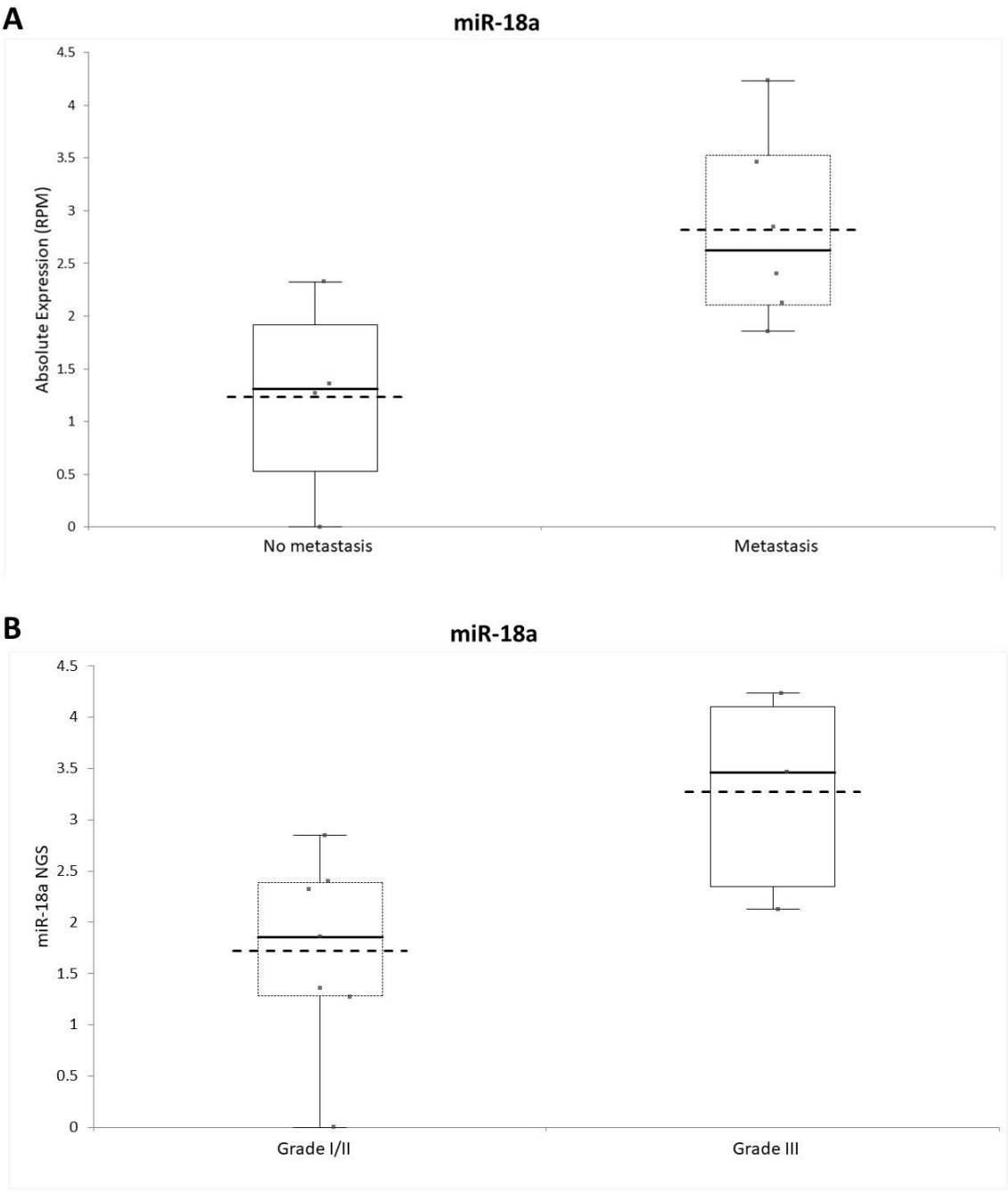

Figure 19. Box and whisker plots absolute miR-18a expression by RNAseq between metastasis (A) and grade (B) groups. Bold horizontal lines are median values, dashed lines represent means. A. CMT dogs with and without lymphatic invasion

(metastasis). B. CMT dogs with high grade tumors (Grade III) versus Grade I/II tumors.

To evaluate the association of circulating microRNA with tumor hormone receptor status, ER and PR IHC were performed by UC Davis Veterinary Histology Laboratory. However, estrogen receptor and progesterone receptor IHC slides were deemed non-diagnostic after review with two board-certified anatomic pathologists (JK, GM) due to weak and inconsistent positive control immunolabeling, non-specific staining, and aberrant patterns for those typically expected (see Appendix 5A-E for examples).

4.3.4. Tumor pre-microRNA in situ hybridization

BaseScope™ ISH revealed cfa-pre-miR-18a, cfa-pre-miR-19b, and cfa-pre-miR-34c were expressed at varying levels in tumor tissues from all ten patients in the CMT group (Figure 20). These target pre-microRNA were generally expressed by neoplastic carcinoma cells and occasionally adjacent normal mammary epithelial cells, with minimal detection in stromal or inflammatory cells (Figure 21). Probe signals were detected in both the nucleus and cytoplasm of cells (Figure 21).

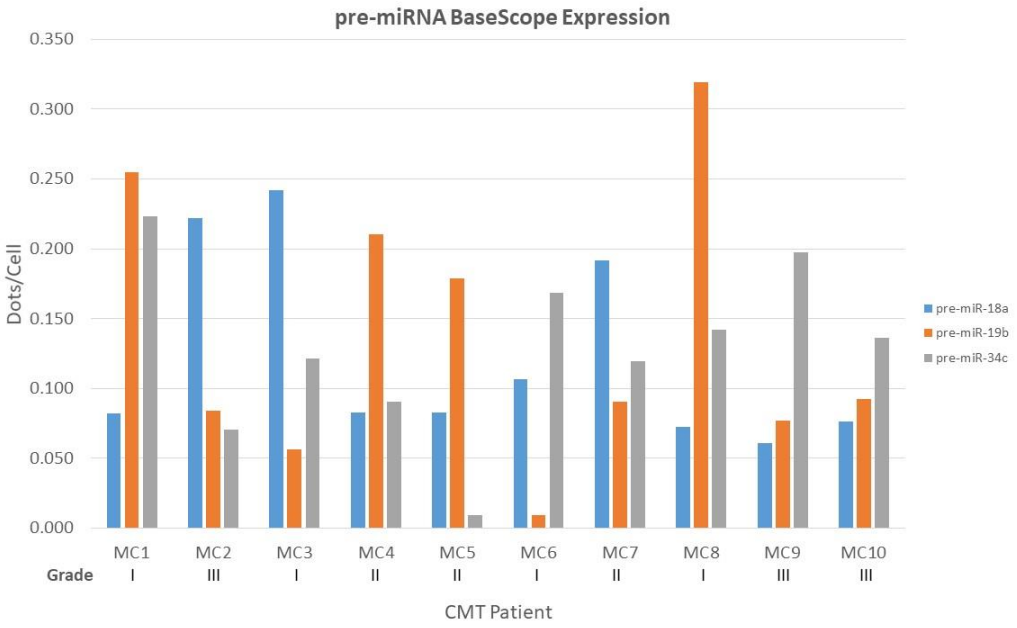

Figure 20. Image analysis of pre-microRNA expression by BaseScope™ *in situ hybridization* (ISH) for pre-miR-18a, pre-miR-19b, and pre-miR-34c. Data is expressed as dots (probes) per cell. Results are an average of three random 20x fields per tumor slide.

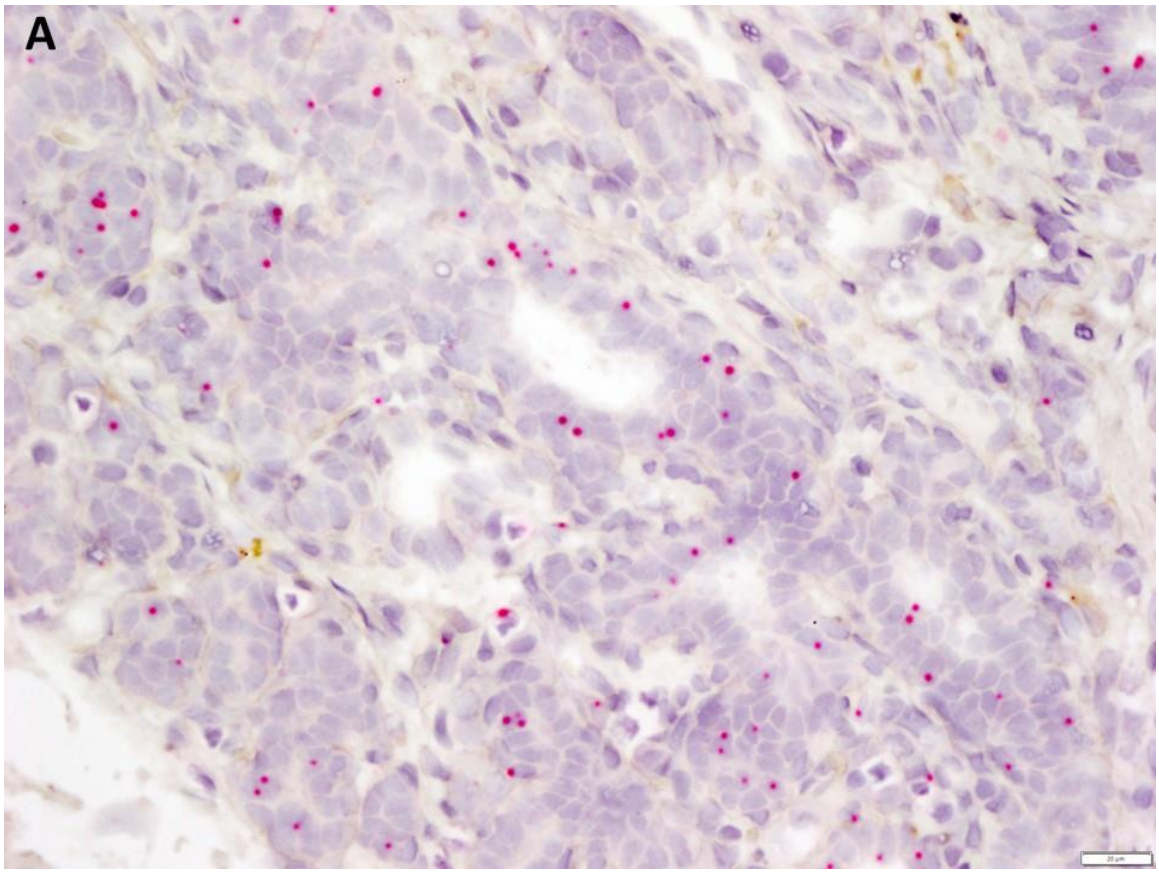
A

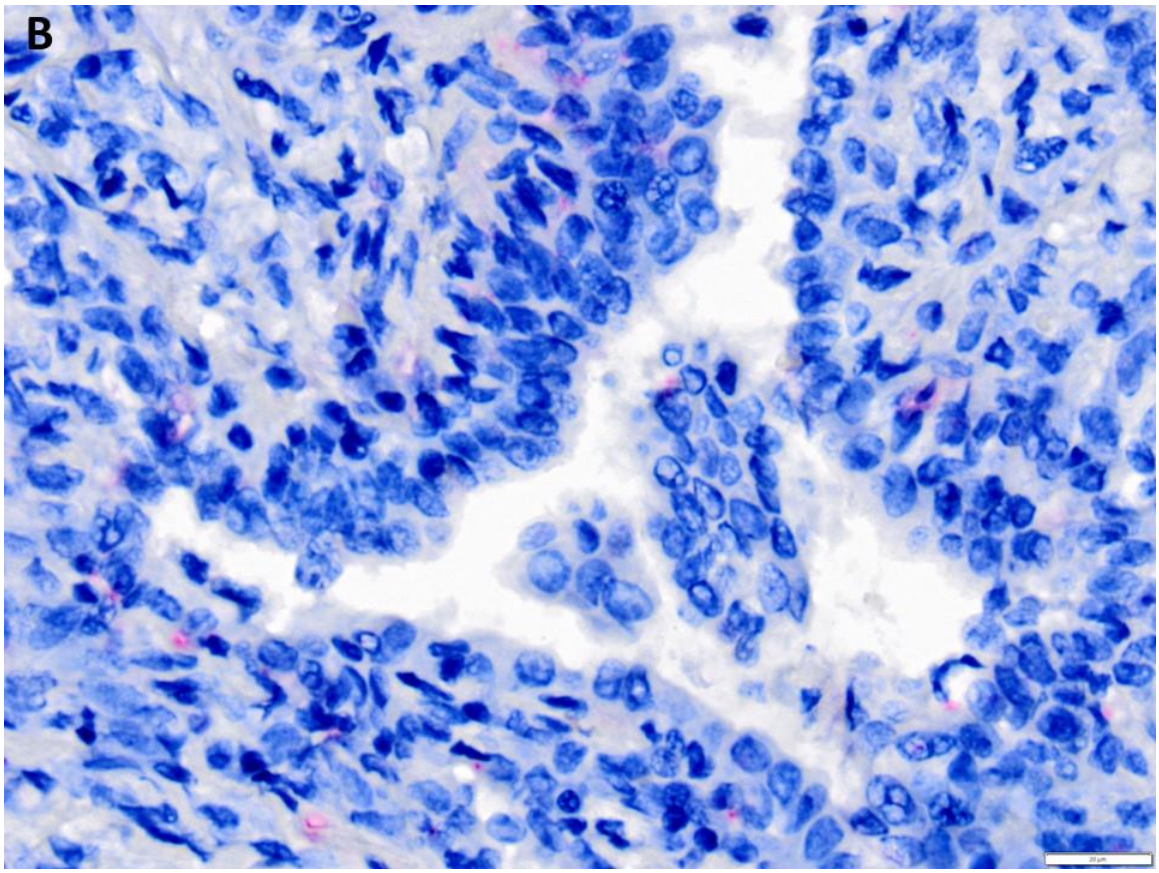
B

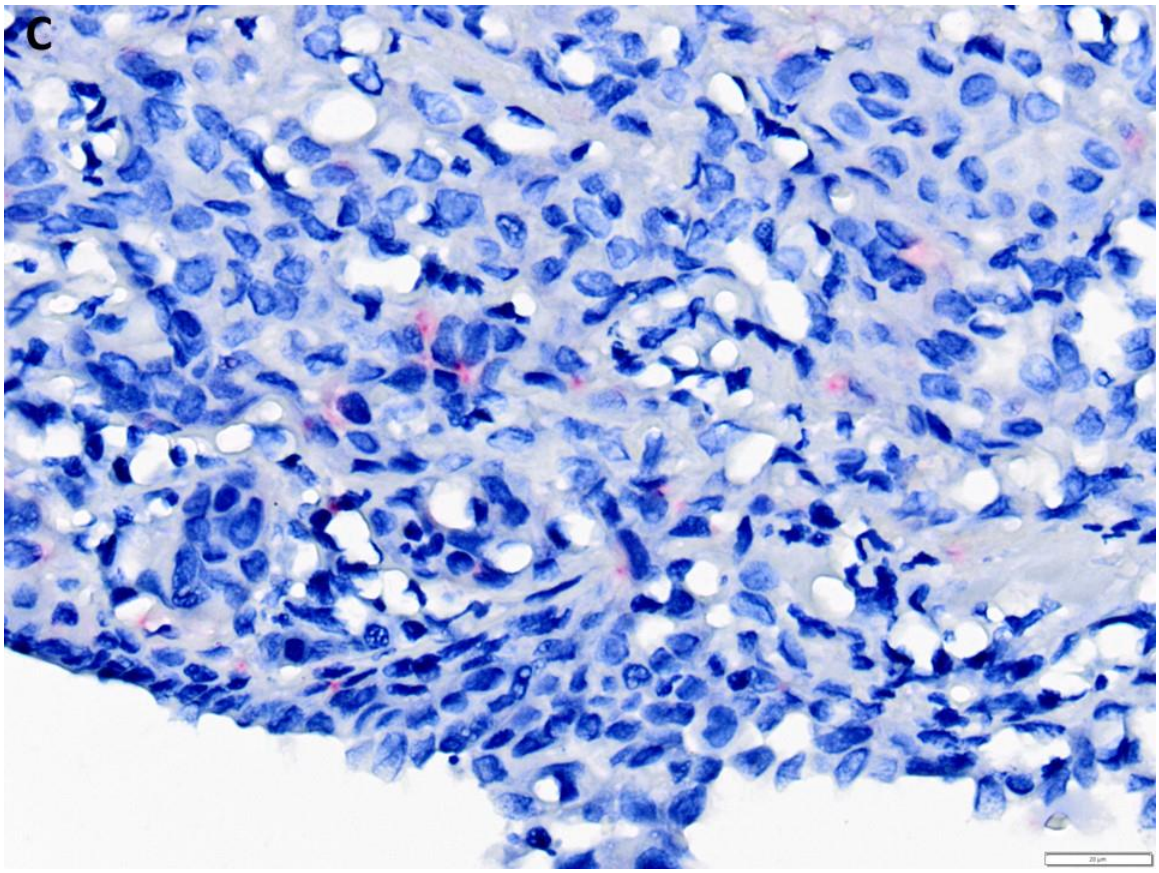

Figure 21. Representative photomicrographs from BaseScope™ *in situ hybridization* (ISH) assay. Each red dot represents an ISH probe bound to a single molecule of target pre-microRNA. The intensity of probe staining reflects the number of ZZ amplification linkers that bound to the original pre-miRNA hybridization probe, rather than different copy number of molecules, and is also influenced by batch differences in FastRed and hematoxylin stains. A = cfa-pre-miR-18a, Grade III anaplastic carcinoma; B = cfa-pre-miR-19b, Grade I carcinoma in situ; C = cfa-pre-miR-34c, Grade II solid carcinoma. Alkaline phosphatase based detection system; FastRed chromogen; hematoxylin tissue counterstain. x400 magnification, scale bar = 20 µm.

There was no statistically significant difference in pre-miRNA expression by inflammatory status, lymphatic invasion, or grade. Expression of the precursor miRNA did not significantly correlate with serum miR-18a, miR-19b, or miR-34c expression by RNAseq or dPCR (Table 12).

Table 12: Correlation between tumor pre-miRNA ISH and circulating miRNA expression.

Comparison	Pearson's r	p-value
Tissue pre-miR-18a ISH vs serum miR-18a (RNAseq)	-0.574	0.083
Tissue pre-miR-18a ISH vs serum miR-18a (dPCR)	0.490	0.150
Tissue pre-miR-19b ISH vs serum miR-19b (RNAseq)	-0.125	0.730
Tissue pre-miR-19b ISH vs serum miR-19b (dPCR)	-0.039	0.915
Tissue pre-miR-34c ISH vs serum miR-34c (RNAseq)	-0.370	0.292
Tissue pre-miR-34c ISH vs serum miR-34c (dPCR)	0.011	0.975

Section 4.4. Discussion

To investigate the potential for serum miRNA to predict relevant prognostic factors, circulating cfa-miR-18a, cfa-miR-19b, cfa-miR-29b, cfa-miR-34c, cfa-miR-122, cfa-miR-125a, and cfa-miR-181a were compared among CMT subgroups for those with inflammatory carcinoma, Grade III versus Grade I/IItumors and presence or absence of lymphatic invasion, as these are well-known histopathologic factors that impact patient outcome (Rasotto et al., 2017; Clemente et al., 2010; Perez Alenza et al., 2001).

Circulating miR-18a by RNAseq was significantly higher in dogs with histologic evidence of tumor lymphatic invasion. In addition, miR-18a by RNAseq was prominently higher in dogs with Grade III tumors, though this narrowly missed statistical significance ($p=0.051$). Thus, circulating miR-18a merits further evaluation as a possible predictive marker of metastasis and possible high-grade CMT tumors in larger prospective longitudinal studies. Additionally, given that serum miR-18a expression was significantly different by RNAseq but not dPCR, the impact of assay methodology on quantification between RNAseq, dPCR and qPCR should be investigated, and a consensus gold standard should be established.

No other serum miRNA were significantly different between lymphatic invasion, inflammatory carcinoma, or high-grade status by RNAseq or dPCR methods. Regardless, the promising circulating miRNA identified in Chapters 2 and 3 should still be evaluated in a large prospective cohort. For many of these histopathologic parameters, the group sizes were very small ($n=3$ for Grade III tumors and inflammatory carcinoma), which likely decreased the statistical power to detect any small but real changes. Finally, the number of histologic subtypes were too variable to compare serum miRNA expression statistically, but subtypes such as micropapillary and cribriform mammary carcinomas are known to have a worse prognosis, so a larger sample size may be able to study the relationship of miRs to these rarer variants.

There was no statistically significant correlation between circulating miRNA and survival times for the 8/10 dogs where that data was available. However, it is difficult to draw definitive conclusions from this patient population for several reasons. First, the sample size was modest and did not include two of the CMT patients. Second, the

treatment protocols and clinical course varied widely between patients in the cohort. Patients MC2, MC5, and MC6 were treated with an experimental dendritic cell fusion vaccine and gemcitabine following surgical resection of the CMT (Bird et al., 2019). Three additional dogs (MC4, MC7, and MC9), received this same protocol, but developed inflammatory mammary carcinoma and died shortly thereafter. Two patients received only surgical resection of their tumor with no follow-up chemotherapy, radiation treatment, or other adjunctive therapy. A prospective study with a far larger sample size is necessary to determine what relationship, if any, there is between these circulating miRNA and response to treatment, progression free survival, risk of relapse, and overall survival.

Unfortunately, it was not possible to evaluate the association of hormone receptor status and tissue or circulating miRNA as the IHC assay was non-diagnostic. ER and PR IHC are non-standard assays that typically use modified anti-human monoclonal antibodies, and very few veterinary laboratories run this test (EJF, personal communications). qPCR for ER and PR mRNA was considered, but rejected based on concerns that formalin-fixation and prolonged storage (in some cases a decade or more) of FFPE tissues would induce too much degradation of RNA and subsequent uncertainty about any results. Future research should directly evaluate the impact of miRNA on ER and PR expression through *in vitro* studies that transfect relevant miRNA mimics and inhibitors to CMT cell lines and measure resulting mRNA and protein expression changes by qPCR and western blot/flow cytometry, respectively.

The preliminary ISH results document that the precursors for miR-18a, miR-19b, and miR-34c were primarily expressed by neoplastic ductular and tubular mammary

epithelial cells, and to a lesser extent, normal mammary epithelial cells, rather than skin, adnexa, stroma, inflammatory cells, etc. The expression of these precursor miRNA by tumor cells could suggest they are one probable source of these miRNA in serum, although the quantification of precursors in tissue did not correlate with the circulating mature miRNA (Table 3). One possible reason for this mismatch is many tumors develop defects in exportin-5 or other proteins in the pri-miRNA/pre-miRNA/mature maturation pathway that impair normal miRNA processing (Melo et al., 2010). Another possibility that cannot be neglected is that additional tissues throughout the body contribute miRNA to the circulating pool in serum. For example, a previous CMT study showed that primary and metastatic tumors from the same patient can have divergent miRNA expression patterns (Bulkowska et al., 2017).

Chapter 5: Conclusions

Canine mammary tumors (CMT) are one of the most common forms of cancer in reproductively-intact female dogs and share numerous clinical and molecular features with women with breast cancer. Key among these are shared genetic features such as alterations to estrogen, progesterone, and HER-2 hormone receptors, as well as loss of function of tumor suppressor genes like p16/INK4A, PTEN, and p53 (Pinho et al., 2012). Recently, microRNA have been shown to be dysregulated in both breast cancer and CMT, and miR-141 may directly cause decreased p16 expression (Lutful Kabir et al., 2015). Multiple studies have identified miRNA such as miR-29b and miR-181a that are up-regulated in canine mammary carcinoma cell lines and tumor tissue (Boggs et al., 29b, Lutful Kabir, 2014). The miRNA profile of CMT even varies between primary and metastatic tumors in the same patient (Bulkowska et al., 2017). Studies evaluating candidate circulating miRNA biomarkers found plasma miR-126 and miR-214 were up-regulated in mammary carcinoma, along with multiple other types of carcinomas and sarcomas (Heishima et al., 2017).

The research in this dissertation set forth to explore the possible role of secreted exosomes and miRNA as diagnostics biomarkers in CMT, and their correlation with histopathologic and molecular tumor features. In Chapter 2, we demonstrated that conditioned media from both normal and malignant canine mammary epithelial cells contains numerous extracellular vesicles ~150-200 nm in size that express CD9 antigen, compatible with exosomes. These CMT exosomes are broadly similar to exosomes

previously identified in urine from dogs with chronic renal disease (Ichii et al., 2017) and plasma from dogs with myxomatous mitral valve disease (Yang et al., 2017).

Small RNA deep-sequencing (RNAseq) of this exosome-rich conditioned media revealed hundreds of miRNA, many of which were significantly different between CMT and CMEC groups.. Some of the most significantly up-regulated exosomal miRNA in CMT *in vitro* include cfa-miR-18a, cfa-miR-19a/b, cfa-miR-29b/c, cfa-miR-34c, and cfa-miR-181a/c. Several of these, such as miR-19a/b, miR-18a, miR-29b, and miR-181c were previously shown to be up-regulated in three of these parent CMT cell lines by qRT-PCR microarray (Lutful Kabir, 2014). miR-29b was one of a few miRNA up-regulated in CMT and specifically tubular-papillary carcinoma tumor tissue by qRT-PCR (Boggs et al., 2008). RNAseq results of three miRNA of interest—miR-18a, miR-19a, and miR-181a—were validated by qRT-PCR.

Chapter 3 evaluated serum miRNA from clinical patients with CMT and a cohort of healthy intact and spayed female dogs. Our hypothesis was that the serum miRNA profile would bear similarity to the exosomal miRNA identified in cell culture because one of the main sources of circulating microRNA (but not the only source) are exosomes secreted by tumor cells. RNAseq revealed differential expression of numerous miRNA between CMT and healthy dogs. Many of the up-regulated circulating miRNA in these patients were indeed similar to the cell culture exosome profile identified in Chapter 2, including miR-18a, miR-19b, miR-29b/c, miR-34c, miR-181c, miR-215, and miR-345.

In silico bioinformatics analysis in Chapters 2 and 3 sheds light on the individual genes and processes/pathways regulated by this cohort of miRNA. Genes enriched in the exosomal miRNA seed sequence targets above expected for chance include those for

epithelial tissue and mammary gland development (ESR1, FRS2, HIF1A, PDE4D). Other relevant pathways included oncogenes involved in cell proliferation (E2F8, LRP2, MDM4, APPL1, and ANXA7) and MAPK signaling (RAP1A, RAP1B, RAPGEF2, TAOK1, ATF2, CACNA1C, MAPK8, MAP3K12 and RPS6KA5). Circulating miRNA were predicted to target a number of critical oncogenes and those impacting the EMT and metastatic behavior.

Several of these serum miRNA showed promising ability to discriminate clinical CMT patients from healthy controls. The best raw diagnostic performance overall was for serum miR-125a, with an ROC-AUC of 0.930. However, the discrepancy in direction of fold-regulation (up-regulated in dPCR versus down-regulated in RNAseq) merits further exploration of the reasons for mismatch and limits excitement about this marker. Serum miR-19b, on the other hand, had a strong initial diagnostic performance with an ROC-AUC of 0.880, diagnostic sensitivity that ranged from good to perfect (80% at 13,000 copies/uL cut-off to 100% at 11,600 copies/uL cut-off), and diagnostic specificity that ranged from good to high (80% at 11,600 copies/uL cut-off and 90% at 13,000 copies/uL cut-off). Serum miR-19b revealed another interesting data point: One of the outlier healthy controls HS3 had the highest absolute circulating miR-19b concentration of any subject in the study, and on clinical follow-up developed cancer with pulmonary metastasis from an unknown primary tumor within the next year. Besides the association with BC/CMT, up-regulated serum/plasma miR-19b has been identified as a candidate biomarker for people with gastric cancer (Wang et al., 2017), prostatic cancer (Zou et al., 2019), and non-small-cell lung cancer (Wu et al., 2014), raising the tantalizing possibility that the very high miR-19b in HS3 was not an aberrant outlier but increased in blood

early before a tumor was clinically apparent. This hypothesis merits close analysis in a follow-up study.

Chapter 4 explored the relationship of circulating miRNA to clinical parameters such as survival time and histopathologic characteristics. While the serum miRNA evaluated generally did not show statistical correlation with survival or statistical differences between the tumor characteristics, circulating miR-18a by RNAseq was significantly higher in patients with lymphatic invasion (metastasis) and near the boundary of significance for Grade III tumor patients. This echoes the findings of Bulkowska et al. (2017) that identified a number of miRNA, including miR-18a, that were up-regulated in Grade III tumors relative to Grade I/II. This raises the possibility that some peripheral blood miRNA, such as serum miR-18a, may non-invasively predict tumor histopathologic characteristics. If verified by larger studies, this suggests a panel of miRNA may provide additional prognostic information to veterinarians when a mammary mass is detected on initial examination.

Chapter 4 also evaluated the expression of precursor miRNA for pre-miR-18a, pre-miR-19b, and pre-miR-34c in these 10 CMT biopsy tissues by ISH. These pre-miRNA were all expressed by neoplastic CMT cells, with minimal presence in adjacent stroma, adnexa, or inflammatory cells. This indicates that one probable source of the serum miRNA in these patients is the tumor itself. However, there was no correlation between pre-miRNA and mature circulating miRNA. This is not totally unexpected, as tumors may have alterations in pre-miRNA processing that affect export (Melo et al., 2010). Multiple tissues can also contribute to a given serum miRNA level.

This research represents the first comprehensive profiling of exosomal and serum microRNA in dogs with CMT. The microRNA expression by exosome-enriched cell-free media and CMT patient sera in this dissertation bears some similarities as well as differences to results from other previously published microRNA studies for this tumor type, summarized in Table 13.

Table 13: Comparison of results from other microRNA biomarker studies for CMT. Differences in analytical methods, fold-regulation, and specific features are listed. The reference "Fish, 2019" refers to this dissertation.

microRNA	Sample Type	Analytical methods	Direction Change	Biomarker/Biological Role	Reference(s)
miR-15a	Tumor tissue; serum	qPCR, RNAseq	Down-regulated (tissue); up-regulated (serum)	Significantly lower in ductal carcinoma subtype tissue. Higher in CMT patient sera by RNAseq.	Boggs et al., 2008; Fish et al., 2018
miR-16	Tumor tissue	qPCR	Down-regulated	Significantly lower in ductal carcinoma subtype.	Boggs et al., 2008
miR-18a	Cultured CMT cells; tumor tissue; exosomes; serum	qPCR microarray, hybridization microarray, RNAseq, qPCR	Up-regulated (cells, exosomes, serum, and Grade III tumors); down-regulated (Grade I/II tumors)	Serum levels associated with lymphatic invasion and possibly tumor grade. Differential expression by tumor grade (up-regulated in high grade tumors, down-regulated in low grade tumors).	Lutful Kabir, 2014; Boggs et al., 2008; Fish et al., 2018; Fish, 2019
miR-19a	CMT cells; tumor tissue; exosomes; serum	qPCR microarray, hybridization microarray, RNAseq, qPCR	Up-regulated (cells, exosomes, serum, and Grade III tumors); down-regulated (Grade I/II tumors)	Differential expression by tumor grade.	Lutful Kabir, 2014; Boggs et al., 2008; Fish et al., 2018; Fish, 2019
miR-19b	Cultured CMT cells; tumor tissue; serum	qPCR microarray, hybridization microarray, RNAseq, qPCR, dPCR	Up-regulated (cells, serum, and Grade III tumors); down-regulated (Grade I/II tumors)	Serum levels had robust diagnostic performance. May be increased early in malignancy before systemic signs available. Differential expression by tumor grade.	Lutful Kabir, 2014; Bulkowska et al., 2017; Fish, 2019
miR-21	Cultured CMT cells; tumor tissue; exosomes	qPCR microarray, hybridization microarray, qPCR, RNAseq	Up-regulated (Generic CMT; Grade III tumors); Down-regulated (exosomes; Grade I/II tumors)	Significantly higher in all CMT tissue (Boggs); high in Grade III tumors (Bulkowska); down-regulated in Grade I/II tumors; down-regulated in CMT exosomes.	Lutful Kabir, 2014; Boggs et al., 2008; Fish et al., 2018
miR-29b	Tumor tissue; cultured CMT cells; serum	qPCR, qPCR microarray, RNAseq, dPCR	Up-regulated	Significantly higher in all CMT tissue, cultured CMT cells; serum.	Boggs et al., 2008; Lutful Kabir 2014; Fish, 2019
miR-29c	Tumor tissue, serum	Hybridization microarray, qPCR, RNAseq, dPCR	Down-regulated (tissue); up-regulated (serum)	Down-regulated in metastatic and non-metastatic tumor samples; up-regulated in serum.	Bulkowska et al., 2017; Fish 2019
miR-125a	Serum; tumor tissue	Hybridization microarray, qPCR, RNAseq, dPCR	Down-regulated (serum by RNAseq; Grade III tumors); up-regulated (serum by dPCR; Grade I/II tumors)	Divergent expression in serum based on analytical method (down-regulated RNAseq, up-regulated dPCR). Differential expression by grade. dPCR expression had strong diagnostic performance.	Fish, 2019; Bulkowska et al., 2017
miR-126	Serum; exosomes	qPCR, RNAseq, dPCR	Up-regulated	Up-regulated in CMT exosomes and serum from dogs with a variety of tumors (including mammary carcinoma).	Heishima et al., 2017; Fish et al., 2018; Fish, 2019
miR-141	Cultured CMT cells	qPCR microarray	Up-regulated	Experimentally validated to down-regulate p16/INK4A (Luciferase reporter assay).	Lutful Kabir et al., 2015
miR-181a	Cultured CMT cells; exosomes; tumor tissue	Hybridization microarray, qPCR, qPCR microarray, RNAseq	Up-regulated (cells; exosomes; Grade III tumors); down-regulated (Grade I/II tumors)	Upregulated in cultured cells and exosomes. Differential expression in tumor tissue.	Lutful Kabir, 2014; Fish et al., 2018; Bulkowska et al., 2017
miR-181b	Tumor tissue; cultured CMT cells	qPCR, qPCR microarray	Up-regulated	Significantly higher in tubular papillary subtype tissue and CMT cells.	Boggs et al., 2008; Lutful Kabir, 2014
miR-181c	Exosomes; serum	RNAseq, qPCR, dPCR	Up-regulated	Significantly higher in both CMT exosomes in culture and clinical CMT patient sera.	Fish et al., 2018; Fish, 2019
miR-214	Serum; exosomes; tumor tissue	Hybridization microarray, qPCR, RNAseq, dPCR	Up-regulated (Serum; Grade I/II tumors); Down-regulated (exosomes; Grade III tumors)	Up-regulated in serum from dogs with a variety of tumors (including mammary carcinoma), down-regulated in CMT exosomes. Differential expression by grade.	Heishima et al., 2017; Fish et al., 2018

Unique to this project, the complementary use of three different modalities for profiling (RNAseq, qRT-PCR, and dPCR) makes the results robust, and allowed detecting all possible miRNA, including novel sequences, rather than the limited set for which current qPCR probes and microarrays exist. This data indicates that several circulating miRNA, including miR-19b, and potentially miR-34c and miR-125a, have good ability to discriminate patients with CMT from healthy intact and spayed female dog. Serum miR-18a may be associated with patients that have metastasis and high-grade tumors. Figure 22 illustrates a proposed model for the biological and diagnostic role of these exosomal and circulating miRNA in CMT.

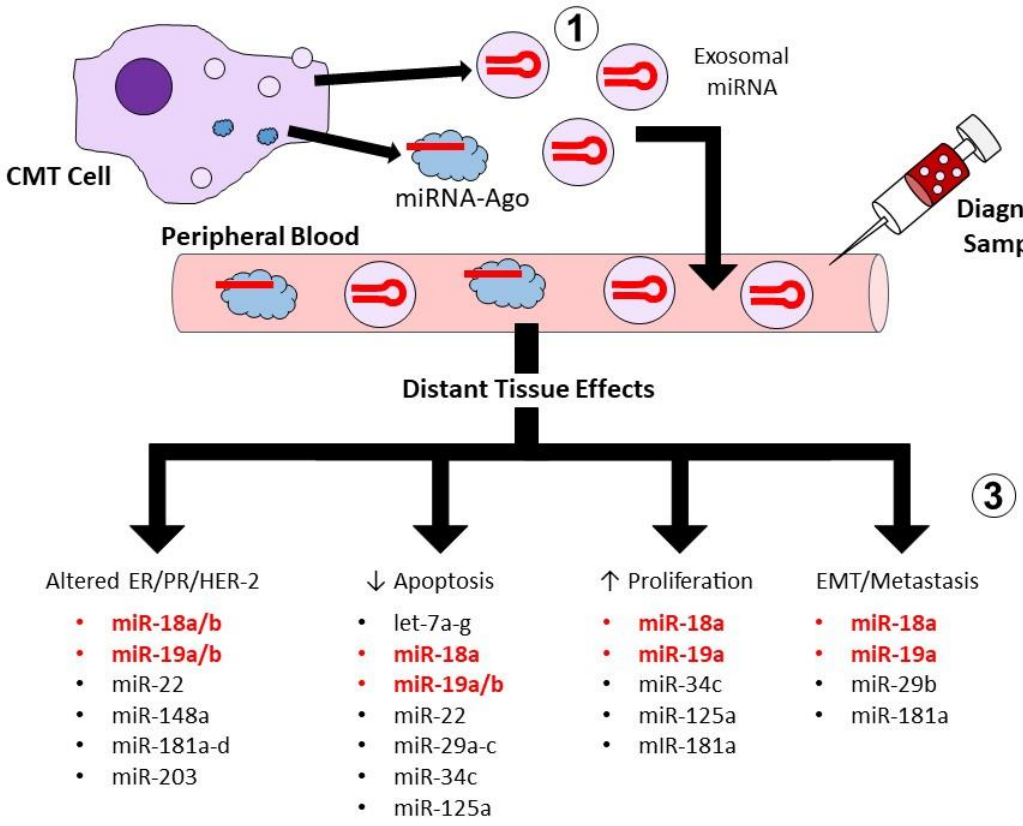

Figure 22. Proposed model of CMT circulating miRNA secretion and effects. (1) CMT secrete miRNA into adjacent tissues and peripheral blood through exosomes and/or bound to proteins such as Argonaute (AGO); See Chapter 2. (2) These exosomal miRNA and/or AGO-miRNA enter peripheral blood, allowing sampling for diagnostic applications. Many of these miRNA, particularly miR-19b, can discriminate CMT patients from controls with good diagnostic accuracy; See Chapter 3. (3) *In silico* analysis in Chapters 2 and 3 show that these exosomal and circulating miRNA are predicted to regulate genes that alter hormone receptors ER/PR/HER-2/EGFR; decrease cytostasis and apoptosis through tumor suppressors like PTEN, Rb, and p53; promote EMT, metastasis and chemoresistance; and positively regulate cell cycle proliferation. Chapter 4 demonstrated that at least one of these circulating miRNA, miR-18a, correlates with clinical tumor behavior including lymphatic invasion (metastasis) and high grade mammary carcinoma. miR-18 and miR-19 genes are bolded in red to highlight their influence on all four processes and their proposed utility for diagnostic (miR-19b) or prognostic (miR-18a) purposes.

Obviously, the bar of correctly identifying dogs with cancer from healthy dogs is a modest one, and larger clinical studies need to verify the performance of these circulating miRNA against dogs with other forms of neoplasia, non-neoplastic mammary pathology/hyperplasia (i.e. mastitis, lactation, pregnancy), and a wide variety of confounding system illnesses.

This research illustrates the need to determine the optimal method for miRNA quantification and establishing standardization. The four techniques used to profile miRNA in this dissertation (RNAseq, qRT-PCR, dPCR, and pre-miRNA-ISH) found some results that were concordant, and others that were discordant. Each of these operates on different underlying molecular principles, so some mismatch is likely inevitable. Wherever possible, results from two or more modalities were provided side-by-side to allow comparison, since there is no single gold-standard test. For findings such as up-regulation of miR-19b that were consistent across *in vitro* and clinical studies, and different sequencing and PCR assays, we have high confidence in the robustness of that data. Indeed, miR-19b represents one of the most viable diagnostic biomarkers identified in this research. For others, such as miR-18a, that appeared to be a promising marker of metastasis and high-grade CMT, but had divergent results between RNAseq and PCR, we can only recommend follow-up with larger-scale prospective longitudinal clinical studies.

This research raised a number of unanswered questions that inform future directions for our research. The CMT exosomes contained miRNA cargo predicted to drive neoplastic transformation, invasion, and aggressive behavior. Whether or not these exosomes actually exert these biological effects is currently unknown. This could be validated by incubating conditioned media from CMT cells with CMEC cells, normal canine fibroblasts, and other cell types, and observing any changes to proliferation rate, survival, anoikis, and EMT-like behavior. Likewise, the *in silico* target prediction provides compelling evidence that these exosomal and circulating miRNA regulate hormone receptors, but the lack of reliable ER/PR IHC prevents drawing any inferences about the ability for these to be associated with changes to hormone receptors *in vivo*.

The best way to experimentally address this problem would be to transfect CMT and CMEC cells *in vitro* with synthetic miRNA mimics and inhibitors for miR-18a, miR-19b, miR-181a and others, then study changes to candidate genes such as ESR1 and PTEN by qRT-PCR and western blot. Finally, the diagnostic and prognostic utility of these serum miRNA needs to be evaluated prospectively in a large cohort over time to determine any correlations with response to treatment and survival.

References

1. Agostini, M., and Knight, R. A. (2014). miR-34: from bench to bedside. Oncotarget. 5(4), 872–881.

2. Aguilera-Rojas, M., Badewien-Rentzsch, B., Plendl, J., Kohn, B., and Einspanier, R. (2018). Exploration of serum- and cell culture-derived exosomes from dogs. BMC Vet. Res. 14(1), 179.

3. Antolín S., Calvo L., Blanco-Calvo M., Santiago M.P., Lorenzo-Patiño M.J., Haz-Conde M., Santamarina, I., Figueroa, A., Antón-Aparicio, L.M., and Manuel Valladares-Ayerbes, M. (2015). Circulating miR-200c and miR-141 and outcomes in patients with breast cancer. BMC Cancer. 15:297.

4. Baer, C., Claus, R., Frenzel, L.P., Zucknick, M., Park, Y.J., Gu, L. Weichenhan, D., Fischer, M., Pallasch, C.P., Herpel, E., et al. (2012). Extensive promoter DNA hypermethylation and hypomethylation is associated with aberrant microRNA expression in chronic lymphocytic leukemia. Cancer Res. 72(15), 3775–3785.

5. Bahmanpour, Z., Sheervalilou, R., Choupani, J., Shekari Khaniani, M., Montazeri, V., and Mansoori Derakhshan, S. (2019). A new insight on serum microRNA expression as novel biomarkers in breast cancer patients. J. Cell. Physiol. 1–13. DOI: 10.1002/jcp.28656.

6. Bailey, W. J., Barnum, J. E., Erdos, Z., Lafranco-Scheuch, L., Lane, P., Vlasakova, K., Sistare, F.D., and Glaab, W. E. (2019). A performance evaluation of liver and skeletal muscle-specific miRNAs in rat plasma to detect drug-induced injury. Toxicol. Sci. 168(1), 110–125.

7. Baioni, E., Scanziani, E., Vincenti, M. C., Leschiera, M., Bozzetta, E., Pezzolato, M., Desiato, R., Bertolini, S., Maurella, C., and Ru, G. (2017). Estimating canine cancer incidence: findings from a population-based tumour registry in northwestern Italy. BMC Vet. Res. 13(1), 203.

8. Bartel, D.P. (2004). MicroRNAs: Genomics, biogenesis, mechanism, and function. Cell. 116(2), 281–297.

9. Baxter, A.A., Phan, T.K., Hanssen, E., Liem, M., Hulett, M.D., Mathivanan, S., and Poon, I.K.H. (2019). Analysis of extracellular vesicles generated from monocytes under conditions of lytic cell death. Sci. Rep. 9(1), 7538.

10. Beauvais, W., Cardwell, J.M., and Brodbelt, D.C. (2012). The effect of neutering on the risk of mammary tumours in dogs - a systematic review. J. Small Anim. Pract. 53(6), 314–322.

11. Benjamin, S.A., Lee, A.C., and Saunders, W.J. (1999). Classification and behavior of canine mammary epithelial neoplasms based on life-span observations in beagles. Vet. Pathol. 36(5), 423–436.

12. Berezikov, E. (2011). Evolution of microRNA diversity and regulation in animals. Nat. Rev. Genet. 12(12), 846–860.

13. Bernstein, E., Kim, S.Y., Carmell, M.A., Murchison, E.P., Alcorn, H., Li, M.Z., Mills, A.A., Elledge, S.J., Anderson, K.V., and Hannon, G.J. (2003). Dicer is essential for mouse development. Nature Genet. 35(3), 215–217.

14. Bhardwaj, P., Au, C.C., Benito-Martin, A., Ladumor, H., Oshchepkova, S., Moges, R., and Brown, K.A. (2019). Estrogens and breast cancer: Mechanisms involved in

obesity-related development, growth and progression. J. Steroid Biochem. Mol. Biol. 189, 161–170.

15. Bird, R.C., DeInnocentes, P., Church Bird, A.E., van Ginkel, F.W., Lindquist, J., and Smith, B.F. (2011). An autologous dendritic cell canine mammary tumor hybrid-cell fusion vaccine. Cancer Immunol. Immunother. 60(1), 87–97.

16. Bird, R.C., DeInnocentes P., Bird, C.A., Lutful Kabir, F.M., Martinez-Romero, E.G., Smith, A.N., Smith, B.F. (2019). Autologous hybrid cell fusion vaccine in a spontaneous intermediate model of breast carcinoma. J Vet Sci (Under Review).

17. Block, G.E., Jensen, E.V, and Polley, T.Z. (1975). The prediction of hormonal dependency of mammary cancer. Ann. Surge. 182(3), 342–352.

18. Boggs, R.M., Wright, Z.M., Stickney, M.J., Porter, W.W., and Murphy, K.E. (2008). MicroRNA expression in canine mammary cancer. Mamm. Genome. 19(7-8), 561-9.

19. Borge, K.S., Nord, S., Van Loo, P., Lingjærde, O.C., Gunnes, G., Alnæs, G.I.G., Solvang, H.K., Lüders, T., Kristensen, V.N., Børresen-Dale, A.L., et al. (2015). Canine mammary tumours are affected by frequent copy number aberrations, including amplification of MYC and loss of PTEN. PLoS One. 10(5), e0126371. doi: 10.1371/journal.pone.0126371.

20. Bulkowska, M., Rybicka, A., Senses, K.M., Ulewicz, K., Witt, K., Szymanska, J., Taciak, B., Klopfleisch, R., Hellmén, E., Dolka, I., et al. (2017). MicroRNA expression patterns in canine mammary cancer show significant differences between metastatic and non-metastatic tumours. BMC Cancer. 17(1), 728.

21. Calin, G.A., Dumitru, C.D., Shimizu, M., Bichi, R., Zupo, S., Noch, E., Aldler, H., Rattan, S., Keating, M., Rai, K., et al. (2002). Nonlinear partial differential equations and

applications: Frequent deletions and down-regulation of micro- RNA genes miR15 and miR16 at 13q14 in chronic lymphocytic leukemia. Proc. Natl. Acad. Sci. 99(24), 15524–15529.

22. Calle, E.E., and Kaaks, R. (2004). Overweight, obesity and cancer: epidemiological evidence and proposed mechanisms. Nat. Rev. Cancer. 4(8), 579–591.

23. Campomenosi, P., Gini, E., Noonan, D. M., Poli, A., D'Antona, P., Rotolo, N., Dominioni, L., and Imperatori, A. (2016). A comparison between quantitative PCR and droplet digital PCR technologies for circulating microRNA quantification in human lung cancer. BMC Biotechnol. 16(1), 60. doi: 10.1186/s12896-016-0292-7.

24. Campo-Paysaa, F., Sémon, M., Cameron, R.A., Peterson, K.J., and Schubert, M. (2011). microRNA complements in deuterostomes: origin and evolution of microRNAs. Evol. Dev. 13(1), 15–27.

25. Canadas, A., França, M., Pereira, C., Vilaça, R., Vilhena, H., Tinoco, F., Silva, M.J., Ribeiro, J., Medeiros, R., Oliveira, P., et al. (2019). Canine mammary tumors: Comparison of classification and grading methods in a survival study. Vet. Pathol. 56(2), 208–219.

26. Carthew, R.W., and Sontheimer, E.J. (2009). Leading edge review origins and mechanisms of miRNAs and siRNAs. Cell. 136(4):642-55.

27. Cassali, G.D., Gobbi, H., Malm, C., and Schmitt, F.C. (2007). Evaluation of accuracy of fine needle aspiration cytology for diagnosis of canine mammary tumours: comparative features with human tumours. Cytopathology. 18(3):191-6.

28. Chang, S.C., Chang, C.C., Chang, T.J., and Wong, M.L. (2005). Prognostic factors associated with survival two years after surgery in dogs with malignant mammary tumors: 79 cases (1998-2002). J. Am. Vet. Med. Assoc. 15:227(10),1625-9.

29. Chang, T.C., Wentzel, E.A., Kent, O.A., Ramachandran, K., Mullendore, M., Lee, K. H., Feldmann, G., Yamakuchi, M., Ferlito, M., Lowenstein, C.J., et al. (2007). Transactivation of miR-34a by p53 broadly influences gene expression and promotes apoptosis. Mol. Cell. 26(5), 745–752.

30. Chang, C.C., Tsai, M.H., Liao, J.W., Chan, J.P., Wong, M.L., and Chang, S.C. (2009). Evaluation of hormone receptor expression for use in predicting survival of female dogs with malignant mammary gland tumors. J. Am. Vet. Med. Assoc. 15;235(4), 391-6.

31. Charrin, S., Jouannet, S., Boucheix, C., Rubinstein, E. (2014). Tetraspanins at a glance. J. Cell. Sci. 127, 3641-3648.

32. Chen, Y.C., Chen, Y.Y., Liao, J.W., and Chang, S.-C. (2018). Expression and prognostic value of c-met in canine mammary tumours. Vet. Comp. Oncol. 16(4), 670–676.

33. Cheng, L., Sharples, R.A., Scicluna, B.J., and Hill, A.F. (2014). Exosomes provide a protective and enriched source of miRNA for biomarker profiling compared to intracellular and cell-free blood. J. Extracell. Vesicles. 3: 10.3402/jev.v3.23743.

34. Cho, H.S., Mason, K., Ramyar, K.X., Stanley, A.M., Gabelli, S.B., Denney, D.W., and Leahy, D.J. (2003). Structure of the extracellular region of HER2 alone and in complex with the Herceptin Fab. Nature. 421(6924), 756–760.

35. Christodoulou, F., Raible, F., Tomer, R., Simakov, O., Trachana, K., Klaus, S.,

Snyman, H., Hannon, G.J., Bork, P., and Arendt, D. (2010). Ancient animal microRNAs and the evolution of tissue identity. Nature. 463(7284), 1084–1088.

36. Chu, C.P., and Nabity, M.B. (2019). Comparison of RNA isolation and library preparation methods for small RNA sequencing of canine biofluids. Vet. Clin. Pathol. doi: 10.1111/vcp.12743. [Epub ahead of print]

37. Cimmino, A., Calin, G.A., Fabbri, M., Iorio, M.V., Ferracin, M., Shimizu, M., Wojcik, S.E., Aqeilan, R.I., Zupo, S., Dono, M., et al. (2005). miR-15 and miR-16 induce apoptosis by targeting BCL2. Proc. Natl. Acad. Sci. 102(39), 13944–13949.

38. Ciravolo, V., Huber, V., Ghedini, G. C., Venturelli, E., Bianchi, F., Campiglio, M., Morelli, D., Villa, A., Della Mina, P., Menard, S., et al. (2012). Potential role of HER2-overexpressing exosomes in countering trastuzumab-based therapy. J. Cell. Physiol. 227(2), 658–667.

39. Clemente, M., Pérez-Alenza, M.D., and Peña, L. (2010). Metastasis of canine inflammatory versus non-inflammatory mammary tumours. J. Comp. Pathol. 143(2–3), 157–163.

40. Croce, C.M. (2009). Causes and consequences of microRNA dysregulation in cancer. Nat. Rev. Genet. 10(10), 704–714.

41. Dadiani, M., Bossel Ben-Moshe, N., Paluch-Shimon, S., Perry, G., Balint, N., Marin, I., Pavlovski, A., Morzaev, D., Kahana-Edwin, S., Yosepovich, A., et al. (2016). Tumor evolution inferred by patterns of microRNA expression through the course of disease, therapy, and recurrence in breast cancer. Clin. Cancer. Res. 22(14), 3651–3662.

42. Dennis, G., Sherman, B.T., Hosack, D.A., Yang, J., Gao, W., Lane, H.C., and Lempicki, R.A. (2003). DAVID: Database for Annotation, Visualization, and Integrated Discovery. Genome Biol. 4(5), P3.

43. DeSantis, C.E., Miller, K.D., Goding Sauer, A., Jemal, A., and Siegel, R. L. (2019). Cancer statistics for African Americans, 2019. CA. Cancer J. Clin. 69(3), 211–233.

44. Dorn, C.R., Taylor, D.O., Schneider, R., Hibbard, H.H., and Klauber, M.R. (1968). Survey of animal neoplasms in Alameda and Contra Costa Counties, California. II. Cancer morbidity in dogs and cats from Alameda County. J. Natl. Cancer. Inst. 40(2), 307–318.

45. Egenvall, A., Bonnett, B. N., Öhagen, P., Olson, P., Hedhammar, Å., and Euler, H. von. (2005). Incidence of and survival after mammary tumors in a population of over 80,000 insured female dogs in Sweden from 1995 to 2002. Prev. Vet. Med. 69(1–2), 109–127.

46. Friedman, R.C., Farh, K.K.H., Burge, C.B., and Bartel, D.P. (2009). Most mammalian mRNAs are conserved targets of microRNAs. Genome Res. 19(1), 92–105.

47. Gam, L.H. (2012). Breast cancer and protein biomarkers. World J. Exp. Med. 2(5), 86–91.

48. Gamba, C.O., Dias, E.J., Ribeiro, L.G.R., Campos, L.C., Estrela-Lima, A., Ferreira, E., and Cassali, G.D. (2013). Histopathological and immunohistochemical assessment of invasive micropapillary mammary carcinoma in dogs: A retrospective study. Vet. J. 196(2), 241–246.

49. Garcia, D.M., Baek, D., Shin, C., Bell, G.W., Grimson, A., and Bartel, D. P. (2011). Weak seed-pairing stability and high target-site abundance decrease the proficiency of lsy-6 and other microRNAs. Nat. Struct. Mol. Biol. 18(10), 1139–1146.

50. Girgert, R., Emons, G., and Gründker, C. (2019). Estrogen signaling in ERα-negative breast cancer: ERβ and GPER. Front. Endocrinol. 9,781.

51. Goldschmidt, M., Peña, L., Rasotto, R., and Zappulli, V. (2011). Classification and grading of canine mammary tumors. Vet. Pathol. 48(1), 117–131.

52. Gonzalez-Villasana, V., Rashed, M.H., Gonzalez-Cantú, Y., Bayraktar, R., Luis Menchaca-Arredondo, J., Manuel Vazquez-Guillen, J., Rodriguez-Padilla, C., Lopez-Berestein, G., and Resendez-Perez, D. (2019). Presence of circulating miR-145, miR-155, and miR-382 in exosomes isolated from serum of breast cancer patients and healthy donors. Dis. Markers. Article ID 6852917, https://doi.org/10.1155/2019/6852917.

53. Grimm, S.L., Hartig, S.M., and Edwards, D.P. (2016). Progesterone receptor signaling mechanisms. J. Mol. Biol. 428(19), 3831–3849.

54. Grimson, A., Srivastava, M., Fahey, B., Woodcroft, B. J., Chiang, H. R., King, N., Degnan, B.M., Rokhsar, D.S., and Bartel, D.P. (2008). Early origins and evolution of microRNAs and Piwi-interacting RNAs in animals. Nature. 455(7217), 1193–1197.

55. Griffiths-Jones, S., Hui, J.H.L., Marco, A., and Ronshaugen, M. (2011). MicroRNA evolution by arm switching. EMBO Rep. 12(2), 172–177.

56. Grishok, A., Pasquinelli, A. E., Conte, D., Li, N., Parrish, S., Ha, I., Baillie, D.L., Fire, A., Ruvkun, G., and Mello, C.C. (2001). Genes and mechanisms related to RNA interference regulate expression of the small temporal RNAs that control C. elegans developmental timing. Cell. 106(1), 23–34.

57. Guo, L., Zhao, Y., Yang, S., Cai, M., Wu, Q., and Chen, F. (2013). Genome-wide screen for aberrantly expressed miRNAs reveals miRNA profile signature in breast cancer. Mol. Biol. Rep. 40(3), 2175–2186.

58. Gurunathan, S., Kang, M.-H., Jeyaraj, M., Qasim, M., & Kim, J.-H. (2019). Review of the isolation, characterization, biological function, and multifarious therapeutic approaches of exosomes. Cells. 8(4), 307.

59. Hahn, W.C., Counter, C.M., Lundberg, A.S., Beijersbergen, R.L., Brooks, M.W., and Weinberg, R.A. (1999). Creation of human tumour cells with defined genetic elements. Nature. 400(6743), 464–468.

60. Hammond, S.M., Bernstein, E., Beach, D., and Hannon, G.J. (2000). An RNA-directed nuclease mediates post-transcriptional gene silencing in Drosophila cells. Nature. 404(6775), 293–296.

61. Hammond, S.M. (2015). An overview of microRNAs. Adv. Drug Deliv. Rev. 87, 3–14.

62. Hampe, J.F., and Misdorp, W. (1974). Tumours and dysplasias of the mammary gland. Bull. World Health Organ. 50, 111–133.

63. Hanahan, D., and Weinberg, R.A. (2011). Hallmarks of cancer: The next generation. Cell. 144(5), 646–674.

64. Hankinson, S.E., Willett, W.C., Manson, J.E., Colditz, G.A., Hunter, D.J., Spiegelman, D., Barbieri, R.L., and Speizer, F. E. (1998). Plasma sex steroid hormone levels and risk of breast cancer in postmenopausal women. J. Natl. Cancer. Inst. 90(17), 1292–1299.

65. He, X., He, L., and Hannon, G.J. (2007). The guardian's little helper: microRNAs in the p53 tumor suppressor network. Cancer Res. 67(23), 11099–11101.

66. He, W.A., Calore, F., Londhe, P., Canella, A., Guttridge, D.C., and Croce, C.M. (2014). Microvesicles containing miRNAs promote muscle cell death in cancer cachexia via TLR7. Proc. Natl. Acad. Sci. 111(12), 4525-4529.

67. Heishima, K., Ichikawa, Y., Yoshida, K., Iwasaki, R., Sakai, H., Nakagawa, T., Tanaka, Y., Hoshino, Y., Okamura, Y., Murakami, M., et al. (2017). Circulating microRNA-214 and -126 as potential biomarkers for canine neoplastic disease. Sci. Rep. 7(1), 2301.

68. Hertel, J., Lindemeyer, M., Missal, K., Fried, C., Tanzer, A., Flamm, C., Hofacker, I.L., and Stadler, P. (2006). The expansion of the metazoan microRNA repertoire. BMC Genomics. 7(1), 25.

69. Hsu, L.H., Chu, N.M., Lin, Y.F., and Kao, S.H. (2019). G-Protein coupled estrogen receptor in breast cancer. Int. J. Mol. Sci. 20(2), 306.

70. Humphreys, D.T., Westman, B.J., Martin, D.I.K., and Preiss, T. (2005). MicroRNAs control translation initiation by inhibiting eukaryotic initiation factor 4E/cap and poly(A) tail function. Proc. Natl. Acad. Sci. 102(47), 16961–16966.

71. Hutvagner, G., and Zamore, P.D. (2002). A microRNA in a multiple-turnover RNAi enzyme complex. Science. 297(5589), 2056–2060.

72. Ichii, O., Ohta, H., Horino, T., Nakamura, T., Hosotani, M., Mizoguchi, T., Morishita, K., Nakamura, K., Hoshino, Y., Takagi, S., et al. (2017). Urinary exosome-derived microRNAs reflecting the changes of renal function and histopathology in dogs. Sci Rep. 7, Article number: 40340.

73. Iorio, M.V., Croce, C.M. (2012). MicroRNA dysregulation in cancer: diagnostics, monitoring and therapeutics: A comprehensive review. EMBO Mol. Med.4(3), 143-59.

74. Irizarry, K.J., Chan, A., Kettle, D., Kezian, S., Ma, D., Palacios, L., Li, Q.Q., Keeler, C.L., and Drechsler, Y. (2016). Bioinformatics analysis of chicken miRNAs associated with monocyte to macrophage differentiation and subsequent IFNg stimulated activation. microRNA..6(1), 53-70.

75. Ji, Y., Lee, D., Kim, V., Muth, D. C., and Witwer, K. W. (2015). Validated microRNA target databases: An evaluation. Drug Dev Res. 76(7), 389-96.

76. Johnson, J.I., Decker, S., Zaharevitz, D., Rubinstein, L.V, Venditti, J.M., Schepartz, S., Kalyandrug, S., Christian, M., Arbuck, S., Hollingshead, M., et al. (2001). Relationships between drug activity in NCI preclinical in vitro and in vivo models and early clinical trials. Br. J. Cancer. 84(10), 1424–1431.

77. Jones-Rhoades, M.W., Bartel, D.P., and Bartel, B. (2006). MicroRNAs and their regulatory roles in plants. Annu. Rev. Plant Biol. 57(1), 19–53.

78. Khanna, C., Lindblad-Toh, K., Vail, D., London, C., Bergman, P., Barber, L., Breen, M., Kitchell, B., McNeil, E., Modiano, J.F., et al. (2006). The dog as a cancer model. Nat. Biotechnol. 24(9), 1065–1066.

79. King, H.W., Michael, M.Z., and Gleadle, J.M. (2012). Hypoxic enhancement of exosome release by breast cancer cells. BMC Cancer, 12(1), 421.

80. Kinzler, K.W., and Vogelstein, B. (1996). Lessons from hereditary colorectal cancer. Cell. 87(2), 159–170.

81. Koliha, N., Wiencek, Y., Heider, U., Jüngst, C., Kladt, N., Krauthäuser, S., Johnston, I.C., Bosio, A., Schauss, A., and Wild, S. (2016). A novel multiplex bead-based platform highlights the diversity of extracellular vesicles. J. Extracell. Vesicles. 5, 29975.

82. Korkola, J., and Gray, J.W. (2010). Breast cancer genomes--form and function. Curr. Opin. Genet. Dev. 20(1), 4–14.

83. Lai, Y.C., Fujikawa, T., Maemura, T., Ando, T., Kitahara, G., Endo, Y., Yamato, O., Koiwa, M., Kubota, C., and Miura, N. (2017). Inflammation-related microRNA expression level in the bovine milk is affected by mastitis. PLoS One, 12(5), e0177182.

84. Lamote, I., Meyer, E., Massart-Leën, A. M., and Burvenich, C. (2004). Sex steroids and growth factors in the regulation of mammary gland proliferation, differentiation, and involution. Steroids. 69(3), 145–159.

85. Le, M.T.N., Hamar, P., Guo, C., Basar, E., Perdigão-Henriques, R., Balaj, L., and Lieberman, J. (2014). miR-200–containing extracellular vesicles promote breast cancer cell metastasis. J. Clin. Invest. 124(12), 5109–5128.

86. Lee, R.C., Feinbaum, R.L., and Ambros, V. (1993). The C. elegans heterochronic gene lin-4 encodes small RNAs with antisense complementarity to lin-14. Cell. 75(5), 843–854.

87. Lee, M., Ban, J.J., Im, W., and Kim, M. (2016). Influence of storage condition on exosome recovery. Biotechnol. Bioprocess Eng. 21(2), 299–304.

88. Li, Q., Liu, M., Ma, F., Luo, Y., Cai, R., Wang, L., Xu, N., and Xu, B. (2014). Circulating miR-19a and miR-205 in serum may predict the sensitivity of luminal A subtype of breast cancer patients to neoadjuvant chemotherapy with epirubicin plus paclitaxel. PLoS One. 9(8): e104870.

89. Li, C., Zhang, J., Ma, Z., Zhang, F., and Yu, W. (2018). miR-19b serves as a prognostic biomarker of breast cancer and promotes tumor progression through PI3K/AKT signaling pathway. Onco Targets Ther. 11, 4087–4095.

90. Liang, Z., Li, Y., Huang, K., Wagar, N., and Shim, H. (2011). Regulation of miR-19 to breast cancer chemoresistance through targeting PTEN. Pharm. Res. 28(12), 3091–3100.

91. Lim, H.Y., Im, K.S., Kim, N.H., Kim, H.W., Shin, J.I., Yhee, J.Y., and Sur, J.H.. (2015). Effects of obesity and obesity-related molecules on canine mammary gland tumors. Vet Pathol.;52(6):1045-51.

92. Livak, K.J., and Schmittgen, T.D. (2001). Analysis of relative gene expression data using real-time quantitative PCR and the 2(-Delta Delta C(T)) method. Methods. 25(4), 402-8.

93. Lötvall, J., Hill, A.F., Hochberg, F., Buzás, E.I., Di Vizio, D., Gardiner, C., Gho, Y.S., Kurochkin, I.V., Mathivanan, S., Quesenberry, P., et al.. (2014). Minimal experimental requirements for definition of extracellular vesicles and their functions: a position statement from the International Society for Extracellular Vesicles. J. Extracell. Vesicles. 3, 26913.

94. Lu, J., Getz, G., Miska, E.A., Alvarez-Saavedra, E., Lamb, J., Peck, D., Sweet-Cordero, A., Ebert, B.L., Mak, R.H., Ferrando, A.A., et al. (2005). MicroRNA expression profiles classify human cancers. Nature. 435(7043), 834–838.

95. Lu, W., and Kang, Y. (2019). Epithelial-mesenchymal plasticity in cancer progression and metastasis. Dev. Cell. 49(3), 361–374.

96. Lu, J., Fu, Y., Kumar, S., Shen, Y., Zeng, K., Xu, A., Carthew, R., and Wu, C.I. (2008). Adaptive evolution of newly emerged micro-RNA genes in Drosophila. Mol. Biol. Evol. 25(5), 929–938.

97. Lund, E., Güttinger, S., Calado, A., Dahlberg, J. E., and Kutay, U. (2004). Nuclear export of microRNA precursors. Science. 303(5654), 95–98.

98. Lutful Kabir, F.M. (2014). Altered expression profiles and defects in a group of cell cycle regulators and tumor suppressor genes (INK4) and evaluation of comprehensive expression profiles of canine miRNAs in spontaneous canine breast cancer models. PhD dissertation, Auburn University. https://etd.auburn.edu/handle/10415/4429.

99. Lutful Kabir, F.M., DeInnocentes, P., Bird, R.C. (2015). Altered microRNA expression profiles and regulation of INK4A/CDKN2A tumor suppressor genes in canine breast cancer models. J. Cell Biochem.116(12), 2956-69.

100. Lutful Kabir, F.M., DeInnocentes, P., Agarwal, P., Mill, C.P., Riese, D.J., and Bird, R.C. (2017). Estrogen receptor-α, progesterone receptor, and c-erbB/HER-family receptor mRNA detection and phenotype analysis in spontaneous canine models of breast cancer. J Vet Sci. 18(2), 149-158.

101. Macías, M., Rebmann, V., Mateos, B., Varo, N., Perez-Gracia, J. L., Alegre, E., and González, Á. (2019). Comparison of six commercial serum exosome isolation methods suitable for clinical laboratories. Effect in cytokine analysis. Clin. Chem. Lab. Med. doi: 10.1515/cclm-2018-1297. [Epub ahead of print].

102. MacLeod, R.A., Dirks, W.G., Matsuo, Y., Kaufmann, M., Milch, H., and Drexler, H. G. (1999). Widespread intraspecies cross-contamination of human tumor cell lines arising at source. Int. J. Cancer. 83(4), 555–563.

103. Mahdavi, M., Nassiri, M., Kooshyar, M. M., Vakili-Azghandi, M., Avan, A., Sandry, R., Pillai, S., Lam, A.K., and Gopalan, V. (2018). Hereditary breast cancer; Genetic penetrance and current status with BRCA. J. Cell. Physiol. 234(5), 5741-5750.

104. Mall, C., Rocke, D.M., Durbin-Johnson, B., and Weiss, R.H. (2013). Stability of miRNA in human urine supports its biomarker potential. Biomark Med. 7(4), 623-31.

105. Malumbres M., Barbacid M. (2009). Cell cycle, CDKs and cancer: a changing paradigm. Nat. Rev. Cancer. 9(3), 153-166.

106. Masters, J.R. (2002). HeLa cells 50 years on: the good, the bad and the ugly. Nat. Rev. Cancer. 2(4), 315–319.

107. McAnena, P., Tanriverdi, K., Curran, C., Gilligan, K., Freedman, J. E., Brown, J. A. L., and Kerin, M. J. (2019). Circulating microRNAs miR-331 and miR-195 differentiate local luminal a from metastatic breast cancer. BMC Cancer. 19(1), 436.

108. Melo, S.A., Moutinho, C., Ropero, S., Calin, G. A., Rossi, S., Spizzo, R., Fernandez, A.F., Davalos, V., Villanueva, A., Montoya, G., et al. (2010). A genetic defect in Exportin-5 traps precursor microRNAs in the nucleus of cancer nells. Cancer Cell. 18(4), 303–315.

109. Melo, S.A.A., Sugimoto, H., O'Connell, J.T., Kato, N., Villanueva, A., Vidal, A., Qiu, L., Vitkin, E., Perelman, L.T., Melo, C.A., et al. (2014). Cancer exosomes perform cell-independent microRNA biogenesis and promote tumorigenesis. Cancer Cell. 26(5), 707–721.

110. Meister, G. (2013). Argonaute proteins: functional insights and emerging roles. Nat. Rev. Genet. 14(7), 447–459

111. Merlo, D.F., Rossi, L., Pellegrino, C., Ceppi, M., Cardellino, U., Capurro, C., Ratto, A., Sambucco, P.L., Sestito, V., Tanara, G., et al. (2008). Cancer incidence in pet dogs: findings of the Animal Tumor Registry of Genoa, Italy. J. Vet. Intern. Med. 22, 976–984.

112. Michael, M. Z., O' Connor, S. M., van Holst Pellekaan, N. G., Young, G. P., & James, R. J. (2003). Reduced accumulation of specific microRNAs in colorectal neoplasia. Molecular Cancer Research : MCR, 1(12), 882–891.

113. Misdorp, W., Else, R.W., Hellmen, E., Lipscomb, T.P. (1999). Histologic classification of mammary tumors of the dog and the cat, 2nd ser., vol. 7. Armed Force Institute of Pathology and World Health Organization.

114. Mitchell, P.S., Parkin, R.K., Kroh, E.M., Fritz, B.R., Wyman, S.K., Pogosova-Agadjanyan, E.L., Peterson, A., Noteboom, J., O'Briant, K.C., Allen, A., et al. (2008). Circulating microRNAs as stable blood-based markers for cancer detection. Proc. Natl. Acad. Sci. 105(30), 10513-8.

115. Moe, L. (2001). Population-based incidence of mammary tumours in some dog breeds. J. Reprod. Infertil. Suppl. 57, 439–443.

116. Musavi Shenas, M.H., Eghbal-Fard, S., Mehrisofiani, V., Abd Yazdani, N., Rahbar Farzam, O., Marofi, F., and Yousefi, M. (2019). MicroRNAs and signaling networks involved in epithelial-mesenchymal transition. J. Cell. Physiol. 234(5), 5775–5785.

117. Nair, S.S., and Kumar, R.. (2012). Chromatin remodeling in cancer: A gateway to regulate gene transcription. Mol. Oncol. 6(6), 611-619.

118. Nieto, A., Peña, L., Pérez-Alenza, M.D., Sánchez, M. A., Flores, J. M., and Castaño, M. (2000). Immunohistologic detection of estrogen receptor alpha in canine mammary

tumors: Clinical and pathologic associations and prognostic significance. Vet. Pathol. 37(3), 239–247.

119. Niu, J., Xue, A., Chi, Y., Xue, J., Wang, W., Zhao, Z., Fan, M., Yang, C.H., Shao, Z.M., Pfeffer, L.M., et al. (2016). Induction of miRNA-181a by genotoxic treatments promotes chemotherapeutic resistance and metastasis in breast cancer. Oncogene. 35(10), 1302–1313.

120. Nottrott, S., Simard, M. J., and Richter, J. D. (2006). Human let-7a miRNA blocks protein production on actively translating polyribosomes. Nat. Struct. Mol. Biol. 13(12), 1108-14.

121. O'Brien, K., Rani, S., Corcoran, C., Wallace, R., Hughes, L., Friel, A. M., McDonnell, S., Crown, J., Radomski, M.W., and O'Driscoll, L. (2013). Exosomes from triple-negative breast cancer cells can transfer phenotypic traits representing their cells of origin to secondary cells. Eur. J. Cancer. 49(8), 1845–1859.

122. Osaki, T., Sunden, Y., Sugiyama, A., Azuma, K., Murahata, Y., Tsuka, T., Ito, N., Imagawa, T., and Okamoto Y. (2016). Establishment of a canine mammary gland tumor cell line and characterization of its miRNA expression. J. Vet. Sci. 17(3), 385-90.

123. Ozsolak, F., Poling, L.L., Wang, Z., Liu, H., Liu, X.S., Roeder, R.G., Zhang, X., Song, J.S., and Fisher, D.E. (2008). Chromatin structure analyses identify miRNA promoters. Genes Dev. 22(22), 3172–3183.

124. Papadaki, C., Stratigos, M., Markakis, G., Spiliotaki, M., Mastrostamatis, G., Nikolaou, C., Mavroudis, D. and Agelaki, S. (2018). Circulating microRNAs in the early prediction of disease recurrence in primary breast cancer. Breast Cancer Res. 20(1), 72.

125. Parolini, I., Federici, C., Raggi, C., Lugini, L., Palleschi, S., De Milito, A., Coscia, C., Iessi, E., Logozzi, M., Molinari, A., et al. (2009). Microenvironmental pH is a key factor for exosome traffic in tumor cells. J. Biol. Chem. 284(49), 34211–34222.

126. Pasquinelli, A.E., Reinhart, B.J., Slack, F., Martindale, M.Q., Kuroda, M.I., Maller, B., Hayward, D.C., Ball, E.E., Degnan, B., Müller, P., et al. (2000). Conservation of the sequence and temporal expression of let-7 heterochronic regulatory RNA. Nature, 408(6808), 86–89.

127. Patra, S., Panigrahi, D. P., Praharaj, P.P., Bhol, C.S., Mahapatra, K.K., Mishra, S. R., Behera, B.P., Jena, M., and Bhutia, S. K. (2019). Dysregulation of histone deacetylases in carcinogenesis and tumor progression: a possible link to apoptosis and autophagy. Cell Mol. Life Sci. doi: 10.1007/s00018-019-03098-1. [Epub ahead of print]

128. Peña, L., Gama, A., Goldschmidt, M.H., Abadie, J., Benazzi, C., Castagnaro, M., Díez, L., Gärtner, F., Hellmén, E., Kiupel, M., et al. (2014). Canine mammary tumors: a review and consensus of standard guidelines on epithelial and myoepithelial phenotype markers, HER2, and hormone receptor assessment using immunohistochemistry. Vet Pathol. 51(1), 127–145.

129. Penfornis, P., Vallabhaneni, K.C., Whitt, J., and Pochampally, R. (2016). Extracellular vesicles as carriers of microRNA, proteins and lipids in tumor microenvironment. Int. J. Cancer. 138(1):14-21.

130. Penso-Dolfin, L., Swofford, R., Johnson, J., Alföldi, J., Lindblad-Toh, K., Swarbreck, D., Moxon, S., and Di Palma, F. (2016). An improved microRNA annotation of the canine genome. PLoS One, 11(4), e0153453.

131. Perez-Alenza, D., Rutteman, G.R., Peña, L., Beynen, A.C., and Cuesta, P. (1998). Relation between habitual diet and canine mammary tumors in a case-control study. J. Vet. Intern. Med. 12(3), 132–139.

132. Perez-Alenza, M.D., Peña, L., del Castillo, N., and Nieto, A. I. (2000). Factors influencing the incidence and prognosis of canine mammary tumours. J. Small Anim. Pract. 41(7), 287–291.

133. Pérez-Alenza, M.D., Tabanera, E., and Peña, L. (2001). Inflammatory mammary carcinoma in dogs: 33 cases (1995-1999). J. Am. Vet. Med. Assoc. 219(8), 1110–1114.

134. Perou, C.M., Sørlie, T., Eisen, M.B., van de Rijn, M., Jeffrey, S.S., Rees, C.A., Pollack, J.R., Ross, D.T., Johnsen, H., Akslen, L.A., et al. (2000). Molecular portraits of human breast tumours. Nature. 406(6797), 747–752.

135. Philibert, J.C., Snyder, P.W., Glickman, N., Glickman, L.T., Knapp, D.W., and Waters, D.J. (2003). Influence of host factors on survival in dogs with malignant mammary gland tumors. J. Vet. Intern. Med. 17(1), 102-6.

136. Pinho, S.S., Carvalho, S., Cabral, J., Reis, C.A., and Gärtner, F. (2012). Canine tumors: a spontaneous animal model of human carcinogenesis. Transl. Res.159(3), 165-72.

137. Pinzón, N., Li, B., Martinez, L., Sergeeva, A., Presumey, J., Apparailly, F., and Seitz, H. (2017). microRNA target prediction programs predict many false positives. Genome Res. 27(2), 234–245.

138. Piriyapongsa, J., Mariño-Ramírez, L., and Jordan, I. K. (2007). Origin and evolution of human microRNAs From transposable elements. Genetics. 176(2), 1323–1337.

139. Poitout-Belissent, F., Aulbach, A., Tripathi, N., and Ramaiah, L. (2016). Reducing blood volume requirements for clinical pathology testing in toxicologic studies-points to consider. Vet. Clin. Pathol. 45(4), 534–551.

140. Pospichalova, V., Svoboda, J., Dave, Z., Kotrbova, A., Kaiser, K., Klemova, D., Ilkovics, L., Hampl, A., Crha, I., Jandakova, E., et al. (2015). Simplified protocol for flow cytometry analysis of fluorescently labeled exosomes and microvesicles using dedicated flow cytometer. J. Extracell. Ves. 4, 25530.

141. Queiroga, F.L., Raposo, T., Carvalho, M.I., Prada, J., and Pires, I. (2011). Canine mammary tumours as a model to study human breast cancer: most recent findings. In Vivo. 25(3), 455–465.

142. Raposo-Ferreira, T.M.M., Brisson, B.K., Durham, A.C., Laufer-Amorim, R., Kristiansen, V., Puré, E., , Volk, S.W., and Sorenmo, K. (2018). Characteristics of the epithelial-mesenchymal transition in primary and paired metastatic canine mammary carcinomas. Vet. Pathol.. 55(5), 622-633.

143. Rasotto, R., Berlato, D., Goldschmidt, M.H., and Zappulli, V. (2017). Prognostic significance of canine mammary tumor histologic subtypes: An observational cohort study of 229 cases. Vet. Pathol. 54(4), 571–578.

144. Reinhart, B.J., Slack, F.J., Basson, M., Pasquinelli, A.E., Bettinger, J.C., Rougvie, A. E., Horvitz, H.R., and Ruvkun, G. (2000). The 21-nucleotide let-7 RNA regulates developmental timing in Caenorhabditis elegans. Nature. 403(6772), 901–906.

145. Rhodes, L.V., Martin, E.C., Segar, H.C., Miller, D.F.B., Buechlein, A., Rusch, D.B., Nephew, K.P., Burow, M.E., and Collins-Burow, B. M. (2015). Dual regulation by microRNA-200b-3p and microRNA-200b-5p in the inhibition of epithelial-to-

mesenchymal transition in triple-negative breast cancer. Oncotarget. 6(18). 6(18):16638-52

146. Rivera, P., Melin, M., Biagi, T., Fall, T., Haggstrom, J., Lindblad-Toh, K., and von Euler, H. (2009). Mammary tumor development in dogs is associated with BRCA1 and BRCA2. Cancer Res. 69(22), 8770–8774.

147. Rodriguez, A., Griffiths-Jones, S., Ashurst, J. L., and Bradley, A. (2004). Identification of mammalian microRNA host genes and transcription units. Genome Res. 14(10a), 1902–1910.

148. Sætrom, P., Heale, B.S.E., Snøve, O., Aagaard, L., Alluin, J., and Rossi, J.J. (2007). Distance constraints between microRNA target sites dictate efficacy and cooperativity. Nucl. Acids Res. 35(7), 2333–2342.

149. Saito, Y., Liang, G., Egger, G., Friedman, J.M., Chuang, J.C., Coetzee, G.A., and Jones, P.A. (2006). Specific activation of microRNA-127 with downregulation of the proto-oncogene BCL6 by chromatin-modifying drugs in human cancer cells. Cancer Cell. 9(6), 435–443.

150. Sampath, D., Liu, C., Vasan, K., Sulda, M., Puduvalli, V.K., Wierda, W.G., and Keating, M.J. (2012). Histone deacetylases mediate the silencing of miR-15a, miR-16, and miR-29b in chronic lymphocytic leukemia. Blood, 119(5), 1162–1172.

151. Santos, J.C., Ribeiro, M.L., Sarian, L.O., Ortega, M.M., and Derchain, S.F. (2016). Exosomes-mediate microRNAs transfer in breast cancer chemoresistance regulation. Am. J. Cancer Res. 6(10), 2129–2139.

152. Schindelin, J., Arganda-Carreras, I., Frise, E., Kaynig, V., Longair, M., Pietzsch, T., Preibisch S, Rueden C, Saalfeld S, Schmid B, et al. (2012). Fiji: an open-source platform for biological-image analysis. Nat. Methods. 9(7), 676–682.

153. Schneider, R., Dorn, C.R., and Taylor, D.O. (1969). Factors influencing canine mammary cancer development and postsurgical survival. J. Natl. Cancer Inst. 43(6), 1249–1261.

154. Schneider, R. (1970). Comparison of age, sex, and incidence rates in human and canine breast cancer. Cancer. 26(2), 419–426.

155. Schuh, J.C.L. (2004). Trials, tribulations, and trends in tumor modeling in mice. Toxicol. Pathol. 32; Suppl 1, 53-66.

156. Shinoda, H., Legare, M.E., Mason, G.L., Berkbigler, J.L., Afzali, M.F., Flint, A.F., and Hanneman, W.H. (2014). Significance of ERα, HER2, and CAV1 expression and molecular subtype classification to canine mammary gland tumor. J. Vet. Diagn. Invest. 26(3), 390-403.

157. Siersbæk, R., Kumar, S., and Carroll, J.S. (2018). Signaling pathways and steroid receptors modulating estrogen receptor α function in breast cancer. Genes Dev. 32(17–18), 1141–1154.

158. Simon, D., Schoenrock, D., Nolte, I., BaumgÃ¤rtner, W., Barron, R., and Mischke, R. (2009). Cytologic examination of fine-needle aspirates from mammary gland tumors in the dog: diagnostic accuracy with comparison to histopathology and association with postoperative outcome. Vet. Clin. Pathol. 38(4), 521–528.

159. Simons, M., and Raposo, G. (2009). Exosomes – vesicular carriers for intercellular communication. Curr. Opin. Cell. Biol. 21(4), 575–581.

160. Singh, R., Pochampally, R., Watabe, K., Lu, Z., and Mo, Y.-Y. (2014). Exosome-mediated transfer of miR-10b promotes cell invasion in breast cancer. Mol. Cancer. 26, 13:256.

161. Sochor, M., Basova, P., Pesta, M., Dusilkova, N., Bartos, J., Burda, P., Pospisil, V., and Stopka, T. (2014). Oncogenic MicroRNAs: miR-155, miR-19a, miR-181b, and miR-24 enable monitoring of early breast cancer in serum. BMC Cancer. 14, 448.

162. Sorenmo KU, Worley DR, Goldschmidt MH. (2013). Ch. 27: Tumors of the mammary gland. In: Withrow & MacEwen's Small Animal Clinical Oncology, 5th ed. (Saunders Elsevier, St. Louis), pp. 538-556;.

163. Stein, E.V., Duewer, D.L., Farkas, N., Romsos, E.L., Wang, L., and Cole, K.D. (2017). Steps to achieve quantitative measurements of microRNA using two step droplet digital PCR. PLoS One. 12(11), e0188085.

164. Stroynowska-Czerwinska, A., Fiszer, A., and Krzyzosiak, J.W. (2014). The panorama of miRNA-mediated mechanisms in mammalian cells. Cell. Mol. Life Sci, 71, 2253–2270.

165. Suzuki, H., Maruyama, R., Yamamoto, E., and Kai, M. (2013). Epigenetic alteration and microRNA dysregulation in cancer. Front Genet. 4(258), 1-8.

166. Taylor, D.D., and Gercel-Taylor, C. (2008). MicroRNA signatures of tumor-derived exosomes as diagnostic biomarkers of ovarian cancer. Gynecol. Oncol. 110(1), 13-21.

167. Théry, C., Zitvogel, L., and Amigorena, S. (2002). Exosomes: composition, biogenesis and function. Nat. Rev. Immunol. 2(8), 569–579.

168. Thery, C., Clayton, A., Amigorena, S., Raposo, G., and Clayton, A. (2006). Isolation and characterization of exosomes from cell culture supernatants and biological fluids. Curr. Protoc. Cell Biol. Chapter 3, Unit 3.22.

169. Turchinovich, A., Weiz, L., Langheinz, A., and Burwinkel, B. (2011). Characterization of extracellular circulating microRNA. Nucl. Acids Res. 39(16), 7223–7233.

170. Tymchuk, C.N., Tessler, S. B., and Barnard, R.J. (2000). Changes in sex Hormone-Binding Globulin, Insulin, andSerum Lipids in Postmenopausal Women on aLow-Fat, High-Fiber Diet Combined With Exercise. Nutrition and Cancer, 38(2), 158–162.

171. Uva P, Aurisicchio L, Watters J, Loboda A, Kulkarni A, Castle J, et al. (2009). Comparative expression pathway analysis of human and canine mammary tumors. BMC Genomics.10:135.

172. Vail, D. M., & MacEwen, E. G. (2000). Spontaneously occurring tumors of companion animals as models for human cancer. Cancer Investigation, 18(8), 781–792.

173. von Deetzen MC, Schmeck BT, Gruber AD, Klopfleisch R. (2014). Malignancy associated microRNA expression changes in canine mammary cancer of different malignancies. ISRN Vet Sci.doi:10.1155/2014/148597.

174. van Staalduinen, J., Baker, D., ten Dijke, P., & van Dam, H. (2018). Epithelial–mesenchymal-transition-inducing transcription factors: new targets for tackling chemoresistance in cancer? Oncogene, 37(48), 6195–6211.

175. Wang, C., Bian, Z., Wei, D., & Zhang, J. (2011). miR-29b regulates migration of human breast cancer cells. Molecular and Cellular Biochemistry, 352(1–2), 197–207.

176. Wang, N., Wang, L., Yang, Y., Gong, L., Xiao, B., & Liu, X. (2017). A serum exosomal microRNA panel as a potential biomarker test for gastric cancer. Biochemical and Biophysical Research Communications, 493(3), 1322–1328.

177. Williams, A. E. (2008). Review Functional aspects of animal microRNAs.

180. Wong N, Wang X. (2015). miRDB: an online resource for microRNA target prediction and functional annotations. Nucleic Acids Res.43(D1):46-52.

181. Woo, H.-K., Sunkara, V., Park, J., Kim, T.-H., Han, J.-R., Kim, C.-J., … Cho, Y.-K. (2017). Exodisc for Rapid, Size-Selective, and Efficient Isolation and Analysis of Nanoscale Extracellular Vesicles from Biological Samples. ACS Nano, 11(2), 1360–1370.

182. Wu, L., Fan, J., & Belasco, J. G. (2006). MicroRNAs direct rapid deadenylation of mRNA.

183. Wu, E., Thivierge, C., Flamand, M., Mathonnet, G., Vashisht, A. A., Wohlschlegel, J., … Duchaine, T. F. (2010). Pervasive and Cooperative Deadenylation of 3'UTRs by Embryonic MicroRNA Families. Molecular Cell, 40(4), 558.

184. Wu, C., Cao, Y., He, Z., He, J., Hu, C., Duan, H., & Jiang, J. (2014). Serum levels of miR-19b and miR-146a as prognostic biomarkers for non-small cell lung cancer. The Tohoku Journal of Experimental Medicine, 232(2), 85–95.

185. Wu Q, Guo L, Jiang F, Li L, Li Z, Chen F. (2015). Analysis of the miRNA–mRNA–lncRNA networks in ER+ and ER- breast cancer cell lines. J Cell Mol Med.19(12):2874-2887.

186. Wu, C.-Y., Du, S.-L., Zhang, J., Liang, A.-L., & Liu, Y.-J. (2017). Exosomes and breast cancer: a comprehensive review of novel therapeutic strategies from diagnosis to treatment. Cancer Gene Therapy, 24(1), 6–12.

187. Yang, X., Du, W. W., Li, H., Liu, F., Khorshidi, A., Rutnam, Z. J., & Yang, B. B. (2013). Both mature miR-17-5p and passenger strand miR-17-3p target TIMP3 and induce prostate tumor growth and invasion. Nucleic Acids Research, 41(21), 9688–9704.

188. Yang VK, Loughran KA, Meola DM, Juhr CM, Thane KE, Davis AM, et al. (2017). Circulating exosome microRNA associated with heart failure secondary to myxomatous mitral valve disease in a naturally occurring canine model. J Extracell Vesicles. 12;6(1):1350088.

189. Yates LA, Norbury CJ, Gilbert RJC. (2013). The long and short of microRNA. Cell.153: 516-519.

190. Yu, X., Harris, S. L., & Levine, A. J. (2006). Cancer Research. Cancer Res., 61(18), 6945–6951.

191. Zare, M., Bastami, M., Solali, S., & Alivand, M. R. (2018). Aberrant miRNA promoter methylation and EMT-involving miRNAs in breast cancer metastasis: Diagnosis and therapeutic implications. Journal of Cellular Physiology, 233(5), 3729–3744.

192. Zeng, Y., Yi, R., & Cullen, B. R. (2003). MicroRNAs and small interfering RNAs can inhibit mRNA expression by similar mechanisms. Proceedings of the National Academy of Sciences, 100(17), 9779–9784.

193. Zha, Q. Bin, Yao, Y. F., Ren, Z. J., Li, X. J., & Tang, J. H. (2017). Extracellular vesicles: An overview of biogenesis, function, and role in breast cancer. Tumor Biology, 39(2), 101042831769118.

194. Zheng, D., Ezzeddine, N., Chen, C.-Y. A., Zhu, W., He, X., & Shyu, A.-B. (2008). Deadenylation is prerequisite for P-body formation and mRNA decay in mammalian cells. The Journal of Cell Biology, 182(1), 89–101.

195. Zou, X., Wei, J., Huang, Z., Zhou, X., Lu, Z., Zhu, W., & Miao, Y. (2019). Identification of a six-miRNA panel in serum benefiting pancreatic cancer diagnosis. Cancer Medicine, 8(6), cam4.2145.

Appendix 1: Complete list of differentially expressed exosomal miRNAs. Fold-change and direction of regulation refer to the CMT group versus the CMEC group expression.

miR	Gene ID	Fold-change	Regulation	p-value	p-value (corrected)
miR-9	MI0008125_1	33.36	up	0.00E+00	0.00E+00
miR-9	MI0008081_1	33.36	up	0.00E+00	0.00E+00
miR-9	MI0008086_1	33.36	up	0.00E+00	0.00E+00
miR-122	MI0008015_1	24.08	up	0.00E+00	0.00E+00
miR-183	MI0008017_1	23.75	up	0.00E+00	0.00E+00
miR-182	MI0010336_1	18.90	up	0.00E+00	0.00E+00
miR-106b	MI0008109_1	14.72	up	0.00E+00	0.00E+00
mIR-31	MI0007994_1	14.32	up	0.00E+00	0.00E+00
miR-429	MI0001644_1	12.47	up	0.00E+00	0.00E+00
miR-203	MI0010363_1	11.79	up	0.00E+00	0.00E+00
miR-18a	MI0010324_1	10.34	up	0.00E+00	0.00E+00
miR-146a	MI0008094_1	10.13	up	0.00E+00	0.00E+00
miR-181c	MI0008034_1	9.99	up	0.00E+00	0.00E+00
miR-96	MI0010356_1	9.65	up	0.00E+00	0.00E+00
miR-135b	MI0010334_1	9.25	up	0.00E+00	0.00E+00
miR-181b	MI0008153_1	8.75	up	0.00E+00	0.00E+00
miR-181b	MI0008127_1	8.75	up	0.00E+00	0.00E+00
miR-196a	MI0010360_1	8.69	up	0.00E+00	0.00E+00
miR-200b	MI0010361_1	8.11	up	0.00E+00	0.00E+00
miR-181a	MI0008152_1	7.78	up	0.00E+00	0.00E+00
miR-181a	MI0008126_1	7.62	up	0.00E+00	0.00E+00
miR-15b	MI0008083_1	7.26	up	0.00E+00	0.00E+00
miR-371	MI0007996_1	7.11	up	0.00E+00	0.00E+00
miR-371	MI0007996_2_1	7.11	up	0.00E+00	0.00E+00
miR-363	MI0008176_1	7.01	up	0.00E+00	0.00E+00
miR-103	MI0010357_1	6.82	up	0.00E+00	0.00E+00

miR-1841	MI0008096_1	6.28	up	4.44E-16	6.49E-16
miR-30b	MI0008013_1	5.82	up	0.00E+00	0.00E+00
miR-200a	MI0010362_1	5.46	up	0.00E+00	0.00E+00
miR-34c	MI0008106_1	5.43	up	0.00E+00	0.00E+00
miR-146b	MI0008073_1	5.35	up	0.00E+00	0.00E+00
miR-331	MI0010394_1	5.24	up	0.00E+00	0.00E+00
miR-147	MI0010371_1	5.24	up	0.00E+00	0.00E+00
miR-155	MI0008078_1	5.10	up	0.00E+00	0.00E+00
miR-20a	MI0008052_1	4.99	up	0.00E+00	0.00E+00
miR-19b	MI0008054_1	4.96	up	0.00E+00	0.00E+00
miR-19b	MI0008174_1	4.96	up	0.00E+00	0.00E+00
miR-107	MI0008072_1	4.92	up	0.00E+00	0.00E+00
miR-181d	MI0008035_1	4.66	up	0.00E+00	0.00E+00
miR-200c	MI0008070_1	4.53	up	0.00E+00	0.00E+00
miR-345	MI0008129_1	4.41	up	5.33E-15	7.54E-15
miR-130a	MI0008029_1	4.08	up	0.00E+00	0.00E+00
miR-29c	MI0008122_1	4.06	up	0.00E+00	0.00E+00
miR-29c	MI0015960_1	4.06	up	0.00E+00	0.00E+00
miR-15a	MI0008048_1	4.03	up	0.00E+00	0.00E+00
miR-19a	MI0008051_1	3.84	up	0.00E+00	0.00E+00
miR-16	MI0008084_1	3.71	up	0.00E+00	0.00E+00
miR-93	MI0008110_1	3.56	up	0.00E+00	0.00E+00
miR-1343	MI0027953_1	3.53	up	0.00E+00	0.00E+00
miR-7	MI0010330_1	3.51	up	0.00E+00	0.00E+00
miR-874	MI0010429_1	3.51	up	4.76E-07	5.65E-07
miR-103	MI0008098_1	3.48	up	0.00E+00	0.00E+00
miR-7	MI0008033_1	3.46	up	0.00E+00	0.00E+00
miR-27a	MI0008040_1	3.46	up	0.00E+00	0.00E+00
miR-1839	MI0008087_1	3.43	up	0.00E+00	0.00E+00
miR-196a	MI0008068_1	3.43	up	0.00E+00	0.00E+00
miR-20b	MI0010322_1	3.41	up	0.00E+00	0.00E+00
miR-660	MI0008186_1	3.39	up	0.00E+00	0.00E+00
miR-215	MI0010343_1	3.29	up	8.72E-06	9.96E-06
miR-186	MI0008108_1	3.27	up	0.00E+00	0.00E+00

miR-495	MI0008140_1	3.25	up	8.10E-12	1.07E-11
miR-339	MI0008115_1	3.25	up	0.00E+00	0.00E+00
miR-421	MI0008181_1	3.16	up	4.40E-14	6.13E-14
miR-16	MI0008049_1	3.14	up	0.00E+00	0.00E+00
miR-27b	MI0008009_1	3.12	up	0.00E+00	0.00E+00
miR-543	MI0008139_1	3.10	up	0.00E+00	0.00E+00
miR-205	MI0010340_1	3.05	up	0.00E+00	0.00E+00
miR-29a	MI0008022_1	3.03	up	0.00E+00	0.00E+00
miR-192	MI0008031_1	3.03	up	0.00E+00	0.00E+00
miR-340	MI0010391_1	3.01	up	0.00E+00	0.00E+00
miR-503	MI0008170_1	2.95	up	0.00E+00	0.00E+00
miR-1296	MI0028014_1	2.93	up	2.45E-10	3.11E-10
miR-499	MI0008059_1	2.91	up	0.00E+00	0.00E+00
miR-7	MI0008085_1	2.89	up	0.00E+00	0.00E+00
miR-486	MI0008027_2	2.87	up	4.44E-16	6.49E-16
miR-212	MI0008155_1	2.87	up	6.12E-08	7.41E-08
miR-30d	MI0008012_1	2.81	up	0.00E+00	0.00E+00
miR-615	MI0010419_1	2.73	up	5.27E-05	5.99E-05
miR-184	MI0010337_1	2.71	up	4.44E-16	6.49E-16
miR-130b	MI0008064_1	2.66	up	3.81E-10	4.77E-10
miR-590	MI0008114_1	2.64	up	0.00E+00	0.00E+00
miR-23a	MI0008039_1	2.58	up	0.00E+00	0.00E+00
miR-185	MI0008065_1	2.55	up	0.00E+00	0.00E+00
miR-335	MI0008020_1	2.53	up	0.00E+00	0.00E+00
miR-22	MI0008157_1	2.51	up	0.00E+00	0.00E+00
miR-125b	MI0008077_1	2.50	up	0.00E+00	0.00E+00
miR-1307	MI0008071_1	2.46	up	0.00E+00	0.00E+00
miR-1301	MI0027930_1	2.43	up	2.22E-16	3.32E-16
miR-375	MI0010368_1	2.38	up	4.60E-11	5.97E-11
miR-23b	MI0008008_1	2.31	up	0.00E+00	0.00E+00
miR-125b	MI0008103_1	2.30	up	0.00E+00	0.00E+00
miR-324	MI0010395_1	2.27	up	6.64E-09	8.25E-09
miR-126	MI0008154_1	2.25	up	1.22E-13	1.68E-13
miR-542	MI0008171_1	2.25	up	5.30E-11	6.77E-11
miR-6529	MI0027868_1	2.23	up	4.73E-11	6.08E-11
miR-323	MI0008137_1	2.19	up	8.21E-07	9.69E-07

miR-365	MI0001657_1	2.17	up	0.00E+00	0.00E+00
miR-365	MI0001647_1	2.16	up	0.00E+00	0.00E+00
miR-92a	MI0008055_1	2.16	up	0.00E+00	0.00E+00
miR-374b	MI0008180_1	2.16	up	0.00E+00	0.00E+00
miR-1306	MI0008066_1	2.13	up	0.00E+00	0.00E+00
miR-29b	MI0008121_1	2.11	up	0.00E+00	0.00E+00
miR-502	MI0008187_1	2.10	up	0.00E+00	0.00E+00
miR-92a	MI0008175_1	2.10	up	0.00E+00	0.00E+00
miR-410	MI0008149_1	1.97	up	3.84E-11	5.02E-11
miR-101	MI0008107_1	1.95	up	0.00E+00	0.00E+00
miR-32	MI0007992_1	1.95	up	4.17E-14	5.86E-14
miR-376a	MI0008141_1	1.93	up	5.33E-15	7.54E-15
miR-376a	MI0008142_1	1.93	up	5.33E-15	7.54E-15
miR-376a	MI0008143_1	1.93	up	5.33E-15	7.54E-15
miR-381	MI0010390_1	1.92	up	0.00E+00	0.00E+00
miR-454	MI0010426_1	1.91	up	3.81E-10	4.77E-10
miR-8859a	MI0027950_1	1.89	up	0.00E+00	0.00E+00
miR-140	MI0008100_1	1.88	up	0.00E+00	0.00E+00
miR-425	MI0008038_1	1.87	up	0.00E+00	0.00E+00
miR-500	MI0008185_1	1.85	up	0.00E+00	0.00E+00
miR-2387	MI0027966_1	1.84	up	1.14E-03	1.26E-03
miR-30a	MI0008000_1	1.83	up	0.00E+00	0.00E+00
miR-758	MI0010424_1	1.82	up	3.43E-11	4.51E-11
miR-329b	MI0010398_1	1.82	up	6.91E-09	8.54E-09
miR-382	MI0008145_1	1.80	up	2.95E-06	3.44E-06
miR-24	MI0008010_1	1.78	up	0.00E+00	0.00E+00
miR-144	MI0008158_1	1.75	up	9.22E-04	1.03E-03
miR-24	MI0008041_1	1.75	up	0.00E+00	0.00E+00
miR-101	MI0007995_1	1.73	up	0.00E+00	0.00E+00
miR-301b	MI0010349_1	1.68	up	4.74E-06	5.49E-06
miR-148b	MI0008069_1	1.68	up	0.00E+00	0.00E+00
miR-485	MI0008146_1	1.65	up	2.96E-08	3.60E-08

miR-125a	MI0008005_1	1.65	up	0.00E+00	0.00E+00
miR-379	MI0008134_1	1.62	up	0.00E+00	0.00E+00
let-7g	MI0008036_1	1.62	up	0.00E+00	0.00E+00
miR-18b	MI0010323_1	1.62	up	2.79E-06	3.27E-06
miR-21	MI0008165_1	1.61	up	0.00E+00	0.00E+00
miR-505	MI0010407_1	1.59	up	3.46E-13	4.71E-13
miR-494	MI0010404_1	1.57	up	0.00E+00	0.00E+00
miR-380	MI0008136_1	1.55	up	6.32E-06	7.27E-06
miR-138a	MI0008056_1	1.52	up	9.49E-04	1.06E-03
miR-26a	MI0008058_1	-1.51	down	0.00E+00	0.00E+00
miR-26a	MI0007990_1	-1.51	down	0.00E+00	0.00E+00
miR-222	MI0010346_1	-1.56	down	0.00E+00	0.00E+00
miR-8884	MI0027983_1	-1.65	down	1.15E-08	1.41E-08
miR-490	MI0010372_1	-1.66	down	1.82E-03	1.99E-03
miR-30c	MI0008024_1	-1.77	down	0.00E+00	0.00E+00
miR-30c	MI0008001_1	-1.77	down	0.00E+00	0.00E+00
miR-99a	MI0008102_1	-1.79	down	0.00E+00	0.00E+00
miR-99a	MI0008075_1	-1.79	down	0.00E+00	0.00E+00
miR-127	MI0008132_1	-1.80	down	8.70E-05	9.83E-05
miR-30e	MI0008023_1	-1.87	down	5.28E-12	7.04E-12
miR-889	MI0027984_1	-1.87	down	0.00E+00	0.00E+00
miR-374a	MI0008179_1	-2.33	down	0.00E+00	0.00E+00
miR-455	MI0007999_1	-2.71	down	6.24E-14	8.63E-14
miR-145	MI0010359_1	-2.81	down	0.00E+00	0.00E+00
miR-574	MI0008080_1	-3.18	down	8.45E-08	1.01E-07
miR-152	MI0008162_1	-3.25	down	0.00E+00	0.00E+00
miR-148a	MI0008018_1	-3.36	down	0.00E+00	0.00E+00
miR-8865	MI0027958_1	-3.53	down	1.82E-03	1.99E-03
miR-676	MI0008188_1	-3.71	down	3.65E-03	3.97E-03
miR-105a	MI0010377_1	-4.63	down	6.60E-08	7.94E-08
miR-143	MI0008092_1	-5.78	down	0.00E+00	0.00E+00
miR-196b	MI0008016_1	-6.92	down	1.64E-02	1.77E-02
miR-1	MI0008118_1	-7.52	down	0.00E+00	0.00E+00
miR-1	MI0008060_1	-7.52	down	0.00E+00	0.00E+00
miR-214	MI0010342_1	-9.13	down	4.89E-13	6.61E-13

miR-504	MI0010406_1	-10.06	down	1.11E-16	1.67E-16
miR-383	MI0008026_1	-10.41	down	1.28E-12	1.72E-12
miR-199	MI0008151_1	-14.03	down	0.00E+00	0.00E+00
miR-199	MI0008042_1	-14.03	down	0.00E+00	0.00E+00
miR-199	MI0008124_1	-19.70	down	0.00E+00	0.00E+00
miR-10a	MI0008161_1	-41.07	down	0.00E+00	0.00E+00
miR-206	MI0008002_1	-91.77	down	0.00E+00	0.00E+00

Appendix 2: Serum miRNA fold-change and corrected p-values for CMT group compared to healthy controls (RNAseq).

microRNA	**Fold-change**	**p-value**
cfa-miR-34c	6.08	0.00E+00
cfa-miR-135a-5p	4.08	0.00E+00
cfa-miR-199	3.93	0.00E+00
cfa-miR-182	3.93	0.00E+00
cfa-miR-199	3.88	0.00E+00
cfa-miR-199	3.88	0.00E+00
cfa-miR-30b	3.69	0.00E+00
cfa-miR-135a-5p	3.51	0.00E+00
cfa-miR-19b	3.15	0.00E+00
cfa-miR-19b	3.14	0.00E+00
cfa-miR-23a	2.92	0.00E+00
cfa-miR-29b	2.78	0.00E+00
cfa-miR-29b	2.78	0.00E+00
cfa-miR-504	2.74	2.50E-09
cfa-miR-421	2.59	0.00E+00
cfa-miR-223	2.56	0.00E+00
cfa-miR-374b	2.47	0.00E+00
cfa-miR-215	2.38	4.83E-05
cfa-miR-345	2.36	1.28E-09
cfa-miR-502	2.28	0.00E+00
cfa-miR-106b	2.25	0.00E+00
cfa-miR-1842	2.21	0.00E+00
cfa-miR-107	2.19	0.00E+00
cfa-miR-331	2.17	0.00E+00
cfa-miR-15b	2.09	0.00E+00
cfa-miR-1839	2.04	0.00E+00
cfa-miR-23b	2.03	0.00E+00
cfa-miR-9	1.99	0.00E+00
cfa-miR-9	1.99	0.00E+00

cfa-miR-9	1.99	0.00E+00
cfa-miR-103	1.97	0.00E+00
cfa-miR-103	1.95	0.00E+00
cfa-miR-18a	1.94	0.00E+00
cfa-miR-374a	1.93	0.00E+00
cfa-miR-339	1.92	0.00E+00
cfa-miR-200c	1.91	1.17E-07
cfa-miR-365	1.83	0.00E+00
cfa-miR-365	1.83	0.00E+00
cfa-miR-183	1.81	5.38E-14
cfa-miR-20a	1.80	0.00E+00
cfa-miR-362	1.80	0.00E+00
cfa-miR-8884	1.79	0.00E+00
cfa-miR-190b	1.78	2.84E-16
cfa-miR-221	1.76	0.00E+00
cfa-miR-425	1.75	0.00E+00
cfa-miR-1843	1.74	6.19E-04
cfa-miR-203	1.66	2.80E-03
cfa-miR-127	1.66	2.47E-04
cfa-miR-16	1.62	0.00E+00
cfa-miR-181c	1.62	0.00E+00
cfa-miR-132	1.61	0.00E+00
cfa-miR-15a	1.61	0.00E+00
cfa-miR-350	1.59	0.00E+00
cfa-miR-197	1.58	0.00E+00
cfa-miR-218	1.56	0.00E+00
cfa-miR-218	1.56	0.00E+00
cfa-miR-301b	1.55	4.29E-06
cfa-miR-133a	1.54	3.62E-03
cfa-miR-133c	1.54	3.62E-03
cfa-miR-8865	1.54	2.58E-04
cfa-miR-551b	1.53	0.00E+00
cfa-miR-16	1.52	0.00E+00
cfa-miR-29c	1.52	0.00E+00
cfa-miR-29c	1.52	0.00E+00
cfa-miR-32	1.52	0.00E+00
cfa-let-7d	-1.56	0.00E+00
cfa-miR-155	-1.57	0.00E+00
cfa-miR-139	-1.60	2.22E-06
cfa-miR-486	-1.64	0.00E+00
cfa-miR-423a	-1.65	0.00E+00

cfa-miR-99b	-1.73	0.00E+00
cfa-miR-10a	-1.74	0.00E+00
cfa-miR-6529	-1.84	0.00E+00
cfa-let-7b	-1.93	0.00E+00
cfa-miR-375	-1.97	0.00E+00
cfa-miR-122	-2.88	0.00E+00
cfa-miR-125a	-3.46	0.00E+00

Appendix 3: miRNA predicted to target the Estrogen Receptor ESR1, ranked by binding probability.

Target rank	Target Score	miRNA name	Gene Symbol
1	99	cfa-miR-18b	ESR1
2	99	cfa-miR-18a	ESR1
3	98	cfa-miR-8795	ESR1
4	94	cfa-miR-188	ESR1
5	91	cfa-miR-8853	ESR1
6	87	cfa-miR-22	ESR1
7	79	cfa-miR-181a	ESR1
8	79	cfa-miR-181b	ESR1
9	79	cfa-miR-181d	ESR1
10	79	cfa-miR-181c	ESR1
11	74	cfa-miR-222	ESR1
12	74	cfa-miR-221	ESR1
13	71	cfa-miR-19a	ESR1
14	71	cfa-miR-19b	ESR1
15	69	cfa-miR-148b	ESR1
16	69	cfa-miR-329a	ESR1
17	69	cfa-miR-152	ESR1
18	69	cfa-miR-148a	ESR1
19	66	cfa-miR-632	ESR1
20	63	cfa-miR-203	ESR1
21	59	cfa-miR-323	ESR1
22	59	cfa-miR-874	ESR1
23	54	cfa-miR-486	ESR1
24	53	cfa-miR-8850	ESR1
25	50	cfa-miR-299	ESR1

Appendix 4: Full gene names and abbreviations for bioinformatic analysis results.

ABHD2	Abhydrolase domain containing 2
ABI3BP	ABI family member 3 binding protein
ACER3	Alkaline ceramidase 3
ACVR1B	Activin A receptor type 1B
ADAMTS20	ADAM metallopeptidase with thrombospondin type 1 motif 20
ADAMTSL3	ADAMTS like 3
ADARB1	Adenosine deaminase, RNA specific B1
ADCY6	Adenylate cyclase 6
ADM	Adrenomedullin
AGO3	Argonaute RISC catalytic component 3
AGO4	Argonaute RISC catalytic component 4
APBB2	Amyloid beta precursor protein binding family B member 2
ARF4	ADP ribosylation factor 4
ARFGEF1	ADP ribosylation factor guanine nucleotide exchange factor 1
ARID1B	AT-rich interaction domain 1B
ARID3A	AT-rich interaction domain 3A
ARID3B	AT-rich interaction domain 3B
ARID4A	AT-rich interaction domain 4A
ARID4B	AT-rich interaction domain 4B
ASCL1	Achaete-scute family bHLH transcription factor 1
ASIC2	Acid sensing ion channel subunit 2
ATRX	ATRX, chromatin remodeler
ATXN1	Ataxin 1
AVL9	AVL9 cell migration associated
BEND3	BEN domain containing 3
BMF	Bcl2 modifying factor

BNC2	Basonuclin 2
CACUL1	CDK2 associated cullin domain 1
CAMK1D	Calcium/calmodulin dependent protein kinase ID
CAMK2D	Calcium/calmodulin dependent protein kinase II delta
CAMK2G	Calcium/calmodulin dependent protein kinase II gamma
CARM1	Coactivator associated arginine methyltransferase 1
CASP3	Caspase 3
CBL	Cbl proto-oncogene
CCDC80	Coiled-coil domain containing 80
CCDC88A	Coiled-coil domain containing 88A
CCNE2	Cyclin E2
CDC42BPA	CDC42 binding protein kinase alpha
CDH2	Cadherin 2
CDK1	Cyclin dependent kinase 1
CELSR3	Cadherin EGF LAG seven-pass G-type receptor 3
CHD1	Chromodomain helicase DNA binding protein 1
CITED2	Cbp/p300 interacting transactivator with Glu/Asp rich carboxy-terminal domain 2
CNBP	CCHC-type zinc finger nucleic acid binding protein
CNOT6	CCR4-NOT transcription complex subunit 6
CNOT6L	CCR4-NOT transcription complex subunit 6 like
CNOT7	CCR4-NOT transcription complex subunit 7
COL1A1	Collagen type I alpha 1 chain
COL1A2	Collagen type I alpha 2 chain
CPLX1	Complexin 1
CPLX2	Complexin 2
CREB1	CAMP responsive element binding protein 1
CSK	C-terminal Src kinase
CTR9	CTR9 homolog, Paf1/RNA polymerase II complex component

DAB2	DAB2, clathrin adaptor protein
DDX5	DEAD-box helicase 5
DDX6	DEAD-box helicase 6
DGKH	Diacylglycerol kinase eta
DLL1	Delta like canonical Notch ligand 1
DNAJC3	DnaJ heat shock protein family (Hsp40) member C3
EDIL3	EDIL3
EIF4E	Eukaryotic translation initiation factor 4E
EIF5A2	Eukaryotic translation initiation factor 5A2
EOMES	Eomesodermin
EPHB1	EPH receptor B1
EPHB3	EPH receptor B3
ESM1	Endothelial cell specific molecule 1
ESR1	Estrogen Receptor 1α
FAM76A	Family with sequence similarity 76 member A
FIGN	Fidgetin, microtubule severing factor
FKBP8	FKBP prolyl isomerase 8
FOXO1	Forkhead box O1
FOXO3	Forkhead box O3
FRS2	Fibroblast growth factor receptor substrate 2
FUT9	Fucosyltransferase 9
GATA3	GATA binding protein 3
GCLM	Glutamate-cysteine ligase modifier subunit
GNA12	G protein subunit alpha 12
GSK3B	Glycogen synthase kinase 3 beta
HBEGF	Heparin binding EGF like growth factor
HCN3	Hyperpolarization activated cyclic nucleotide gated potassium channel 3
HDAC1	Histone deacetylase 1

HIPK1	Homeodomain interacting protein kinase 1
HIPK3	Homeodomain interacting protein kinase 3
HMGA2	High mobility group AT-hook 2
HNF1A	HNF1 homeobox A
HSP90B1	Heat shock protein 90 beta family member 1
HSPA5	Heat shock protein family A (Hsp70) member 5
HUWE1	HECT, UBA and WWE domain containing 1, E3 ubiquitin protein ligase
IGF1	Insulin like growth factor 1
IL34	Interleukin 34
INO80	INO80 complex subunit
INSR	Insulin receptor
ITGA6	Integrin subunit alpha 6
ITGB8	Integrin subunit beta 8
JAK2	Janus kinase 2
KANK1	KN motif and ankyrin repeat domains 1
KCNN3	Potassium calcium-activated channel subfamily N member 3
KCTD13	Potassium channel tetramerization domain containing 13
KIAA1467	Family with sequence similarity 234 member B
KIF26B	Kinesin family member 26B
KLB	Klotho beta
KLF3	Kruppel like factor 3
KLF4	Kruppel like factor 4
KLHL20	Kelch like family member 20
KMT2A	Lysine methyltransferase 2A
KMT2D	Lysine methyltransferase 2D
KPNA5	Karyopherin subunit alpha 5
KRAS	KRAS proto-oncogene, GTPase
KRIT1	KRIT1, ankyrin repeat containing

LAMC1	Laminin subunit gamma 1
LATS2	Large tumor suppressor kinase 2
LIMD1	LIM domains containing 1
LIN28B	Lin-28 homolog B
LOC488215	N-acetyllactosaminide beta-1,6-N-acetylglucosaminyl-transferase
LPP	LIM domain containing preferred translocation partner in lipoma
MAB21L1	Mab-21 like 1
MAPK8	Mitogen-activated protein kinase 8
MARK1	Microtubule affinity regulating kinase 1
MDM4	MDM4, p53 regulator
MECP2	Methyl-CpG binding protein 2
MED28	Mediator complex subunit 28
MMP24	Matrix metallopeptidase 24
MORF4L2	Mortality factor 4 like 2
MTDH	Metadherin
MTF2	Metal response element binding transcription factor 2
NAA15	N(alpha)-acetyltransferase 15, NatA auxiliary subunit
NECAB3	N-terminal EF-hand calcium binding protein 3
NFATC2	Nuclear factor of activated T cells 2
NID1	Nidogen 1
NIPBL	NIPBL, cohesin loading factor
NOTCH1	Notch 1
NR6A1	Nuclear receptor subfamily 6 group A member 1
NRP1	Neuropilin 1
OSBPL8	Oxysterol binding protein like 8
PACS1	Phosphofurin acidic cluster sorting protein 1
PAK4	p21 (RAC1) activated kinase 4
PDCD10	Programmed cell death 10

PDE7A	Phosphodiesterase 7A
PHC1	Polyhomeotic homolog 1
PHF19	PHD finger protein 19
PHF8	PHD finger protein 8
PHIP	Pleckstrin homology domain interacting protein
PI15	Peptidase inhibitor 15
PODXL	Podocalyxin like
PPARGC1B	PPARG coactivator 1 beta
PPM1F	Protein phosphatase, Mg2+/Mn2+ dependent 1F
PPP1R13B	Protein phosphatase 1 regulatory subunit 13B
PPP3CA	Protein phosphatase 3 catalytic subunit alpha
PRKAA1	Protein kinase AMP-activated catalytic subunit alpha 1
PRKCE	Protein kinase C epsilon
PROX1	Prospero homeobox 1
PSME3	Proteasome activator subunit 3
PTEN	Phosphatase and tensin homolog
PTK2	Protein tyrosine kinase 2
PTPRJ	Protein tyrosine phosphatase, receptor type J
QKI	QKI, KH domain containing RNA binding
RAB11FIP2	RAB11 family interacting protein 2
RANBP1	RAN binding protein 1
RAP2A	RAP2A, member of RAS oncogene family
RAP2C	RAP2C, member of RAS oncogene family
RARB	Retinoic acid receptor beta
RBBP8	RB binding protein 8, endonuclease
RERE	Arginine-glutamic acid dipeptide repeats
RHBDD1	Rhomboid domain containing 1
RICTOR	RPTOR independent companion of MTOR complex 2

ROBO1	Roundabout guidance receptor 1
ROCK1	Rho associated coiled-coil containing protein kinase 1
ROGDI	Rogdi atypical leucine zipper
RORA	RAR related orphan receptor A
RPS6KB1	Ribosomal protein S6 kinase B1
RRAS	RAS related
RSF1	Remodeling and spacing factor 1
S1PR1	Sphingosine-1-phosphate receptor 1
SDC1	Syndecan 1
SDC4	Syndecan 4
SESN3	Sestrin 3
SETX	Senataxin
SFRP1	Secreted frizzled related protein 1
SGMS1	Sphingomyelin synthase 1
SH3GLB1	SH3 domain containing GRB2 like, endophilin B1
SLC25A5	Solute carrier family 25 member 5
SMARCA2	SWI/SNF related, matrix associated, actin dependent regulator of chromatin, subfamily a, member 2
SMOC2	SPARC related modular calcium binding 2
SORBS2	Sorbin and SH3 domain containing 2
SP3	Sp3 transcription factor
SRGAP2	SLIT-ROBO Rho GTPase activating protein 2
STOX2	Storkhead box 2
SUZ12	SUZ12, polycomb repressive complex 2 subunit
SYT1	Synaptotagmin 1
SYT2	Synaptotagmin 2
TAF9B	TATA-box binding protein associated factor 9b
TET1	Tet methylcytosine dioxygenase 1
TET3	Tet methylcytosine dioxygenase 3

TGFB2	Transforming growth factor beta 2
THY1	Thy-1 cell surface antigen
TOP1	DNA topoisomerase I
TP53INP1	Tumor protein p53 inducible nuclear protein 1
TP63	Tumor protein p63
TRIM71	Tripartite motif containing 71
UBE2A	Ubiquitin conjugating enzyme E2 A
UBE2B	Ubiquitin conjugating enzyme E2 B
UBR2	Ubiquitin protein ligase E3 component n-recognin 2
USP33	Ubiquitin specific peptidase 33
USP37	Ubiquitin specific peptidase 37
UST	Uronyl 2-sulfotransferase
VAV2	Vav guanine nucleotide exchange factor 2
VEGFA	Vascular endothelial growth factor A
WEE1	WEE1 G2 checkpoint kinase
ZBTB20	Zinc finger and BTB domain containing 20
ZMAT1	Zinc finger matrin-type 1
ZMAT3	Zinc finger matrin-type 3
ZMAT4	Zinc finger matrin-type 4
ZMYND11	Zinc finger MYND-type containing 11
ZNF346	Zinc finger protein 346
ZNF385B	Zinc finger protein 385B
ZNF830	Zinc finger protein 830

Appendix 5: Estrogen and progesterone receptor immunohistochemistry.

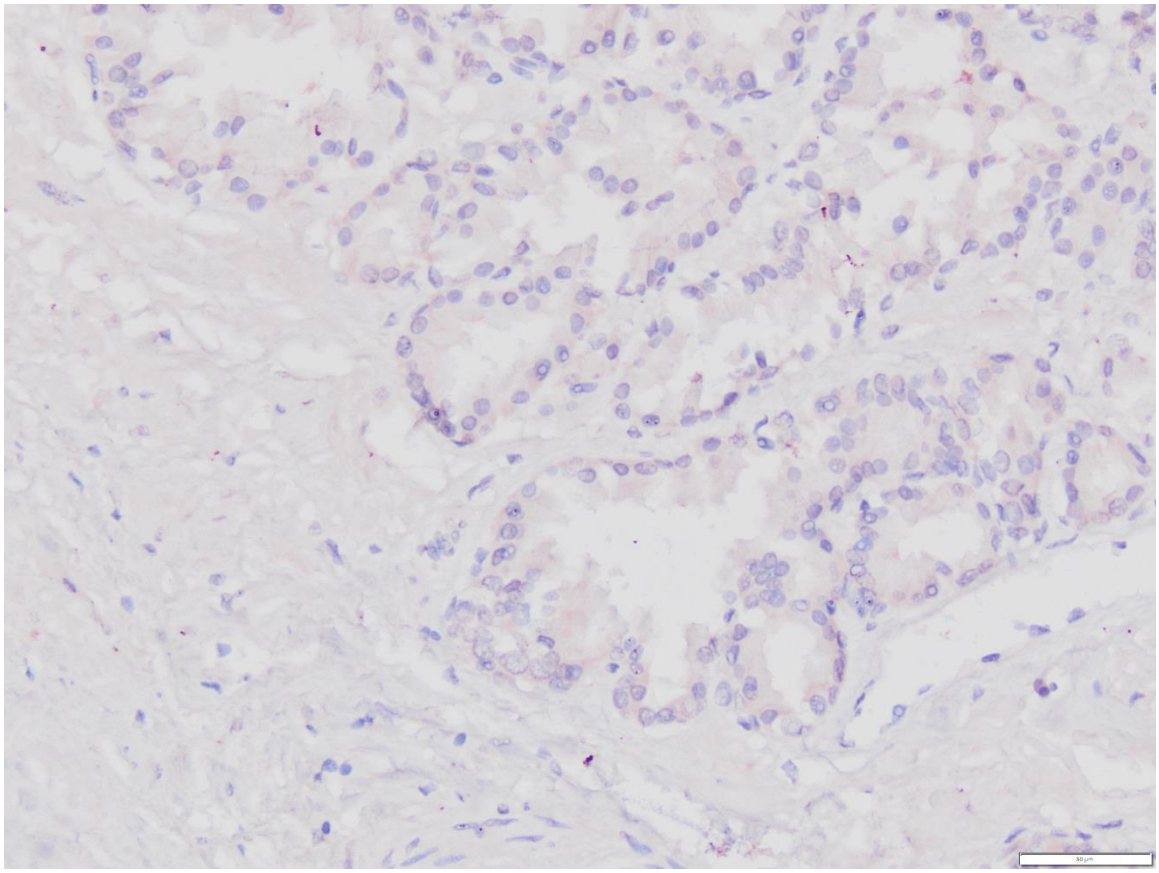

A. Estrogen receptor, positive control. Note the barely perceptible brown-red staining in epithelial cells, with a large amount of non-specific background staining throughout the image. AEC chromogen, hematoxylin counterstain. 200x magnification. Scale bar = 50 µm.

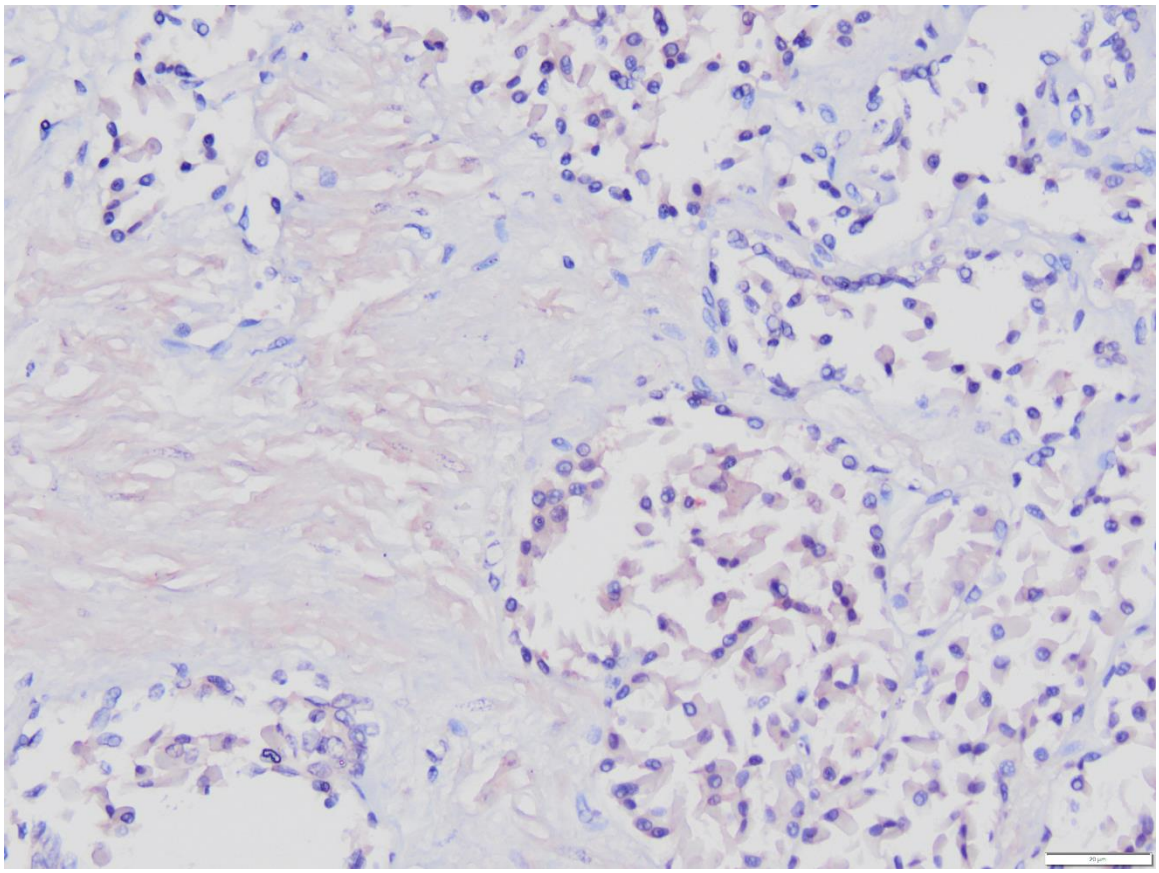

B. Progesterone receptor, positive control. Note the faint brown-red staining in epithelial cells, with a large amount of non-specific background staining throughout the image. AEC chromogen, hematoxylin counterstain. 200x magnification. Scale bar = 50 µm.

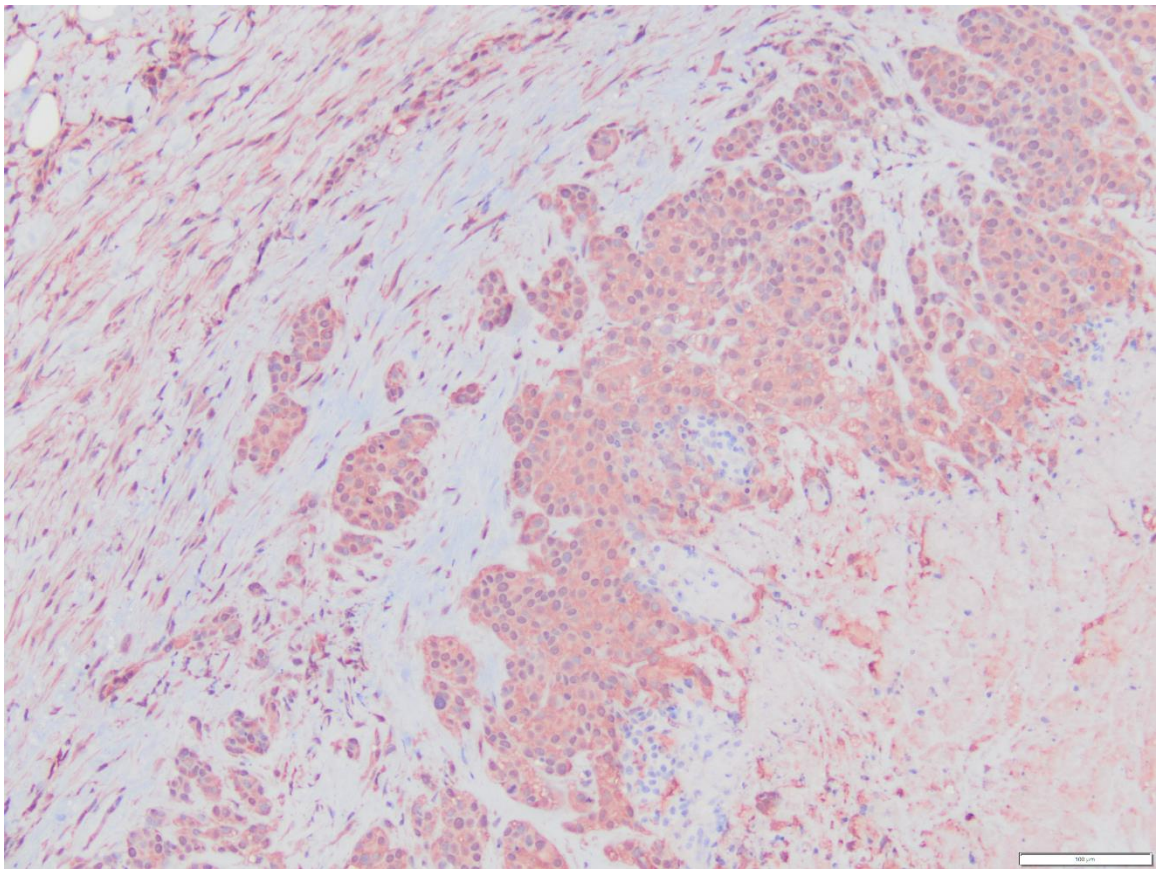

C. Estrogen receptor, MC1 (Grade I mixed carcinoma). There is intense red immunolabeling (greater than positive control) by neoplastic cells as well as adjacent stroma and background, indicating non-specific binding. AEC chromogen, hematoxylin counterstain. 100x magnification. Scale bar = 100 µm.

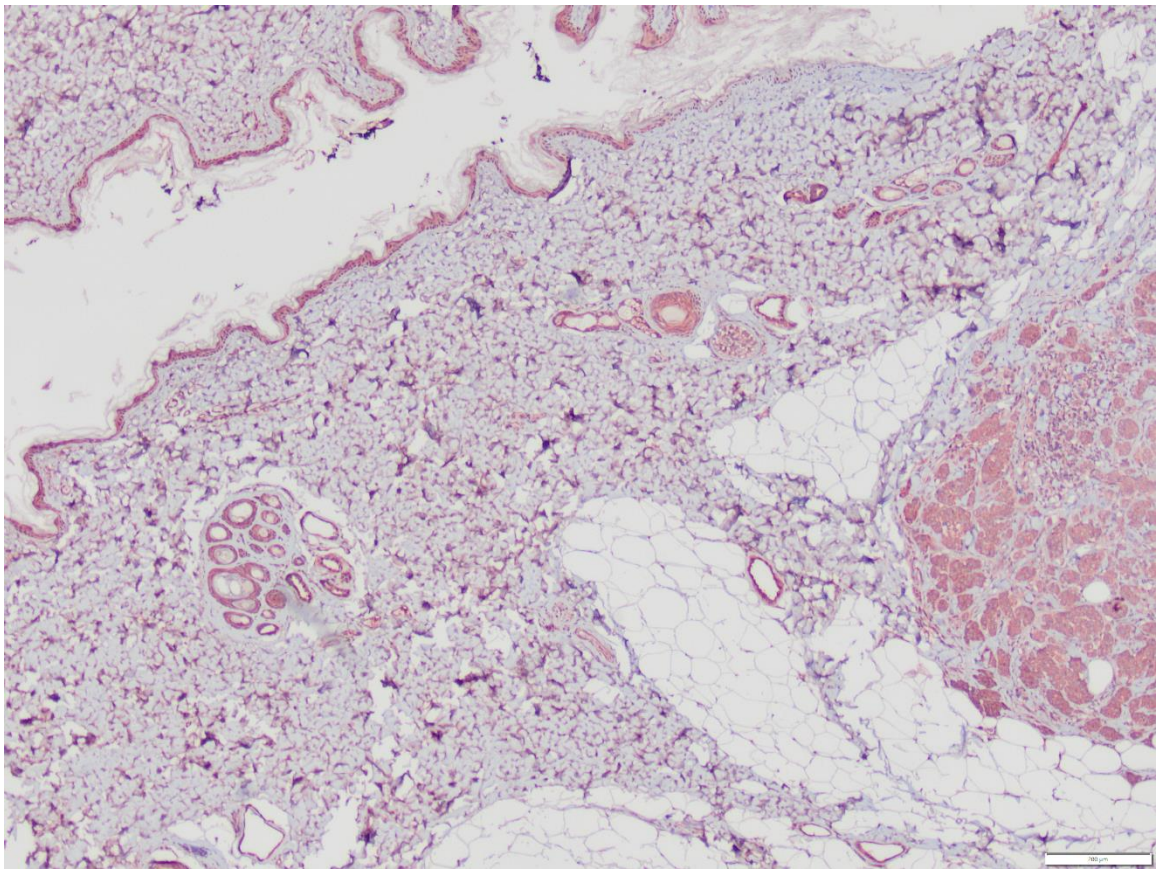

D. Estrogen receptor, MC4 (Grade II micropapillary invasive carcinoma). There is intense red immunolabeling (far greater than positive control) by neoplastic cells as well as adjacent stratified squamous epithelium in the epidermis, subcutis, stroma and background, indicating non-specific binding. AEC chromogen, hematoxylin counterstain. 40x magnification. Scale bar = 200 µm.

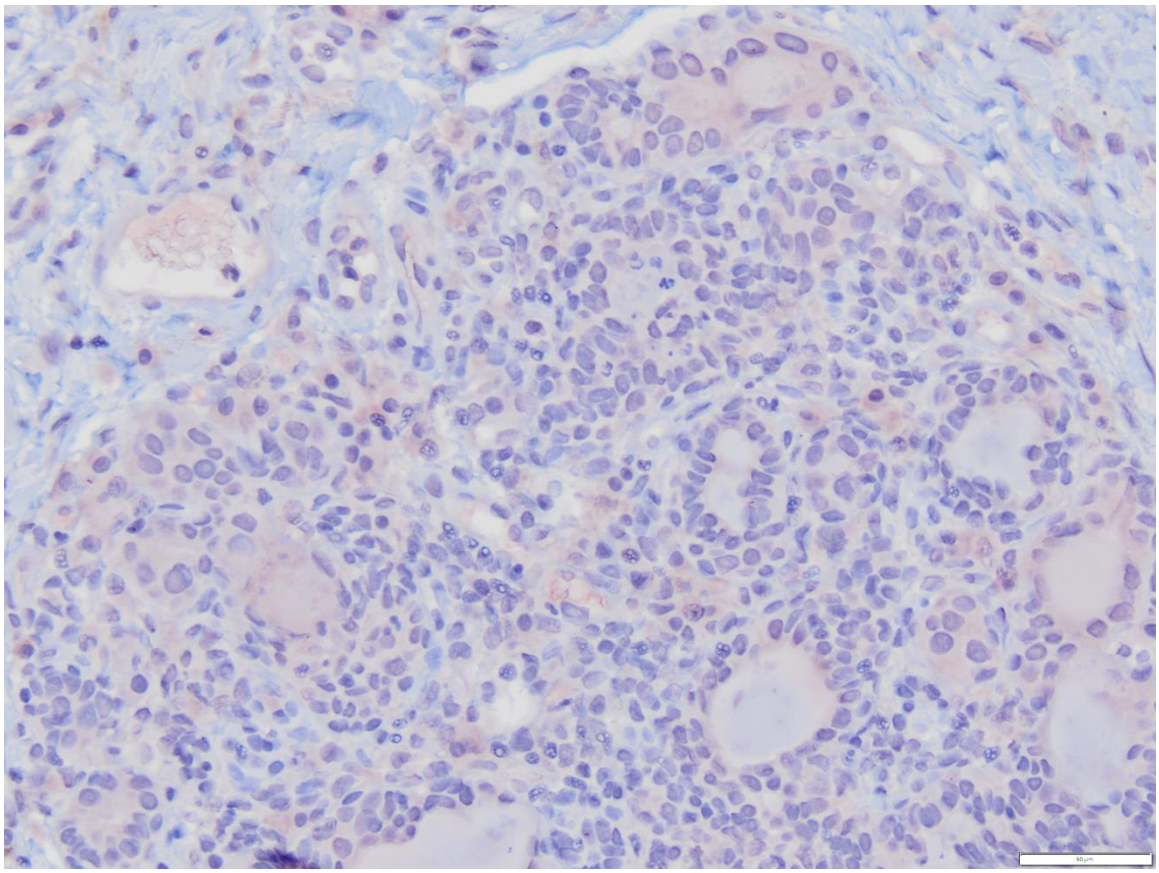

E. Progesterone receptor, MC10 (Grade III tubulopapillary-solid carcinoma). There is weak red immunolabeling approximately equal to or slightly greater than the positive control by neoplastic cells. Any progesterone positivity by a poorly-differentiated Grade III tumor would be highly unusual. AEC chromogen, hematoxylin counterstain. 200x magnification. Scale bar = 50 µm.